



Terms and Conditions of Use of Digitised Theses from Trinity College Library Dublin

Copyright statement

All material supplied by Trinity College Library is protected by copyright (under the Copyright and Related Rights Act, 2000 as amended) and other relevant Intellectual Property Rights. By accessing and using a Digitised Thesis from Trinity College Library you acknowledge that all Intellectual Property Rights in any Works supplied are the sole and exclusive property of the copyright and/or other IPR holder. Specific copyright holders may not be explicitly identified. Use of materials from other sources within a thesis should not be construed as a claim over them.

A non-exclusive, non-transferable licence is hereby granted to those using or reproducing, in whole or in part, the material for valid purposes, providing the copyright owners are acknowledged using the normal conventions. Where specific permission to use material is required, this is identified and such permission must be sought from the copyright holder or agency cited.

Liability statement

By using a Digitised Thesis, I accept that Trinity College Dublin bears no legal responsibility for the accuracy, legality or comprehensiveness of materials contained within the thesis, and that Trinity College Dublin accepts no liability for indirect, consequential, or incidental, damages or losses arising from use of the thesis for whatever reason. Information located in a thesis may be subject to specific use constraints, details of which may not be explicitly described. It is the responsibility of potential and actual users to be aware of such constraints and to abide by them. By making use of material from a digitised thesis, you accept these copyright and disclaimer provisions. Where it is brought to the attention of Trinity College Library that there may be a breach of copyright or other restraint, it is the policy to withdraw or take down access to a thesis while the issue is being resolved.

Access Agreement

By using a Digitised Thesis from Trinity College Library you are bound by the following Terms & Conditions. Please read them carefully.

I have read and I understand the following statement: All material supplied via a Digitised Thesis from Trinity College Library is protected by copyright and other intellectual property rights, and duplication or sale of all or part of any of a thesis is not permitted, except that material may be duplicated by you for your research use or for educational purposes in electronic or print form providing the copyright owners are acknowledged using the normal conventions. You must obtain permission for any other use. Electronic or print copies may not be offered, whether for sale or otherwise to anyone. This copy has been supplied on the understanding that it is copyright material and that no quotation from the thesis may be published without proper acknowledgement.

**A NOVEL METHOD FOR THE MEASUREMENT OF FLOW-
INDUCED PLATELET ACTIVATION AT NANOSCALE
RESOLUTION LEVEL**

by

María José Santos-Martínez

being a thesis submitted for the degree of
Doctor of Philosophy (Pharmacology)

at

**UNIVERSITY OF DUBLIN
TRINITY COLLEGE**

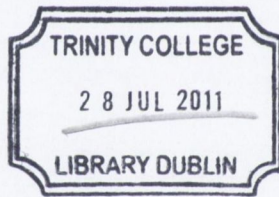


under the supervision and direction of

Professor Marek W Radomski

**SCHOOL OF PHARMACY AND PHARMACEUTICAL SCIENCES
TRINITY COLLEGE DUBLIN**

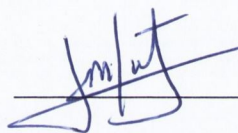
2009



THESIS
9208

DECLARATION

This thesis is submitted by the undersigned to the University of Dublin, Trinity College, for examination for the degree of Doctor of Philosophy. It has not been submitted as an exercise for a degree at this or any other University. I have carried out all the practical work except where duly acknowledged. I agree that the Library may lend or copy this thesis upon request.



María José Santos-Martínez

TABLE OF CONTENTS

Acknowledgements	i
Summary	ii
List of Abbreviations	iv
INTRODUCTION	1
Vascular Haemostasis and Thrombosis	1
Coagulation and Fibrinolytic Systems	1
The Haemostatic Function of Platelets	4
Platelet Adhesion	7
Platelet Activation.....	8
Platelet Aggregation.....	10
Adenosine Diphosphate (ADP)	11
Eicosanoids (PGI ₂ and TXA ₂)	12
Matrix Metalloproteinases and their inhibitors	16
Platelets and Endothelium	21
Platelets and Blood Flow	27
In Vitro Methods for Measurement of Platelet Activation	30
Quartz Crystal Microbalance with Dissipation (QCM-D)	35
AIMS OF PROJECT	39

MATERIALS AND METHODS	41
Reagents	41
Blood Collection and Platelet Isolation	41
Q-Sense™ E₄	41
Components of Q-Sense™ E ₄ System.....	42
Data Acquisition and Analysis.....	46
Operation.....	47
Platelet Aggregation	51
Phase Contrast Microscopy	52
Confocal Microscopy	52
Atomic Force Microscopy (AFM)	53
Rheology	55
Statistics	56
RESULTS	57
Perfusion of Sensor Crystals with PRP led to Platelet Aggregation	57
Effects of Fibrinogen Concentrations on Aggregation	59
Effects of Flow Rate on Platelet Aggregation	59
Platelet Aggregation on Gold and Polystyrene-coated Crystals	60
Imaging of Sensor-Induced Platelet Aggregation	78
Phase Contrast Microscopy	78
Confocal Microscopy	79
Atomic Force Microscopy.....	80

Effects of Platelet Agonists on Platelet Aggregation	82
Pharmacology Modulation of Platelet Aggregation	83
Effects of COX Inhibition on Platelet Aggregation	83
Inhibition of Aggregation by the MMP Inhibitor, Phenanthroline.....	85
Effects of Apyrase and MeSAMP on Platelet Aggregation.....	86
Inhibition of Aggregation by GSNO and SNAP.....	87
Inhibition of Platelet Activation by Prostacyclin	88
Q-Tools Analysis Using Voigt-based Viscoelastic Model	91
Rheology	95
DISCUSSION	99
Method Characteristics	100
Fibrinogen as Coating Surface to Induce Platelet Activation and Aggregation..	100
Influence of Flow Rate on Platelet Aggregation	104
Platelet Agonists	105
Platelet Inhibitors.....	107
Method Evaluation	111
Q-Tools Analysis	113
Atomic Force Microscopy	115
CONCLUSIONS	117
FURTHER DIRECTIONS	119
REFERENCES	123

ACKNOWLEDGEMENTS

This work could not be possible without the help, support and kindness of a great number of people. First of all I would like to thank my supervisor Prof. Marek Radomski for offering me the opportunity of doing my PhD, for believing and trusting in my abilities to carry out this project. Marek, many thanks for your support, guidance and friendship. Special thank to Carlos for helping me out and instilling within me the interest in science and research, something that now I'm really enjoying and makes me very happy. Thanks a million to Paul and David for their guidance in my "first steps" in the lab. I would like to thank as well all my lab mates that I have met along the way; special thanks to Ania, Aneta, Joanna, Iwona, Jesus and Juan Jose for their friendship, support and understanding, particularly in those days where I wasn't in a very good mood. I could not ask for better colleagues in the lab! In addition, I would also like to thank Julio for sorting out all the computer troubles that I had to face over the past three years and obviously for his friendship. I am very grateful as well to all those that helped with my experiments including Prof. Yuri Volkov, Lidia, Adriele, Stephen Paul and Jen. In addition, I would also like to thank John Booth for his instruction in understanding the functioning of Q-Sense and helpful discussions. I would also like to thank all members of the technical and administrative staff in the School of Pharmacy, particularly Derek, Alison, Brian, Aileen and Betty for their support and kindness.

I would like to finish with special thank to my family, for their patience and understanding. I feel really very lucky for having the best family that I could ever have dreamt of!

SUMMARY

Background: Platelet aggregation is essential for vascular haemostasis and thrombosis. Inhibition of platelet aggregation underpins the pharmacological and clinical effects of antiplatelet drugs. These effects are commonly quantified using methods and devices that assess platelet aggregation under static conditions in macroscale. However, current devices neither mimic the conditions found in human microvasculature nor detect microaggregates.

Aim: To provide pharmacological characteristics of a novel method of flow-induced platelet aggregation using a commercially available nanoscale resolution device, the Quartz Crystal Microbalance with Dissipation (Q-Sense™ E₄).

Methods: Blood was collected from healthy volunteers and platelet-rich plasma (PRP) was diluted with Phosphate Buffered Saline (PBS) at final concentrations of 50,000; 100,000; 150,000 and 210,000 platelets/ μ L. Platelet-poor plasma (PPP) was used as control. Gold (G) and polystyrene-coated (PL) quartz crystals coated with fibrinogen were used as sensors. Sensor crystals were mounted and perfused at 37°C at 10-100 μ L/minutes for up to 240 minutes. Platelet aggregation was then measured as changes in frequency f (Hz) and energy dissipation D (1E-6) on the crystal surface. Phase-contrast, confocal imaging, atomic force microscopy and pharmacological agents were used to study platelet activation detected by the device.

Results: Microaggregates were detected in a platelet concentration-, flow- and shear stress-dependent manner. The optimal condition for the measurement of platelet aggregation was found when fibrinogen-coated polystyrene-coated

crystals were perfused with PRP at the flow rate of 100 μ L/minute. Platelet activation and aggregation were also detected by phase-contrast, confocal imaging and atomic force microscopy. In addition, platelet aggregation was modulated by different antiplatelet agents.

Conclusion: This novel method can be used to measure platelet function under flow conditions with nanoscale resolution in physiological, pathological and pharmacological studies.

LIST OF ABBREVIATIONS

ADP	Adenosine diphosphate
ASA	Acetylsalicylic acid
cAMP	Cyclic adenosine monophosphate
cGMP	Cyclic guanosine monophosphate
COX	Cyclooxygenase
<i>D</i>	Energy dissipation
DAG	Diacyl glycerol
ECM	Extracellular matrix
EDRF	Endothelium-derived relaxing factor
<i>f</i>	Frequency
FITC	Fluorescein isothiocyanate
GPIb	Glycoprotein Ib
GPIIb/IIIa	Glycoprotein IIb/IIIa
GPIa/IIa	Glycoprotein Ia/IIa
GPCRs	G protein-coupled receptors
GSNO	S-nitrosoglutathione

IP ₃	Inositol trisphosphate
2-MeSAMP	2-Methylthio-AMP triethylammonium salt hydrate
MMP	Matrix metalloproteinase
MT-MMPs	Membrane-type matrix metalloproteinases
NO	Nitric oxide
NOS	Nitric oxide synthase
eNOS	Endothelial nitric oxide synthase, NOS-3
iNOS	Inducible nitric oxide synthase, NOS-2
nNOS	Neuronal nitric oxide synthase, NOS-1
ONOO ⁻	Peroxynitrate
PAI-1	Plasminogen activator inhibitor 1
PAI-2	Plasminogen activator inhibitor 2
PBS	Phosphate Buffered Saline
PFA	Platelet function analyzer
PG	Prostaglandin
PGI ₂	Prostacyclin
PKC	Protein kinase C

PLC	Phospholipase C
PPP	Platelet-poor plasma
PRP	Platelet-rich plasma
QCM	Quartz Crystal Microbalance
QCM-D	Quartz Crystal Microbalance with Dissipation
QSoft ₄₀₁	Q-Sense software 401
SDS	Sodium Dodecyl Sulphate
SNAP	S-nitroso-N-acetyl-DL-penicillamine
TCIPA	Tumour cell-induced platelet aggregation
TIMP	Tissue inhibitor of matrix metalloproteinases
TP	Thromboxane A ₂ receptor
t-PA	tissue plasminogen activator
TRAP	Thrombin receptor activator peptide
TXA ₂	Thromboxane A ₂
u-PA	Urokinase plasminogen activator
vWF	von Willebrand Factor

INTRODUCTION

VASCULAR HAEMOSTASIS AND THROMBOSIS

Haemostasis is the process responsible for the preservation of the integrity of the circulatory system resulting from vascular damage. Haemostasis and thrombosis represent very complex interactions between the injured vessel wall and the different components of the blood, particularly the coagulation cascade, the fibrinolytic system and platelets. *Thrombosis* is a pathological extension of haemostasis that results from an imbalance between the three main factors involved in the classical Virchow's Triad: *blood*, *blood vessel* and *blood flow*.

COAGULATION AND FIBRINOLYTIC SYSTEMS

After vessel-wall damage, platelets are recruited to the site of injury where they play a central role in the clotting process (primary haemostasis); simultaneously coagulation factors react in a self-amplifying way that is called **coagulation cascade** or secondary haemostasis. This culminates in the generation of thrombin and fibrin and the formation of the clot. Coagulation factors are generally indicated by Roman numerals, with a lowercase *a* to indicate an active form. The coagulation cascade utilizes classically two pathways, the contact activation pathway (known as the intrinsic pathway), and the tissue factor pathway (known as the extrinsic pathway) which lead to fibrin formation. The primary pathway for the initiation of blood coagulation is the tissue factor pathway. The contact pathway of blood coagulation, a powerful tool for *in vitro* studies of the coagulation cascade, is not required for initiation of haemostasis *in vivo*. In fact, a complete deficiency of factor XII, high-molecular-weight kininogen, or prekallikrein is associated with major defects in the initiation of the

contact pathway of coagulation; however patients suffering from these deficiencies do not have a haemorrhagic disorder (Furie and Furie 1988).

Collagen, when exposed to the vascular lumen, results in accumulation and activation of platelets, while exposed tissue factor is responsible for the generation of thrombin. Thrombin not only converts fibrinogen to fibrin but also activates platelets. Tissue factor is constitutively expressed on vascular and non-vascular cells, but is also present in circulating blood. Activated platelets and endothelial cells can secrete the enzyme responsible for the conversion of inactive tissue factor to its active form. In the case of direct tissue damage, tissue factor in the vessel wall or on cell surfaces may already exist in its active form, and the enzyme may not be required (Furie and Furie 2008).

Tissue factor forms a complex with circulating factor VIIa. This complex, which plays the most important role in coagulation, has three substrates: factor VII, factor IX, and factor X. Factor IXa binds to factor VIII. This complex activates factor X to form factor Xa. Factor Xa, generated by the tissue factor-factor VIIa complex or the factor IXa-factor VIII complex, binds factor V on membrane surfaces. This complex converts prothrombin (factor II) to thrombin (factor IIa). The thrombin generated activates factors VIII and V, leading to a burst of thrombin-generating potential. During haemostasis, the tissue factor pathway that is the fuse for initiation of coagulation is inactivated (Furie and Furie 2008). Finally, thrombin cleaves soluble fibrinogen (factor I) into insoluble fibrin to form the definite clot (**figure 1**).

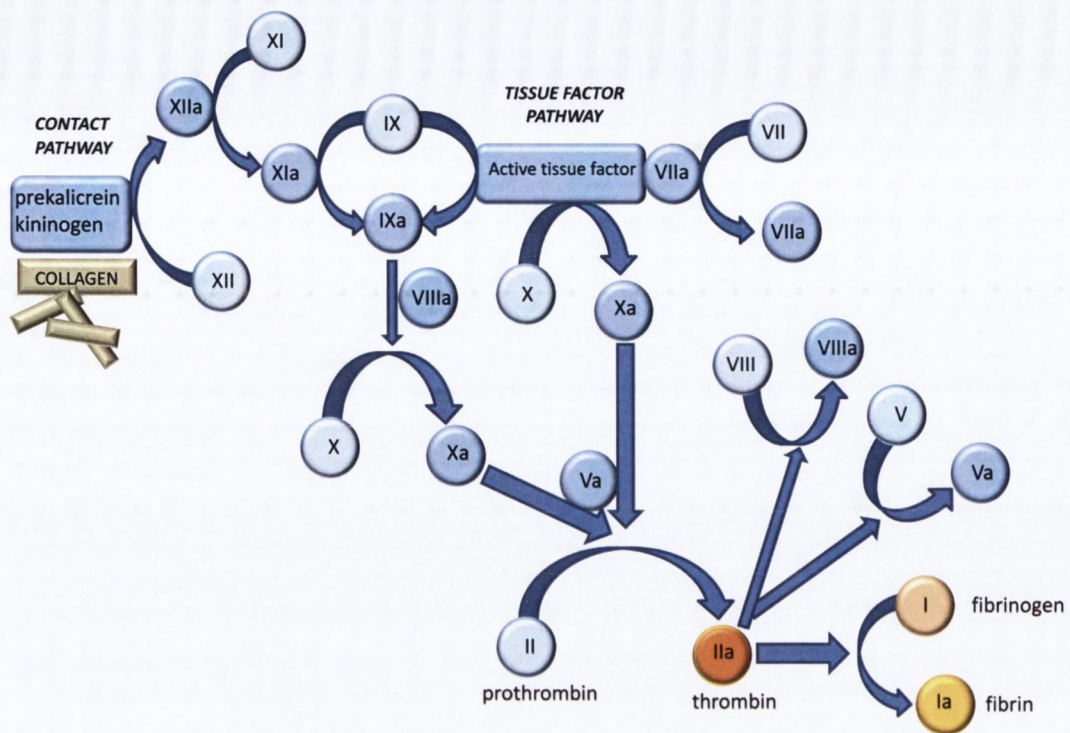


Figure 1: Coagulation cascade
 Blue arrows correspond to activation actions.

Fibrinogen is a 340 KDa glycoprotein synthesised in the liver and its concentration in plasma is 1.5-4 mg/ml. Fibrinogen contains two sets of three polypeptide chains called alpha, beta and gamma that are joined by disulfide bridging within the N-terminal E domain. The molecules are elongated 45-nm structures consisting of two outer D domains, each connected to a central E domain by a coiled-coil segment. These domains contain constitutive binding sites that participate in fibrinogen conversion to fibrin, fibrin assembly, and platelet interactions through glycoprotein GPIIb/IIIa surface receptors (Mosesson, Siebenlist et al. 2001).

The main component of the **fibrinolytic system** is plasmin, which cleaves fibrin. Plasmin derives from plasminogen by the action of tissue plasminogen activator (t-PA) and urokinase plasminogen activator (u-PA). Tissue plasminogen activator is released into the blood very slowly by the damaged

endothelium and after several days therefore the clot is broken down. Both factors, t-PA and u-PA are inhibited by plasminogen activator inhibitor-1 and plasminogen activator inhibitor-2 (PAI-1 and PAI-2). This system may be amplified by a complex formed by thrombin and thrombomodulin. This complex is able to activate protein C which inactivates inhibitors of tissue plasminogen activator leading to increased generation of plasmin. Finally, alpha 2-antiplasmin and alpha 2-macroglobulin are able to inactivate plasmin (**figure 2**).

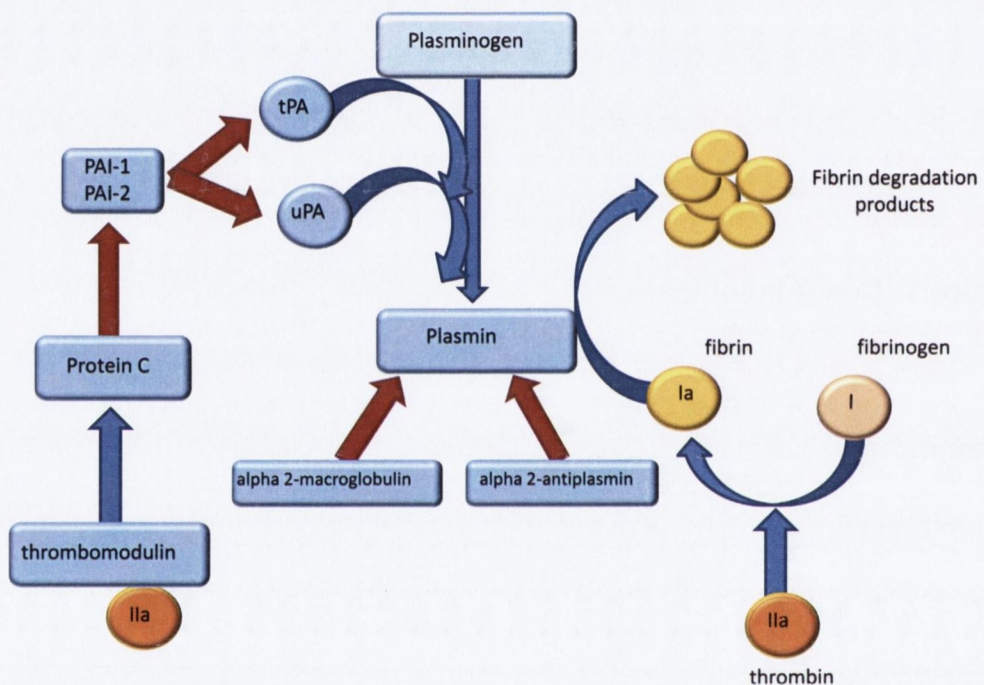


Figure 2: Fibrinolytic system

Blue lines correspond to activation actions and red lines to inhibitory actions.

THE HAEMOSTATIC FUNCTION OF PLATELETS

Platelets are anucleate cell elements derived from megakaryocytes that play a crucial role in haemostasis and thrombosis. Platelets were identified for the first time in 1842 by Donne. At that time platelets were considered just an artefact produced during the preparation of blood specimens (Donne 1842). In 1865 Schultze (Schultze 1865) noted the tendency of platelets to clump but it was

Bizzozero (Bizzozero 1882) who first recognized the importance of platelets as authentic functional entities (Dopheide, Yap et al. 2001) .

Human platelets are 2-4 μm in size and contain numerous alpha (α) and dense (δ) granules, which store factors and platelet receptor proteins that are crucial for platelet function. Like other blood elements, lysosomes, mitochondria and endoplasmic reticulum are also expressed by platelets. Under physiological circumstances platelets have a life span of 7-10 days and are suspended in blood at a concentration of 150,000 to 400,000 platelets/ μL (Michelson 2003). In the absence of any activating stimulus, platelets circulate in a quiescent state being discoid in shape, however, when they become activated, they change their shape extending pseudopodia in many directions (**figure 3**).

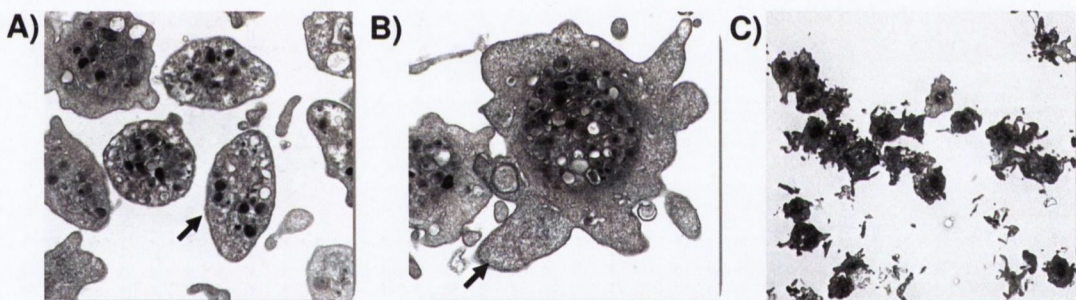


Figure 3: Platelets electron microscopy

A) resting platelets with discoid shape; B) activated platelets with the formation of pseudopodia; C) aggregated platelets forming different plugs. Arrows point to the selected structures.

Endothelial cell-released factors such as nitric oxide (NO) and prostaglandin I₂ (PGI₂, prostacyclin) and CD39, an adenosine diphosphate (ADP)-ase, present on the surface of endothelial cells are inhibitory factors that have to be overcome for platelets to become activated (Michelson 2003). The main trigger for the formation of a haemostatic thrombus after vascular injury is the loss of the endothelial cell barrier between extracellular matrix components and

flowing blood. Platelets respond to this event in three consecutive and integrated phases that involve **adhesion, activation and platelet aggregation** (Ruggeri 2002). When the vascular wall is damaged, circulating platelets are recruited to the site of injury and interact with different subendothelial and plasma proteins leading to a cascade of events mediated mainly by Thromboxane A₂ (TXA₂) (Needleman, Moncada et al. 1976), ADP (Born 1966) and matrix metalloproteinase-2 (MMP-2) (Sawicki, Salas et al. 1997) that may result in haemostatic plug to repair the vascular damage that occurs with daily life, or as a result of thrombus formation (Furie and Furie 2008) (**figure 4**).

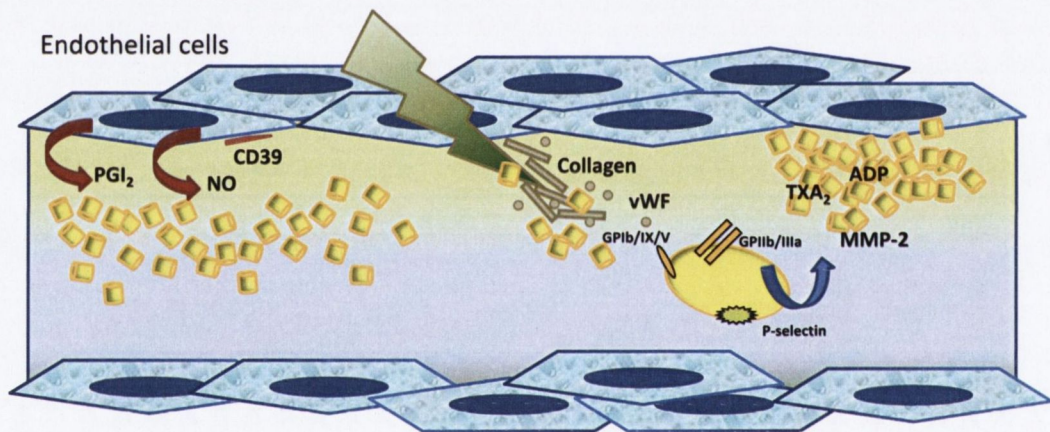


Figure 4: Steps in platelet plug formation

Prior to vascular injury, platelets are maintained in the resting state by the combined action of inhibitory factors. These factors include PGI₂ and NO released from endothelial cells, and CD39, an ADPase on the surface of endothelial cells that hydrolyzes any small amounts of ADP that could cause platelet activation. The development of the platelet plug is initiated by the adhesion of collagen and von Willebrand factor (vWF) to platelet glycoprotein (GP) receptors such as GPIb and spreading on the connective matrix, forming a monolayer. At the same time, P-selectin which is mainly stored in alpha-granules translocates to the membrane surface and GPIIb/IIIa becomes activated. Afterwards, the platelet plug is extended as additional platelets are activated via the release or secretion of TXA₂, ADP, MMP-2 and other platelet agonists. Finally, close contacts between platelets in the growing haemostatic plug, along with a fibrin network, help to maintain and stabilize the platelet aggregate. Platelets are represented as yellow structures.

In addition, evidence also indicates the role of platelets in non-haemostatic processes such as wound repair, angiogenesis, innate immune response, and carcinogenesis (Jurasz, Alonso-Escolano et al. 2004; Jurasz, Santos-Martinez et al. 2006; Medina, Jurasz et al. 2006).

PLATELET ADHESION

When subendothelial components such as collagen and von Willebrand factor (vWF) are exposed to flowing blood, flowing platelets decelerate, adhere to the site of vascular damage and aggregate to arrest bleeding. Membrane receptors are responsible for the initial binding of platelets to the wounded vessel wall allowing the formation of a layer of platelets that supports thrombin generation and the formation of subsequent platelet aggregates (Michelson 2003). Soluble vWF does not bind to platelets to prevent aggregation; however, collagen-immobilized vWF is highly reactive towards flowing platelets. In fact, initial binding and adhesion of platelets to the exposed subendothelium is mediated by GPIb/IX/V complex and collagen receptors, GPVI and GPIa/IIa, in the platelet surface, and by vWF and fibrillar collagen in the vascular site. These adhesive interactions basically depend on the rheological conditions at the site of vascular damaged. At low shear rate, platelet adhesion to the vessel wall primarily involves binding to fibrillar collagen, fibronectin and laminin. However, under high shear stress, such as is found in the microcirculation, the initial adhesion of platelets to the subendothelium is mediated primarily through the interaction of vWF with the platelet receptor GPIb/IX/V complex (Rivera, Lozano et al. 2009). The GPIb/IX/V complex consists of four subunits: GPIb α , GPIb β , GPIX and GPV. The GPIb α subunit is essential for binding vWF, while

both GPIIb/IIIa and GPIIX are important in assembling and anchoring the complex to the platelet surface. The interaction between vWF and its glycoprotein platelet receptor is required to decelerate platelets and allow the platelet collagen receptors to bind to collagen and to firmly adhere to the surface. Indeed, GPIIb/IIIa is considered as an “indirect collagen receptor” and it is essential for platelet interactions with collagen at high shear rates. Platelets contain two main collagen receptors, GPIIb/IIIa and GPVI. The GPIIb/IIIa receptor belongs to the integrin family (integrin $\alpha_2\beta_1$) and GPVI is a type I transmembrane protein. Activation of platelets by collagen requires the engagement of both receptors (Chen and Lopez 2005). The main function of GPIIb/IIIa receptor is to induce a strong attachment of platelets to the collagen surface. The major function of GPVI is to act as a signalling molecule; GPVI is responsible for activation of integrins and also induces granule secretion and TXA₂ formation to fully activate platelets (Clemetson and Clemetson 2001). In fact, blockade of GPIIb/IIIa inhibits collagen-induced aggregation (Coller, Beer et al. 1989) and deficiency or blockade of GPVI inhibits thrombus formation on collagen surfaces under flow conditions (Goto, Tamura et al. 2002).

PLATELET ACTIVATION

Platelet activation begins with the binding of platelet receptors on the subendothelial surface that leads to conformational changes in platelet structure, from discoid-shaped structures to spherical forms that extend pseudopodia; secretion of granules, which enhances the activation process and finally, establishment of fibrinogen bridges between platelets. Collagen and vWF and their receptors work together in platelet adhesion and platelet

activation to mediate thrombus formation. Platelet collagen receptors, GPIa/IIa and GPVI, play an important role on activating platelets in the early stage and work with GPIb/IX/V complex for the initiation of the intracellular signalling, called "inside-out" signalling, that results in platelet aggregation (Chen and Lopez 2005). The binding of vWF to GPIb/IX/X complex leads to the release and activation of the GPIIb/IIIa receptor. The GPIIb/IIIa receptor is a platelet specific surface receptor that belongs to the integrin superfamily ($\alpha_{IIb}\beta_3$ integrin). It is the most abundant receptor on platelet surface; as many as 80,000 copies of GPIIb/IIIa are expressed on the surface of resting platelets with additional pools in the membranes of α -granules and the open-canalicular system (Cramer, Savidge et al. 1990). In resting platelets this integrin has no ligand-binding activity, however the release of the GPIIb/IIIa receptor onto the platelet surface and the conformational change in its structure results in exposure of high affinity-binding sites that facilitate the recognition of circulating soluble fibrinogen. As a result, a haemostatic plug that provides a place for the congregation of coagulation protein complexes that convert fibrinogen to fibrin leading to thrombus formation is produced (Fullard 2004). In addition, the release of adhesive proteins such as vWF, fibrinogen, and fibronectin from α -granules also facilitate blood coagulation (Wencel-Drake, Painter et al. 1985). A number of monoclonal antibodies, such as PAC-1, have been produced to recognize activated conformation of GPIIb/IIIa.

Activated platelets also express on their surface membranes P-selectin. P-selectin (CD62-P) is a 140-KDa transmembrane adhesion receptor identified in platelets (Stenberg, McEver et al. 1985) and endothelial cells. In resting platelets it is limited to the membrane of α -granules but, when platelets are

activated, P-selectin is mobilized to the platelet membrane mainly mediating platelet-leukocyte aggregation (Larsen, Celi et al. 1989; Hamburger and McEver 1990) (**Figure 5**).

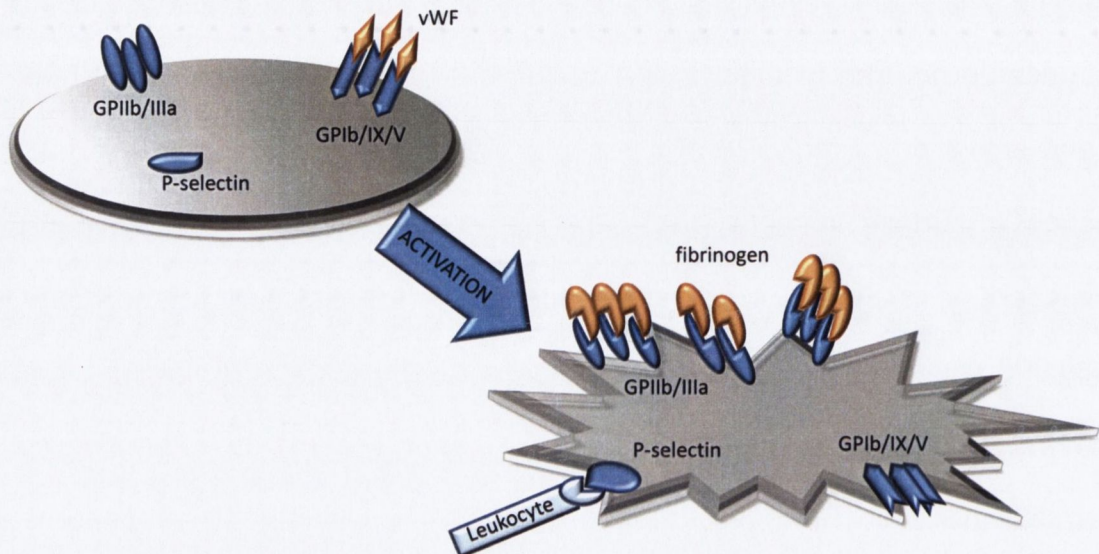


Figure 5: Platelet receptors

GPIb α mainly mediates adhesion by interacting with vWF. When platelets become activated, GPIIb/IIIa mainly mediates platelet aggregation by binding to fibrinogen. P-selectin upon translocation to the membrane surface mediates platelet-leukocyte interactions.

PLATELET AGGREGATION

After deposition of platelets on the exposed vWF and collagen, the next step is the recruitment of additional platelets to form the platelet aggregate. In order for platelets to accumulate on the initial platelet monolayer the activation of GPIIb/IIIa receptors is required to promote the interactions with adjacent platelets and fibrinogen. The recruitment of additional platelets is mediated by a variety of locally accumulating mediators that are produced or released once platelet adhesion has been initiated and some level of platelet activation through platelet adhesion receptors has occurred. These mediators include

ADP and TXA₂, which are secreted or released from activated platelets and thrombin, which is produced on the surface of activated platelets. These diffusible mediators act via G-protein-coupled receptors (GPCRs). G-proteins are centrally involved in the second phase of platelet-dependent thrombus formation. The mediators through the activation of G-protein-mediated signalling pathways can further increase their own formation and release, thus acting as a positive-feedback mechanism that amplifies the initial signals to ensure the rapid activation and recruitment of platelets into a growing thrombus. The activation of G-protein-coupled receptors stimulates phospholipase C (PLC), increases the cytosolic Ca⁺⁺ and causes activation of protein kinase C (PKC). This induces the reorganisation of the cytoskeleton and platelet shape change and suppresses the synthesis of cyclic adenosine monophosphate (cAMP) by inhibiting adenylyl cyclase (Michelson 2003).

Adenosine diphosphate (ADP)

Adenosine diphosphate is stored at high concentrations in δ -granules of platelets and is released upon platelet activation, although red cells are also able to release ADP at sites of vascular injury. Adenosine diphosphate interacts with two GPCRs in the platelet membrane, P2Y₁ and P2Y₁₂. Whereas P2Y₁ couples to G_q (Hechler, Leon et al. 1998) , P2Y₁₂ is coupled to G_i-type G proteins, in particular to G_{i2} (Jantzen, Gousset et al. 1999). The P2Y₁ receptors initiate aggregation through mobilization of calcium stores, whereas the P2Y₁₂ receptors coupled to adenylyl cyclase inhibition are essential for a full aggregation response to ADP and the stabilization of aggregates. However, co-activation of both, P2Y₁ and P2Y₁₂, seems to be required for optimal ADP-

induced aggregation and ADP-promoted thrombus growth (Gachet 2008). Interestingly, platelet responses to thrombin and TXA₂ at low and intermediate concentrations are reduced in the absence of ADP receptors (Fabre, Nguyen et al. 1999) underlining the important role of ADP as a positive-feedback mediator required for sustained platelet activation. The activation of ADP-platelet receptor increases intraplatelet Ca⁺⁺ concentrations and TXA₂ synthesis; induces protein phosphorylation, shape change, granule secretion and activation of GPIIb/IIIa leading to platelet aggregation (Rivera, Lozano et al. 2009).

The target of thienopyridine drugs such as ticlopidine, clopidogrel or prasugrel is the P2Y₁₂ receptor. These drugs are widely used in the prevention of vascular events in patients with cardiovascular disease (Barret, Jones et al. 2008). However, for *in vitro* studies of the ADP-platelet aggregation pathway apyrase (an ADP-scavenger) and 2-Methylthio-AMP triethylammonium salt hydrate (2-MeSAMP, a P2Y₁₂ specific receptor antagonist) are usually used (Jantzen, Gousset et al. 1999; Jurasz, Sawicki et al. 2001; Takasaki, Kamohara et al. 2001; Alonso-Escolano, Strongin et al. 2004; Medina, Jurasz et al. 2006) as thienopyridines are pro-drugs that require metabolic activation *in vivo*.

Eicosanoids (PGI₂ and TXA₂)

Eicosanoids are involved in many biological conditions, such as pain, fever, inflammatory reactions, and the stimulation and inhibition of platelet aggregation. They are products derived from the arachidonic acid metabolism by the action of different enzymes. Cyclooxygenases (COX) such as COX-1 and COX-2, also known as prostaglandin H synthases are expressed on the

luminal membrane of the endoplasmic reticulum. The catalytic domain of each enzyme contains two different catalytic sites, peroxidase and cyclooxygenase. The two reactions performed by COXs are the conversion of arachidonic acid to prostaglandins (PG) including PGG₂ by COX activity and the conversion of PGG₂ to PGH₂ by the peroxidase activity. COX-1 is the constitutively expressed form of the enzyme and it is found in high amounts in cells such as endothelial cells and platelets. In contrast, COX-2 is the inducible form of the enzyme that is responsible for a number of inflammatory reactions. PGH₂ is also converted to PGD₂, PGE₂, PGF_{2α}, prostacyclin and TXA₂ (**Figure 6**).

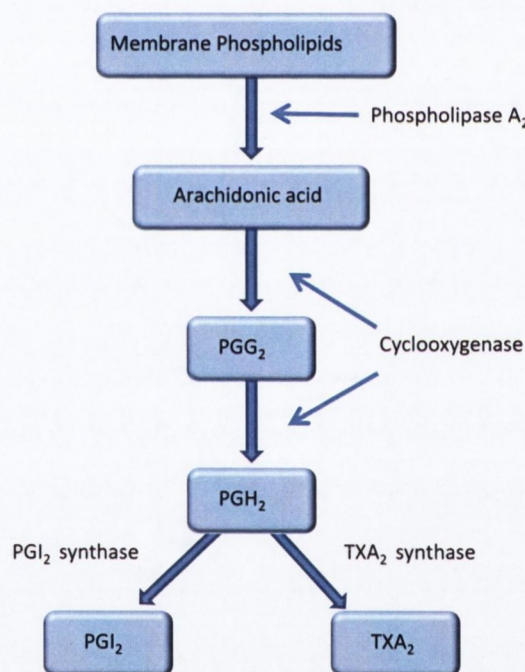


Figure 6: Metabolism of arachidonic acid to PGI₂ and TXA₂

Like ADP, TXA₂ functions as a positive-feedback mediator during platelet activation. **Thromboxane A₂** is an unstable (half-time in plasma less than 30 seconds) arachidonic acid metabolite synthesized by activated platelets through the actions of COX-1 and TXA₂ synthase. TXA₂ is a vasoconstrictor

and a potent platelet agonist that induces shape change, phosphoinositide hydrolysis, Ca^{++} mobilization, protein phosphorylation, secretion and subsequent aggregation. In endothelial cells, where prostacyclin synthase is present, arachidonic acid-synthesized cyclic endoperoxides are converted to prostacyclin, which is a vasodilator and a potent platelet inhibitor. The action of TXA_2 is locally restricted because of its short half-life. The TXA_2 receptor (TP), which is also activated by the prostaglandin endoperoxides PGG_2 and PGH_2 , couples to G_q and $\text{G}_{12}/\text{G}_{13}$ (Knezevic, Borg et al. 1993; Djellas, Manganello et al. 1999). The role of TP has been demonstrated in studies using platelets from TP-deficient animals which are unresponsive to TXA_2 (Nataraj, Thomas et al. 2001). TP-deficient mice have prolonged bleeding times and are unable to form stable thrombi (Thomas, Mannon et al. 1998).

Acetylsalicylic acid (ASA) suppresses platelet secretion by inhibiting COX in platelets and in vessel walls. This action results in reduced synthesis of TXA_2 in platelets and prostacyclin in the vessel wall. Since platelets lack the capacity for *de novo* protein synthesis, the inhibitory effects of ASA persist for the time necessary for the production of new platelets from megakaryocytes to take place. In contrast in the endothelium, the ASA-inactivated COX can be replaced by the *de novo* synthesized enzyme in approximately two days after administration of ASA. Therefore, ASA causes strong inhibition of TXA_2 formation in platelets and modest reduction of prostacyclin synthesis in endothelial cells (Dusting, Moncada et al. 1982).

G-Protein-Mediated Signalling Pathways

As mentioned before, both ADP and TXA₂ will recruit platelets into a growing thrombus by activating multiple G-protein-mediated signalling pathways to induce platelet-shape change and degranulation. ADP activates G_q and G_i through its receptors P2Y₁ and P2Y₁₂, whereas TXA₂ activates mainly G_q and G₁₂/G₁₃ via the TP. G₁₃ has been shown to activate the Rho/Rho-kinase-mediated pathway facilitating shape change. The G_q family will activate PLC which results in the formation of inositol trisphosphate (IP₃) and diacyl glycerol (DAG) leading to an elevation of free cytoplasmic calcium and activation of protein kinase C (PKC). G_i family inhibits adenylyl cyclase and also regulates phosphatidylinositol-3-kinases (PI3-Ks) facilitating aggregation and degranulation (Offermanns 2006) (**Figure 7**).

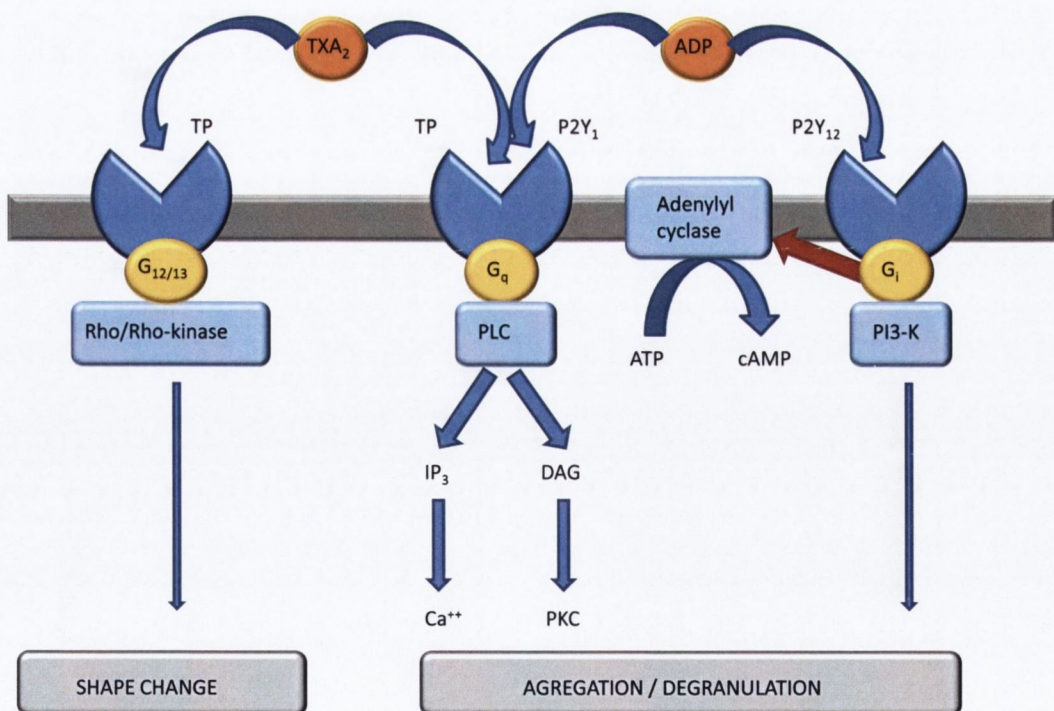


Figure 7: Signalling mechanisms linking the activation of GPCRs by ADP and TXA₂ to G-proteins

Matrix Metalloproteinases and their Inhibitors

Matrix metalloproteinases (MMPs) are a family of zinc- and calcium-dependent proteinases that are involved in the turnover of the extracellular matrix (ECM) of the connective tissue. These enzymes are capable of degrading most components of the ECM and mediate a large variety of biological processes including normal embryonic development and wound healing, as well as pathological processes such as cancer, atherosclerosis or other inflammatory disorders (Sternlicht and Werb 2001; Visse and Nagase 2003).

The MMP family can be divided into several groups based on their substrate specificity and/or structure. Structurally, all MMPs have basically a "pre" domain (N-terminal domain) that is followed by a propeptide ("pro" domain) and a catalytic domain that contains the zinc-binding region, which is essential for the catalytic activity. With some exceptions, like MMP-7, MMP-26 and MMP-23, all of them have a haemopexin/vitronectin-like domain that is connected to the catalytic site by a hinge region (Sternlicht and Werb 2001). Collagenases (MMP-1, -8, -13, and -18) have the ability to digest interstitial collagens of type I, II, and III. Gelatinases, both MMP-9 and MMP-2, degrade type IV collagen and gelatine. The stromelysins (MMP-3, -7, -10 and -11) have much broader substrate specificity and they can degrade a wide range of ECM components, including proteoglycans, type IV collagen, fibronectin, and laminin. These MMPs represent the secreted MMPs and they are produced as latent enzymes. Pro-MMPs bind specific ECM proteins and remain enzymatically inactive until the active catalytic enzyme is released. However, there is a subgroup of MMPs, known as membrane-type MMPs (MT-MMPs) that are not secreted, but remain attached to cell surfaces and mainly activate secreted MMPs. Therefore,

activation of a few select enzymes can initiate a cascade of proteolytic activity of many others. A clear example is the activation of MMP-2 at the cell surface by MT1-MMP by cleaving the MMP-2 pro-domain (Alonso-Escolano, Strongin et al. 2003; Visse and Nagase 2003).

Because MMPs may degrade the components of the ECM, a tight regulation of MMP activity is essential to prevent excessive matrix degradation. A group of endogenous proteins called tissue inhibitors of metalloproteinases (TIMP-1, -2, -3 and -4) regulate MMP activity. TIMPs bind to the active site of the MMPs, thus blocking access to ECM substrates.

In addition to MMPs, another family of proteins endowed with MMP activity are called ADAMs. This is a metalloproteinase-disintegrin family, which not only contains a MMP-like domain, but also a disintegrin region (**A Disintegrin And Metalloproteinase domain**). Approximately forty ADAMs have been identified to date, less than half of them contain a catalytic-site and only several of these proteins are catalytically active (Schlondorff and Blobel 1999; Seals and Courtneidge 2003; Blobel 2005).

It has been shown that platelet aggregation may be mediated via the release of MMP-2 from platelets in addition to TXA₂ (Needleman, Moncada et al. 1976) and ADP (Born 1962). Furthermore, MMP-2 is translocated to the platelet surface during aggregation and it may interact with cell surface proteins and receptors (Sawicki, Salas et al. 1997). Indeed, human recombinant MMP-2 increases GPIIb α levels in platelets adhering to vWF (Radomski, Stewart et al. 2001) and it was suggested that the release of platelet MMP-2 may be associated with binding of platelets to fibrinogen (Martinez, Salas et al. 2001). Interestingly, the proteolytic activation of proMMP-2 to MMP-2 may be

mediated by MT1-MMP on the platelet surface upon activation (Kazes, Elalamy et al. 2000). In addition, MMP-2 amplifies the pro-aggregatory effects of different agonists showing that the enzyme may be involved in facilitation of platelet activation at the level of second messenger system generated during phosphoinositide breakdown (Falcinelli, Guglielmini et al. 2005). MMP-2 is also released from platelets in vivo in humans at a localised site of vessel wall damage in amounts sufficient to potentiate platelet aggregation (Falcinelli, Giannini et al. 2007). All these data show that MMP-2 may be involved in transmission of inside-out and outside-in signaling. Finally, MMP-2 also participates in the interactions between cancer cells and platelets supporting haemotogenous cancer cell metastasis and invasion (Jurasz, Sawicki et al. 2001; Jurasz, North et al. 2003; Alonso-Escolano, Strongin et al. 2004; Jurasz, Alonso-Escolano et al. 2004; Alonso-Escolano, Medina et al. 2006; Medina, Jurasz et al. 2006).

MMP-9 may counteract the pro-aggregatory effect of MMP-2 (Fernandez-Patron, Martinez-Cuesta et al. 1999). This enzyme inhibits the activation of PLC, via the formation of NO and cyclic guanosine monophosphate (cGMP) in human platelets, resulting in inhibition of platelet aggregation (Sheu, Fong et al. 2004). MMP-1 has been shown to increase the number of tyrosine-phosphorylated proteins in platelets and to stimulate trafficking of β_3 integrins to cell contact places. In contrast, MMP-3 does not seem to play any role in platelet function (Galt, Lindemann et al. 2002). ADAM-10 has been also identified in platelets (Colciaghi, Borroni et al. 2002) and its actions on platelets may depend upon cleavage of GPVI that binds collagen (Gardiner, Shen et al. 2007). ADAM-17 (TNF- α converting enzyme, TACE) has been implicated in the

proteolytic cleavage (shedding) of glycoprotein platelet receptors including GPIIb/IIIa (Bergmeier, Piffath et al. 2004) and GPVI (Rabie, Strehl et al. 2005). ADAMTS-13, has been identified as von-Willebrand Factor-cleaving proteinase (Fujikawa, Suzuki et al. 2001).

TIMP-4 appears to be the major intraplatelet endogenous MMP inhibitor. This inhibitor co-localizes with MMP-2 in resting platelets suggesting that TIMP-4 is in complex with MMP-2. Although upon aggregation MMP-2 is translocated to the platelet surface (Sawicki, Sanders et al. 1998), TIMP-4 is not detectable but it is released (Radomski, Jurasz et al. 2002). Hence, the dissociation of TIMP-4 from its complex with MMP-2 may facilitate the interactions of MMP-2 with its receptors and stimulate aggregation. TIMP-2 has been also detected in platelets (Murata, Yamashita et al. 1997). TIMP-2 contributes to the activation of pro-MMP-2 as a trimolecular complex (MT1-MMP/TIMP-2/pro-MMP-2) on the platelet surface. However, when TIMP-2 is over-expressed it binds to MT1-MMP preventing the activation of MMP-2 by the action of free MT1-MMP (Kazes, Elalamy et al. 2000) (**Figure 8**).

A number of synthetic agents inhibit the actions of MMPs. These include such compounds as o-phenanthroline, doxycycline, Batimastat[®], and Marimastat[®]. Ortho-phenanthroline (phenanthroline) is a synthetic inhibitor limited in use to the laboratory. Batimastat and Marimastat have been used in clinical trials to treat advanced cancers, but they did not show any beneficial effect (Santos-Martinez, Medina et al. 2008). This therapeutic failure could be due to a lack of selectivity (for example MMP-2 selective inhibitors are yet to be developed) and/or low efficacy *in vivo* (Pirard 2007). As MMP-2-dependent signalling in platelets is aspirin-insensitive (Sawicki, Salas et al. 1997; Radomski, Stewart et

al. 2001; Chung, Jurasz et al. 2002; Falcinelli, Giannini et al. 2007) the development of selective inhibitors of this enzyme deserves consideration.

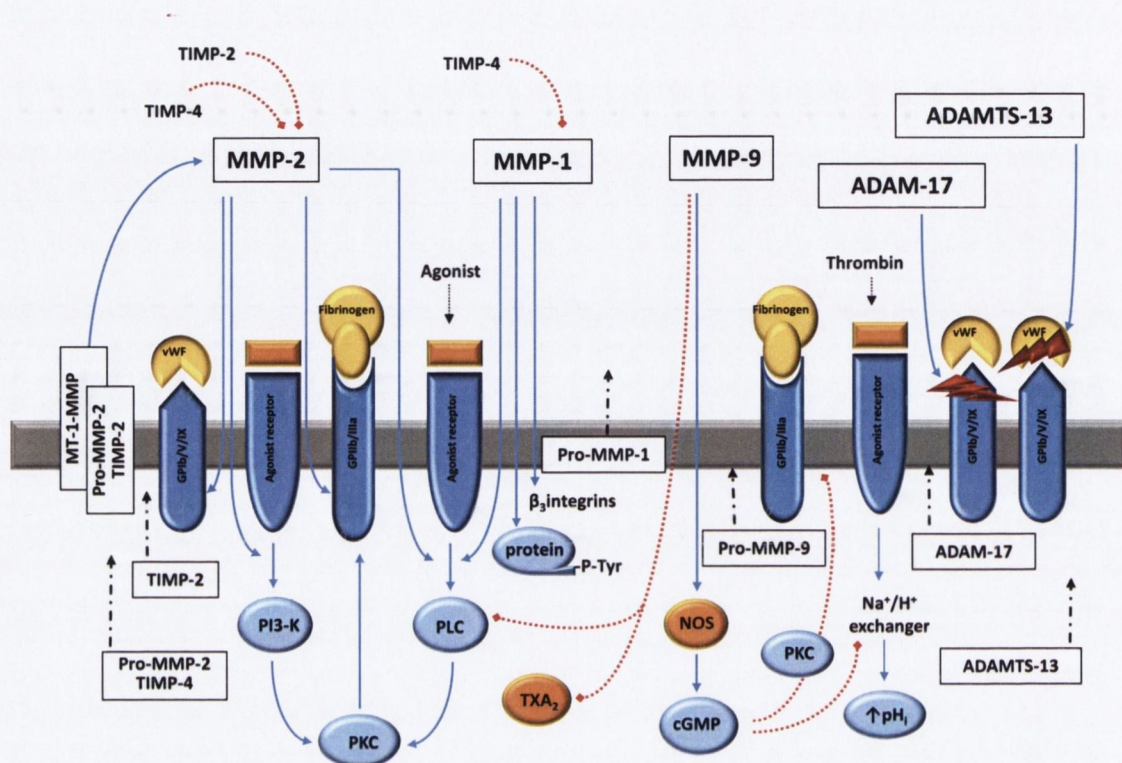



Figure 8: Mechanisms of action of MMPs, ADAMs, ADAMTS and TIMPs on platelets

TIMP-4 acts as a major intraplatelet TIMP regulating the activity of MMPs. MMP-2 amplifies the proaggregatory effects of different agonists via PLC and PI3-K activation, thus modifying GPIIb/IIIa and GPIb/V/IX function. MMP-1 induces tyrosine phosphorylation of intracellular proteins, redistributes β_3 integrins and also primes platelets for aggregation. In contrast, MMP-9 inhibits platelet aggregation by down-regulation of the activation of PLC and TXA_2 formation. This effect of MMP-9 may be dependent upon activation of the NO-cGMP system in platelets. MT1-MMP participates in the activation of MMP-2 via the trimolecular complex. ADAM-17 and ADAMTS-13 are implicated in the proteolytic cleavage of subunits GPIIb α -GPV and vWF, respectively. P-Tyr: tyrosine phosphorylation; pH_i: intracellular pH. Blue lines: activation, red lines: inhibition, black lines: release,  cleavage (adapted from Santos-Martinez et al. 2008)

PLATELETS AND ENDOTHELIUM

The laminar flow profile in the microvasculature results in lateral displacement forces that allow red blood cells to push leukocytes and platelets toward the vessel wall. In principle, platelets only adhere to the vessel wall when the endothelial integrity is disrupted. Endothelial cells, that coat the entire vascular system, play an essential role in the balance between activation and inhibition of the haemostatic system. An intact and healthy endothelium prevents the attachment of platelets and the proteins involved in the initiation of coagulation and platelet aggregation. For this purpose endothelial cells generate and release **nitric oxide** and **prostacyclin**, the two most potent soluble inhibitors of platelet adhesion and aggregation. Prostacyclin and NO, released by the vascular endothelium, synergize with each other in order to inhibit platelet aggregation (Radomski, Palmer et al. 1987a). Prostacyclin and NO stimulate the activity of adenylyl cyclase and guanylyl cyclase and this stimulation results in an increase of intracellular cAMP and cGMP levels, respectively (Moncada, Gryglewski et al. 1976; Best, Martin et al. 1977; Radomski, Palmer et al. 1987b; Gerzer, Karrenbrock et al. 1988). The down-stream signalling include cAMP-dependent protein kinases (PKA), cGMP-dependent protein kinases (PKG), cGMP-gated channels and cAMP-gated channel (Radomski and Moncada 1993). Human platelets contain very high concentrations of PKA and PKG, and selective stimulation of either PKA or PKG correlates with inhibition of platelet activation and aggregation. In addition to inhibition of GPIIb/IIIa activation and fibrinogen binding, the mechanism of PKA- and PKG-mediated platelet regulation involves decreased actin polymerization and myosin light chain kinase activity. Furthermore, there is a reduction of intracellular Ca^{++} via

inhibition of intracellular and plasmalemmal calcium channels and activation of intracellular and plasmalemmal calcium pumps (Jurasz, Radomski et al. 2000). Moreover, it has been shown that GPIb/IX/V can be modified by the phosphorylation of Ser166 by cAMP-dependent kinase (Wyler, Bienz et al. 1986) that is activated by prostacyclin.

Moreover, endothelial cells also express high levels of **CD39**, an ADPase which degrades ADP released from erythrocytes and aggregating platelets as another factor that contributes to the maintenance of platelet haemostasis in physiological conditions (Michelson 2003; Watson 2009). However, platelets can bind to the intact endothelium in inflammatory states. This happens because in inflammation the inhibitory mechanisms described above are impaired and because cytokine-inducible adhesion molecules can be expressed on the surfaces of activated endothelial cells that activate platelets. Moreover, activated endothelial cells can release, from storage granules called Weibel-Palade bodies, vWF and P-selectin, both of them ligands for GPIb α on platelets (Chen and Lopez 2005).

Nitric oxide is a potent regulator of platelet function and is generated for both, endothelial cells and platelets (Radomski, Palmer et al. 1987c; Radomski, Palmer et al. 1990a). When originally described it was named as endothelium-derived relaxing factor (EDRF) because it was found to be an unstable humoral substance released from vascular endothelium capable of mediating the action of endothelium-dependent vasodilators (Furchgott and Zawadzki 1980). Further work from Moncada's and Ignarro's groups identified EDRF as NO (Ignarro, Buga et al. 1987; Palmer, Ferrige et al. 1987). Nitric oxide is generated from L-

arginine and oxygen by the action of the NO synthase (NOS) enzymes (**figure 9**). At present, three isoforms of this enzyme have been cloned: endothelial NOS (eNOS, NOS-3), neuronal NOS (nNOS, NOS-1), and cytokine-inducible NOS (iNOS, NOS-2). Despite its very short half-life NO diffuses freely across membranes, ideal attributes for a paracrine and autocrine signalling molecule. Indeed, NO is considered one of the most important messenger molecules involved in many physiological and pathological processes known to date (**figure 9**).

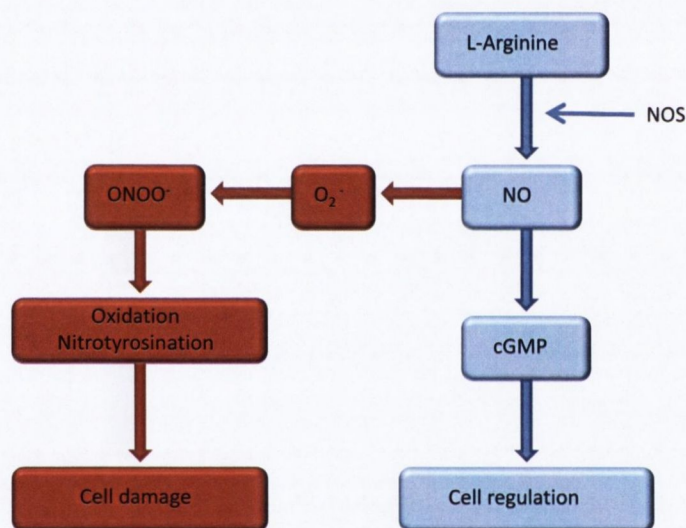


Figure 9: Nitric oxide functions

Nitric oxide is synthesized from L-Arginine by the action of the enzyme NO synthase (NOS). Nitric oxide may then act in a cGMP-dependent manner regulating cell functions or -independent manner generating peroxynitrate (ONOO⁻) leading to cell damage.

Nitric oxide plays an important role in the modulation of vascular homeostasis. When generated by endothelial cells NO not only diffuses to vascular smooth muscle cells resulting in vasodilatation through a cGMP-dependended mechanism (Garg and Hassid 1989) but also reaches the vascular lumen inhibiting platelet

adhesion, aggregation and causing dissipation of preformed aggregates (disaggregation). Nitric oxide is an effective inhibitor of platelet adhesion to the endothelium and components of the extracellular matrix such as collagen, fibrinogen and vWF and therefore, a potent inhibitor of platelet aggregation and inducer of disaggregation (Radomski, Palmer et al. 1987a; Radomski, Palmer et al. 1987b; Radomski, Palmer et al. 1987c; Salas, Moro et al. 1994; Radomski, Stewart et al. 2001). In addition, platelets can also synthesize NO and as a result have the ability to regulate platelet aggregation (Radomski, Palmer et al. 1990a; Radomski, Palmer et al. 1990b). In fact, the release of NO from washed platelets during aggregation with collagen was measured with the use of a microsensors (Malinski, Radomski et al. 1993) The platelet actions of NO are also mediated by cGMP-dependent mechanism (Radomski, Palmer et al. 1987; Moro, Russel et al. 1996) (**figure 10**).

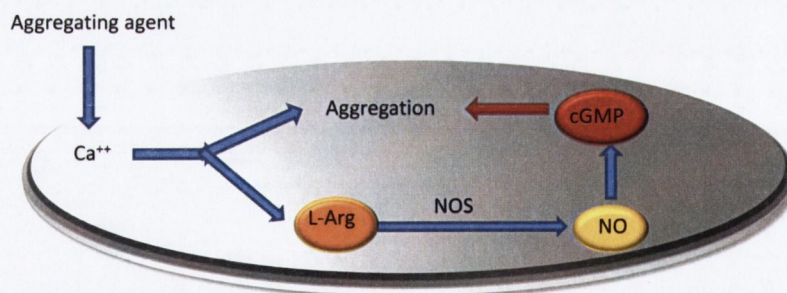


Figure 10: Platelet actions of nitric oxide

In platelets, NO acts in a cGMP-dependent manner inhibiting platelet aggregation. Blue arrows correspond to activation actions and red arrows to inhibitory actions.

To study inhibition of platelet function, NO donors such as S-nitroso-N-acetyl-DL-penicillamine (SNAP), a pharmacological agent and S-nitrosoglutathione (GSNO), an endogenous inhibitor, have been widely used in *in vitro* studies (Radomski, Rees et al. 1992; Salas, Moro et al. 1994; Jurasz, Sawicki et al. 2001).

Prostacyclin is the most potent endogenous inhibitor of the interactions between platelets and the vessel wall. Prostacyclin is synthesized from PGH_2 by the action of the PGI_2 synthase. Prostacyclin is released by vascular endothelial cells and acts as a potent vasodilator, inhibitor of platelet aggregation (anti-thrombotic actions), and modulator of vascular smooth muscle cell proliferation-migration-differentiation (anti-atherosclerotic actions). Indeed, multiple lines of evidence suggest that prostacyclin protects from cardiovascular disease by pleiotropic effects on vascular smooth muscle (Fetalvero KM, Martin KA et al. 2007). Animal studies using prostacyclin receptor knock-out (IP^{-/-}) mice have revealed increased predisposition of these animals to thrombosis, intimal hyperplasia, atherosclerosis, restenosis, as well as reperfusion injury (Cheng 2006). Of additional importance has been the world-wide withdrawal of selective COX-2 inhibitors, due to their discriminating suppression of COX-2-derived-prostacyclin and its cardioprotective effects, leading to increased cardiovascular events, including myocardial infarction and thrombotic stroke.

The actions of PGI_2 are mediated via a seven transmembrane-spanning G-protein coupled receptor (GPCR), known as the human prostacyclin receptor or hIP (Armstrong R 1996). The G-protein then activates adenylate cyclase which

converts ATP into cAMP. Inhibition of platelet aggregation by prostacyclin is mediated by cAMP-dependent mechanism. However, prostacyclin has also been shown to promote vascular smooth muscle cell differentiation at the level of gene expression through the Gs/cAMP/PKA pathway (Fetalvero KM, Martin KA et al. 2007).

Therefore, in vascular haemostasis there are several control mechanisms to limit and break down clots that are not needed. These mechanisms involve, among others, platelet inhibitors and activators as discussed above allowing these cell elements to flow in non-activated state in the vascular system.

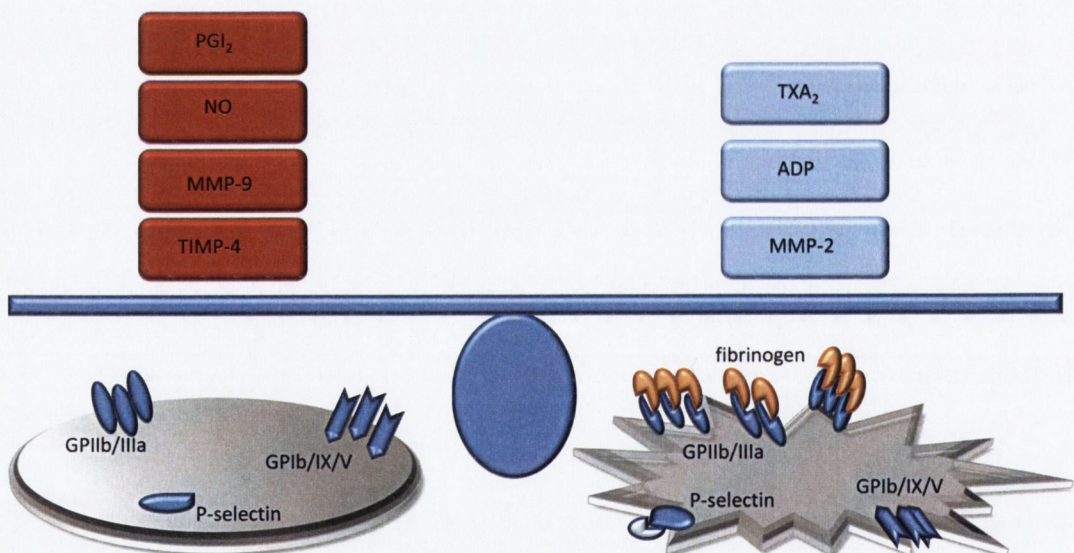


Figure 11: Platelet inhibitors and activators

In physiological conditions, there is a balance between platelet inhibitors (in red) and activators (in blue).

PLATELETS AND BLOOD FLOW

Platelet adhesion to sites of vascular injury is a crucial and initial step in haemostasis and thrombosis. For a platelet to become irreversibly attached to the blood vessel wall, the binding should be strong enough to resist the dispersive haemodynamic forces generated by the blood flow. The two parameters most commonly used to describe the blood flow are shear rate γ and shear stress τ . Shear stress is considered as the most relevant mechanical force to platelet-mediated haemostasis and thrombosis. In fact, it is widely recognized that high shear stress activates platelets (Kroll, Hellums et al. 1996; Turitto and Hall 1998) although it has been also demonstrated that low shear stress can also increase platelet adhesion to the venular wall (Russell, Cooper et al. 2003).

Laminar blood flow is characterized by the presence of blood layers flowing past each other at different velocities (**figure 12**). Shear rate (s^{-1}) is a measure of how rapid fluid layers are flowing past each other and it depends basically on flow rate Q (mL/min) and geometry of the vessel. Physiological shear rates are lowest in large veins ($<50 \text{ s}^{-1}$), increasing gradually, as the diameter of the vessel decreases, to about $1,500 \text{ s}^{-1}$ in arterioles. Shear stress is defined as the force per unit area (dynes/cm^2) between lamina or the force that fluid applies on adjacent stream fluid lamina (Kroll, Hellums et al. 1996; Sakariassen, Hanson et al. 2001). In the flow environment of the arterial circuit, blood is considered as a suspension that behaves as a Newtonian fluid (Turitto 1982) and for a Newtonian fluid, the relationship between shear stress and shear rate is given by the formula: shear rate $\gamma = \text{shear stress } \tau / \text{viscosity } \eta$. Obviously, shear rates and shear stresses change continuously due to

modifications in the architecture of the vessel (for example, thrombus formation) and the corresponding change in local blood flow rate. On the other hand, the viscosity of the blood also changes with local shear rate, as flow rate and shear rate increase, blood viscosity decreases (Zwaginga, Sakariassen et al. 2006). Knowing the viscosity of the blood, the diameter of the vessel and the local flow rate, the shear stress can be calculated. In humans the typical ranges of shear stresses in the vasculature vary from 1-8 dynes/cm² in veins to 20-30 dynes/cm² in arteries and over 350 dynes/cm² in stenotic vessels (Kroll, Hellums et al. 1996). The range of shear stresses over which platelet adhesion and aggregation are observed are around 1-200 dynes/cm² (Kroll, Hellums et al. 1996).

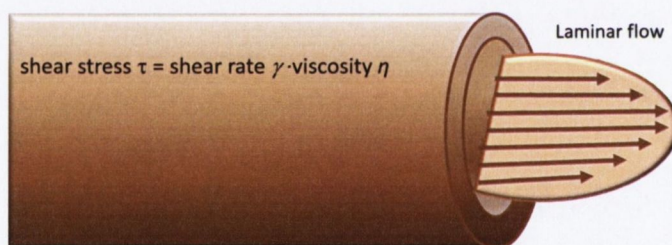


Figure 12: Laminar flow rate in blood vessels

Shear stress is defined as the force per unit area between lamina or the force that fluid applies on adjacent stream fluid lamina. As blood is considered a suspension that behaves as a Newtonian fluid, shear rate $\gamma = \text{shear stress } \tau / \text{viscosity } \eta$.

At very low shear stress, basically used in routine aggregometry, different agonists can activate platelets leading to a conformational change of GPIIb/IIIa receptor that result in binding of fibrinogen and platelet aggregation. However, under conditions of high shear stress ($>30 \text{ dynes/cm}^2$), vWF present in plasma,

or released from α -granules, mediates platelet aggregation mainly via GPIb and GPIIb/IIIa receptors (Ikeda, Handa et al. 1991; Konstantopoulos, Kukreti et al. 1998). In fact, in plasma and under static conditions, vWF binding to the GPIIb/IIIa is minimal (Schullek, Jordan et al. 1984). However, when high shear stresses are applied to platelets, vWF binds to GPIIb/IIIa receptor as well as to the GPIb/IX/V complex, and this binding contributes significantly to direct shear-induced platelet aggregate formation (Kroll, Hellums et al. 1996). In addition, pathological shear stresses also cause the release of ADP from dense granules which has been shown to be associated with high shear stress-mediated platelet activation and subsequent aggregation (Frojmovic, Nash et al. 2002).

IN VITRO METHODS FOR MEASUREMENT OF PLATELET ACTIVATION

To date, different antiplatelet drugs such as aspirin, clopidogrel, prostacyclin, and fibrinogen and thrombin receptor antagonists have been tested to prevent the development or recurrence of thrombotic diseases of the coronary and cerebrovascular circulation with various effectiveness (Maree and Fitzgerald 2007). To improve the therapy of arterial thrombotic disorders and identify novel therapeutic targets it is imperative to study basic mechanisms of platelet thrombus formation. Any potential pharmacological leads thus identified need to be tested under conditions similar or identical to those of blood flow. In fact, the ideal situation to study blood platelet-dependent haemostasis and thrombosis would be using devices that could simulate flow conditions encountered in the vasculature, in other words, the *in vitro* reconstitution of the components of Virchow's triad.

There was little research in arterial thrombosis and relatively little understanding of platelet function before 1960. In 1962, Born developed a simple method for studying the response of platelets to chemical agonists (Born 1962). The method recorded changes in light transmission of a stirred platelet suspension exposed to a platelet agonist when platelet aggregates were forming. This device (commonly called **light aggregometer**) had a profound effect on the study of platelet reactions, and it rapidly came into routine and used worldwide (Kroll, Hellums et al. 1996). Almost two decades later, another novel device to assess platelet function was developed. The new instrument, called **electronic aggregometer** was similar to light aggregometer, but, rather than light transmission, it measured the increase in electrical impedance across

two metal wires that results from platelet aggregation in anticoagulated whole blood (Cardinal and Flower 1980).

Rapid platelet function analyzer (RPFA) is a point-of-care instrument designed to measure the effects of antiplatelet therapy. It is a fully automated platelet aggregometer originally developed to monitor GPIIb/IIIa antagonists within a self-contained cartridge (containing a platelet activator and fibrinogen-coated beads) (Smith, Steinhubl et al. 1999). It features three different cartridges to assess the level of inhibition of platelet aggregation, monitored by light transmission, achieved by aspirin, P2Y₁₂ antagonists or GPIIb/IIIa inhibitors, but not their combination (Zwaginga, Sakariassen et al. 2006).

Light aggregometer has been considered as the historical gold standard of platelet function testing. In fact, it is possible to obtain a large amount of information about many different aspects of platelet function adding a set of agonists to stirred platelets (Harrison, Frelinger et al. 2007). Because platelets are stirred to maintain them in suspension, platelet-platelet interactions in the aggregometer take place under the influence of fluid mechanical shear stress. However, the shear stress varies throughout the stirred platelet suspension and does not mimic flow and shear rates encountered in arterial circulation (Kroll, Hellums et al. 1996). Moreover, platelets are stirred under low shear conditions and only form aggregates after addition of agonists, conditions which do not accurately mimic platelet adhesion, activation and aggregation upon vessel wall damage (Harrison, Frelinger et al. 2007). In addition, the conventional light transmission methods quantifying platelet aggregation have not been sufficiently sensitive to detect micro-aggregates (Pedvis L.G., Wong T. et al. 1988).

A number of different devices have been developed in order to mimic, as close as possible, the processes that take place during vessel wall damage.

Cone and plate analyzer, involves a cone rotating on a plate that generates a controlled shear stress (from less than 2 dynes/cm² to greater than 200 dynes/cm²) allowing the study of the kinetics of aggregate formation. Cell suspensions are placed between the plate, on the bottom, and the upper cone that rotates inducing a constant uniform shear stress. It is considered one of the instruments of choice (the another one is the coaxial cylinder Couette) for studying the effects of bulk shear stress on cellular function (Konstantopoulos, Kukreti et al. 1998). In addition, the imaging of platelet adhesion and aggregation to the plate coated with collagen or extracellular matrix (ECM) can be also investigated (Zwaginga, Sakariassen et al. 2006).

Platelet function analyzer 100 (PFA-100) creates an artificial vessel consisting of a sample reservoir, a capillary and a biologically active membrane with a central aperture (collagen-epinephrine-coated or collagen-ADP-coated). The sample is aspirated from the reservoir at high shear rates (5,000-6,000 s⁻¹) through the capillary and the aperture applying a negative pressure, mimicking in this way the resistance and the injured part of a small artery, and the time necessary for a platelet plug to occlude the aperture is monitored (Kundu, Heilmann et al. 1995). However, it has been demonstrated that this method has limited sensitivity and specificity (Hayward, Harrison et al. 2006; Podda, Bucciarelli et al. 2007).

Coaxial cylinder Couette device was originally invented for studies of viscosity and biological particle suspensions in controlled flow and later on adapted to measurements of platelet function (Xia and Frojmovic 1994). It consists of two coaxial cylindrical chambers separated by a gap where controlled rotation of the inner cylinder generates the desired shear rates (100-8,000 s⁻¹). Using this device sampling of micro-volumes of platelets for further analysis such as flow cytometry is also possible (Frojmovic 2008).

The *in vitro* studies of coagulation-dependent thrombus formation can be also performed using **perfusion chambers**. The most widely employed are the annular perfusion chambers and the parallel-plate perfusion chambers (Zwaginga, Sakariassen et al. 2006).

Annular perfusion chamber, developed by Baumgartner (Baumgartner and Haudenschild 1972), was the first successful and large-scale used *in vitro* device of thrombus formation. In this model, a segment of a vessel is everted and mounted centrally on a bar that is surrounded by an outer cylinder. By varying the flow rate or the distance between the subendothelial surface and the inner wall of the cylinder, the shear rate at the subendothelial surface goes from 50 to 3,300 s⁻¹ (Sakariassen, Hanson et al. 2001).

Parallel plate perfusion chamber was developed by Sakariassen (Sakariassen, Muggli et al. 1989). Similar to the annular chamber, it consists of a rectangular flow channel coated with components capable of inducing thrombus formation. It provides a controlled and well-defined flow environment (Konstantopoulos, Kukreti et al. 1998). Modifying the flow rate or the height

and/or the width of the chamber shear rates vary from 50 to 10,500 s⁻¹ (Sakariassen, Hanson et al. 2001). New generation of perfusion chambers such as miniature parallel-plate perfusion chamber (low flow rate perfusion) or parallel-plate perfusion chambers with stenosis have been also developed in the last decade. However, platelet function measurements using flow-mimicking devices or point-of-care instruments have limited sensitivity, specificity and do not correlate well with the aggregometer that because of lack of better methodology still remains “gold standard” of platelet function testing.

QUARTZ CRYSTAL MICROBALANCE WITH DISSIPATION (QCM-D)

The traditional Quartz Crystal Microbalance (QCM) has been used for very long time to analyze mass changes on rigid surfaces. The principle of analysis of QCM is based on the resonance frequency of a quartz crystal induced by applying an alternating electric field across the crystal. An increase in mass bound to the quartz surface causes the crystal's oscillation frequency f to decrease (negative f shift). It has been shown that for small amounts of mass (compared to the mass of the crystal) and for rigid, evenly distributed, and sufficiently thin adsorbed layers f is proportional to the mass. In this way, the QCM operates as a very sensitive balance and the mass of the adhering layer can be calculated using the Sauerbrey relation with nanogram sensitivity (Sauerbrey 1959).

$$\Delta m = - C \Delta f / n$$

Δm changes in mass Δf changes in frequency $C = 17.7 \text{ ng Hz}^{-1} \text{ cm}^{-2}$ for a 5 MHz quartz crystal $n = 1,3,5,7$ is the overtone number

However, a soft or very thick layer bound to the crystal will result in a high dissipation shift. In this particular case the Sauerbrey relationship underestimates the mass (Hook, Rodahl et al. 1998). A soft film dampens the crystal's oscillation and the damping or energy dissipation D of the crystal's oscillation reveals the film's elasticity. In fact, measuring D , the viscoelasticity of the adsorbed layer can be characterized, something that it is not possible just evaluating the changes in f . Indeed, a low D shift is a representative feature of rigid films, however soft and/or thick films induce a high D shift. Therefore, the combined information from simultaneously recorded changes in f and D is superior to f measurements alone (Fredriksson, Kihlman et al. 1998). Using a

Quartz Crystal Microbalance with Dissipation (QCM-D) such as Q-Sense™ E₄, both parameters, f and D , can be monitored simultaneously and in real-time. This feature makes the technique as a powerful tool to study viscoelastic monolayers (**figure 13** and **figure 14**).

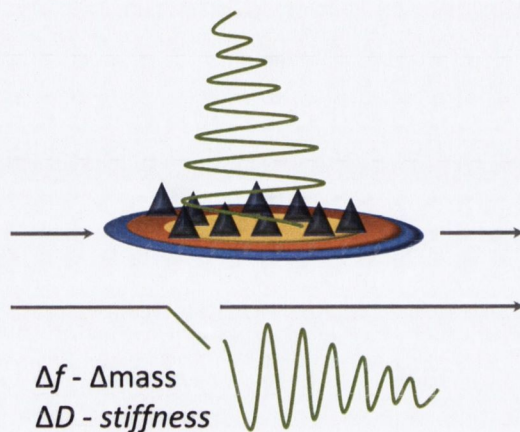


Figure 13: Effects of nm films on f and D of a quartz crystal

Changes in f (Δf) are proportional to mass, changes in D (ΔD) to stiffness. Adapted from: www.q-sense.com.

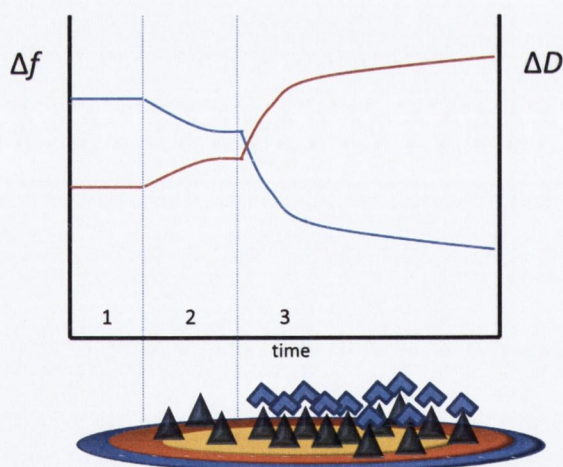


Figure 14: Effects of molecules on f and D of a quartz crystal

The blue line corresponds with changes in f (Δf) and the red line with changes in D (ΔD). 1. Baseline. 2. Binding of a small molecule induces decrease in f and increase in D . 3. Binding of a larger molecule forms a thicker and softer layer and induces a higher f and D shifts. Adapted from: www.q-sense.com.

In addition, if the adsorbed layer is assumed to be uniform across the crystal, it is possible, using the analyzing software QTools, to perform a modelling of the raw data from the acquisition Q-Sense software (QSoft) and calculate the thickness and accumulation of mass. In this case the mass is estimated combining and fitting f and D measurements at three overtones and using a Voigt-based viscoelastic model included in the software (Voinova, Rodahl et al. 1999). In fact, using Q-SenseTM E₄ the formation of thin films (nm) of different biological materials such as proteins or cells onto the crystal surface have been already characterized during the last two decades (Marx 2003; Dixon 2008).

AIMS OF PROJECT

The **general objective** of my research was to develop a novel, sensitive, quantitative and working in nanoscale method for testing platelet function under flow conditions in research and clinical studies.

Specific aims:

- 1) The characterization of platelet aggregation using a commercially available nanoscale resolution device, the Quartz Crystal Microbalance with Dissipation, Q-Sense™ E₄.
- 2) To test the pharmacological effects of antiplatelet agents as measured by the device.

MATERIALS AND METHODS

REAGENTS

All reagents were purchased from Sigma-Aldrich (Dublin, Ireland) unless otherwise indicated. Collagen was obtained from Chronolog (Lab Medics, UK).

BLOOD COLLECTION AND PLATELET ISOLATION

Blood was collected from healthy volunteers who had not taken any drugs known to affect platelet function for at least 14 days prior to the study. Platelet-rich plasma was prepared from blood as previously described (Radomski and Moncada 1983). Afterwards, PRP was diluted with Phosphate Buffered Saline (PBS) at final concentrations of 50,000; 100,000; 150,000 and 210,000 platelets/ μ L. In addition, platelet-poor plasma (PPP) was also used as control.

Q-SENSE™ E₄

The Q-Sense™ E₄ system (Q-Sense AB, Sweden) has four temperature and flow controlled modules set up in parallel configuration. The heart of the system is a quartz crystal sensor that it is placed in a chamber inside the module. Each chamber/flow module has an inlet and outlet. Platelets are perfused using a peristaltic microflow system (ISMATEC, IMS 935).

COMPONENTS OF Q-SENSE™ E₄ SYSTEM

- a) **Sensor crystal:** it is the sensing element itself. It is a 5MHz sensor crystal that consists of a thin disc of quartz sandwiched between two metal electrodes (**figure 15**).

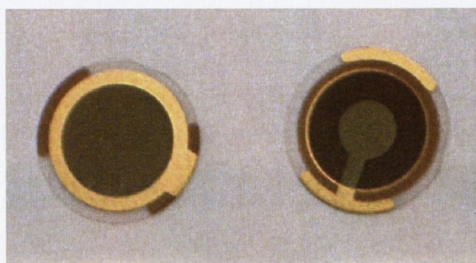


Figure 15: Crystal sensor

Photograph of a gold crystal sensor. On the right, the back side of the sensor, on the left, the active measurement side.

The measurement surface of the sensor is gold, although it can be coated with different materials such as polystyrene. Gold and polystyrene-coated (PL) quartz crystals have been used as sensors for the development of the method. For the polystyrene coating gold crystals were coated with a 0.5% solution of polystyrene in toluene using a spin coater (WS-400BX-6NPP/LITE, Laurell Technology, UK) at 6,000 rpm for 15 seconds.

- b) **Flow module** (QFM₄₀₁): each flow module holds one sensor crystal. They can be easily detached from the chamber platform and disassemble for cleaning. They can be heated/cooled to the set temperature of the chamber platform and they have an inlet and outlet (**figure 16**).

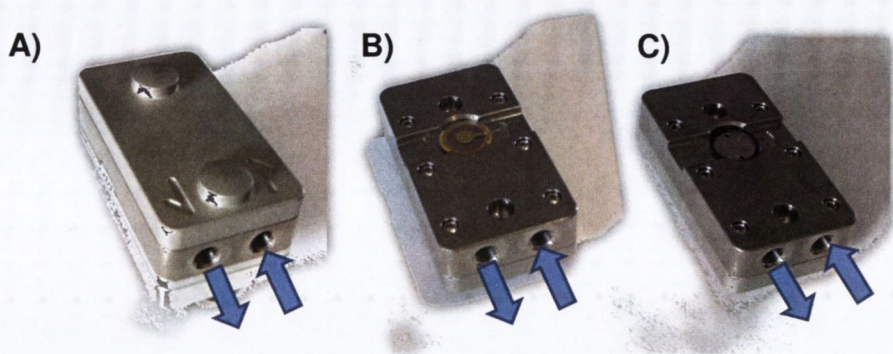


Figure 16: Flow module

A photograph of a single flow module (A) where the blue arrows correspond to the inlet and outlet. Details of the unlocked module (B) with a sensor placed in the chamber (C).

When the sample flows through the inlet it passes through a snake-shaped path, where the temperature becomes stable before entering the chamber where the crystal sensor is placed (**figure 17**).

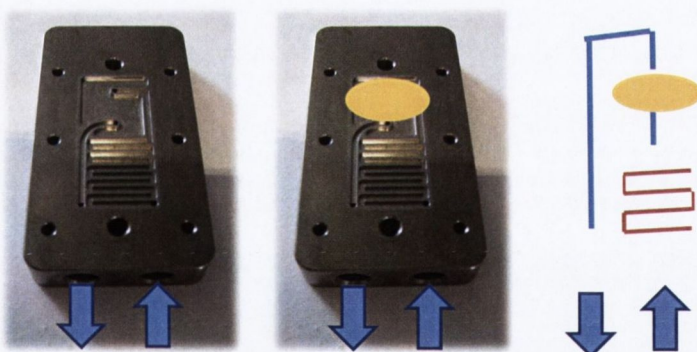


Figure 17: Flow module

A schematic representation of flow module and sensor. The snake-shaped path inside the module allows the stabilisation of the temperature before it reaches the sensor placed in the chamber.

c) Chamber platform (QCP₄₀₁): it is the stand for the flow modules. The platform can hold four modules. The modules are connected with PTFE tubing, to perform the experiments, in parallel configuration. Under the

flow module box file there is a thermoelectric device that controls the temperature environment (**figure 18**).

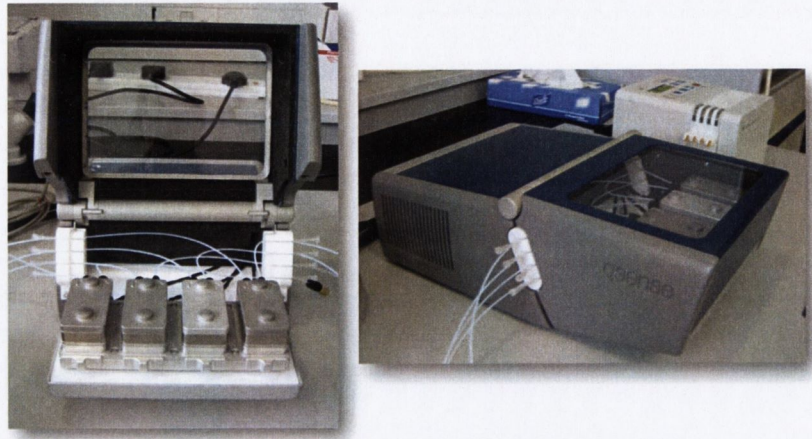


Figure 18: Chamber platform

A photograph of the chamber platform. The modules used in our experiments connected in parallel configuration and inserted in the chamber platform are shown on the photograph.

d) Electronics unit (QE₄₀₁): it is connected with the chamber platform and the computer. It is the unit where the signals are generated and the data is collected before being sent to the computer (**figure 19**).

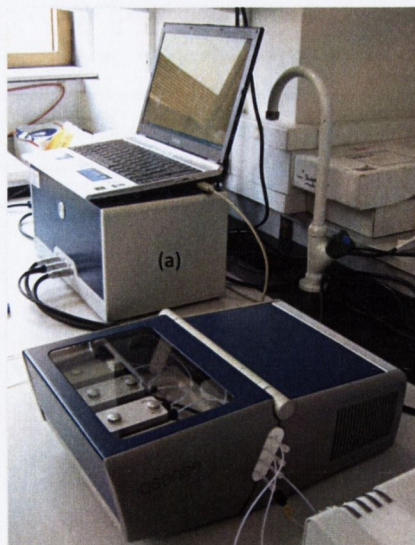


Figure 19: Electronics unit

A photograph of device used in our experiments. The electronics unit (a) connected with the chamber platform and the computer is shown.

- e) **Peristaltic microflow system** (ISMATEC, IMS 935): it is a four-channel digital peristaltic pump that allows a controlled flow rate perfusion from 0 to 1,000 $\mu\text{L}/\text{minute}$ through the system (**figure 20**).
- f) **Block-Heating-System** (Grant QBD1, Grant instruments, UK): it allows a controlled temperature range for the samples before being perfused (**figure 20**).



Figure 20: Q-Sense™ E₄ system

A photograph of system used in our experiments. Samples are kept at 37 °C using a block-heating-system (a) and perfused using a peristaltic pump (b).

DATA ACQUISITION AND ANALYSIS

- a) **Acquisition Q-Sense software 401 (QSoft₄₀₁)**: it acquires and displays at real time and simultaneously temperature and QCM-D measurements (f and D) from the four sensors.

- b) **Analyzing software QTools₃₀₁**: it analyses the data acquired with Q-Soft. Using the “Voight model” included in the software, it is possible to perform a theoretical modeling of the QCM-D raw data leading to a mathematical fit that estimates the adsorbed mass and viscoelastic properties of the layer deposited on the surface-sensor. As viscous layers show different penetration depths of harmonic acoustic frequencies, changes in f and D have to be recorded at three overtones to be modelled.

OPERATION

a) **Sample preparation:** the samples should be prepared very carefully to reduce distortion of the measurements collected by the device. Changes in temperature or the presence of air bubbles can affect the sensor signal. The buffer used (PBS) is degassed and warmed up to 37-38 °C (Ultrasonic bath, BRANSON, 1510, UK) prior to perfusion because, in this way, the risk of formation of bubbles in the system is very much reduced.

b) **Preparation of sensor surfaces:** the crystals should be clean and dry before starting the perfusion (uncoated crystals) or being immersed in the coating solution to avoid non-homogeneous coating that can also interfere with the measurements.

For the fibrinogen-coating, PL and gold quartz crystals were placed in fibrinogen dissolved in PBS at the final concentration of 100 µg/mL and 500 µg/mL and maintained for one hour at room temperature.

c) **Measurements:** before starting an experiment the chamber platform, the electronics unit and the computer have to be properly connected. Once the QSoft₄₀₁ is started, the temperature control has to be increased up to 37 °C (5-10 minutes are needed for equilibration). Crystals are then inserted in the flow module with the active side facing down (resting on the o-ring inside the chamber) to allow the contact of the crystal surface with the sample during the measurements.

Afterwards PBS perfusion is initiated to fill the system; in the case of fibrinogen-coated crystals, for 20 minutes (100 $\mu\text{L}/\text{minute}$) to remove fibrinogen unbound to the surface.

Next, the resonance frequencies of the sensor crystals have to be found as they correspond to the baselines of each crystal. The f and D for the 3rd, 5th, 7th, 9th, 11st and 13rd overtones or resonances have to be obtained for each sensor (**figure 21**).

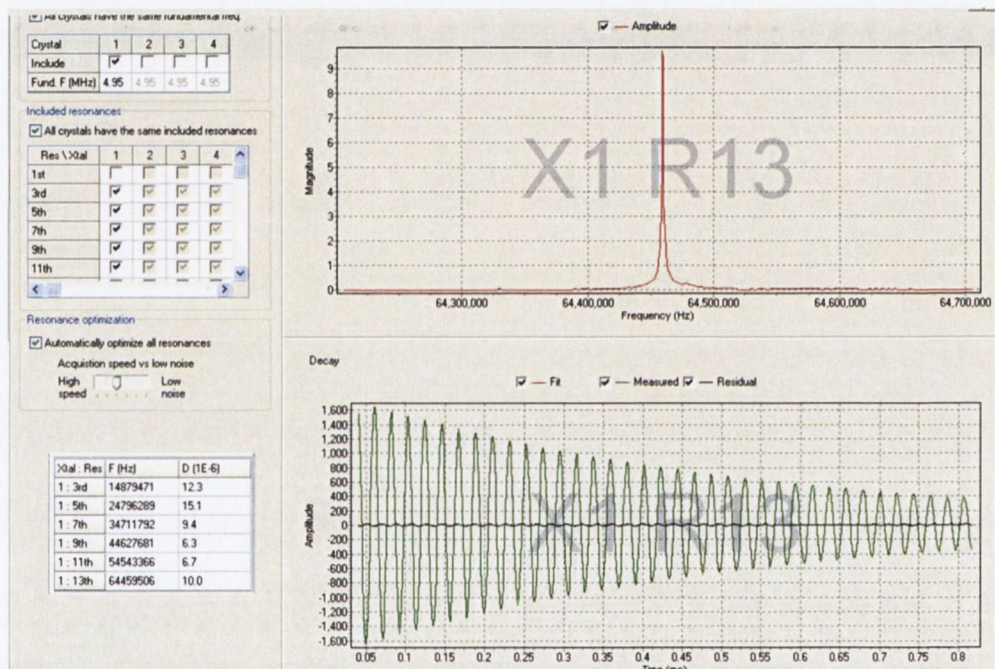


Figure 21: Set up measurement screen

In this case the f and D for the 3rd, 5th, 7th, 9th, 11st and 13rd overtones for the crystal sensor placed in the first module (X1) were obtained. On the left hand side, in a red square, the values obtained for all the resonances are shown. On the right hand side the graphs for the amplitude (red) and decay (green) for the 13rd overtone.

Once the acquisition is started, one f and D vs time graph for each sensor crystal appears on the screen. A chart showing the temperature can also be displayed (**figure 22**).

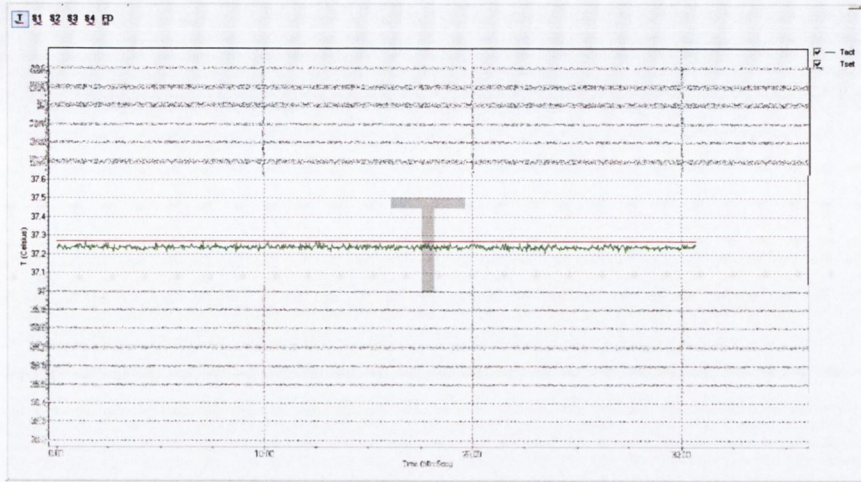


Figure 22: Representative temperature chart

The red line corresponds to the temperature set up value and the green line to the actual temperature value during the experiment.

If the crystal is properly mounted, the temperature is stable and the flow module is bubble-free, the f and D baseline have to be stable and should be recorded for at least two minutes (**figure 23**).

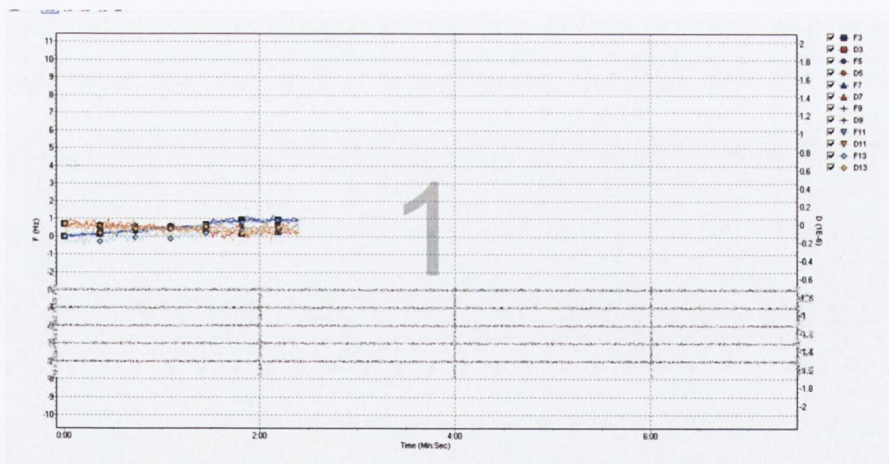


Figure 23: Representative baseline chart

The Q-Sense E₄ is then ready to perform an experiment.

d) Cleaning: once the experiment has been completed, the system and the sensor have to be cleaned.

Following the protocols supplied by Q-Sense:

System cleaning: for this purpose 2% SDS solution is perfused through the device for approximately 15 minutes and then rinsed with purified water for another 15 minutes. Afterwards the chamber should be emptied and dried.

Sensor cleaning: after the system has been cleaned, the sensors are removed from the modules and cleaned. First, they are immersed in 99% ethanol solution and placed and sonicated, in the ultrasonic bath, for five minutes. Afterwards, crystals are immersed in 2% SDS solution, sonicated for another five minutes, rinsed with purified water and dried.

Gold crystals: to remove organic and biological substances from the surface of crystals, sensors are immersed in a 5:1:1 mixture of purified water, ammonia (25%) and hydrogen peroxide at 55-60° C for 5 minutes. Next, the crystals are rinsed with purified water and dried.

Polystyrene-coated crystals: to remove the polystyrene coating for recycling crystals sensors are immersed in a 1:1 solution of toluene and purified water and sonicated for two minutes at 37° C. After that crystals are rinsed again in purified water and dried.

PLATELET AGGREGATION

For the study of **platelet aggregation**, gold and polystyrene-coated quartz crystals have been used as sensors following coating with fibrinogen. Uncoated gold and polystyrene-coated quartz crystals have been also used as controls. Crystal sensors (coated or uncoated) were mounted on the flow chamber and PRP perfused through the device at varying concentrations (50,000; 100,000; 150,000 and 210,000 platelets/ μL) at 37 °C for up to 210 minutes. Platelet aggregation was monitored in real-time by QSoft₄₀₁ and measured as f (Hz) and D (1E-6).

To analyse the effects of **flow rates** and platelet concentrations on **shear stress**, PRP at a final concentration of 210,000 platelets/ μL was perfused through the system at a fixed flow rate (10, 20, 50, and 100 $\mu\text{L}/\text{minute}$) for 30 minutes and platelet aggregation was monitored and measured as changes in f and D .

To study the effects of increasing **concentrations of platelets**, PPP (control) and PRP at final concentrations of 100,000; 150,000 and 210,000 platelets/ μL were perfused for up to 60 minutes and the concentration-response curves were generated.

To investigate the effects of **platelet agonists** on platelet aggregation in our system two platelet agonists have been used: ADP and thrombin receptor activator peptide (TRAP) at final concentrations of 10 and 25 μM , respectively. Both agonists were added prior to initiation of perfusion of PRP (210,000 platelets/ μL) and their effects measured for 30 minutes.

To study the effects of **platelets inhibitors** on platelet aggregation several endogenous and pharmacological inhibitors of platelet aggregation that act at

different levels of the platelet activation process were tested in our system. For experiments using **prostacyclin**, that increases cAMP, the drug at final concentration of 10 ng/mL was added 60 minutes after initiation of perfusion of PPP and PRP (50,000; 100,000; 150,000 and 210,000 platelets/ μ L) and the effects measured for 30 minutes. When **aspirin** (100 μ M) a platelet cyclooxygenase inhibitor; **phenantroline** (100 μ M) a MMP inhibitor; **apyrase** (250 μ g/mL) an ADP scavenger; **2-Methylthio-AMP triethylammonium salt hydrate** (2-MeSAMP) (100 μ M) a selective P2Y₁₂ receptor antagonist; or NO releasing agents such as **S-Nitroso-glutathione** (GSNO) or **S-Nitroso-N-acetyl-DL-penicillamine** (SNAP) at the final concentration of 100 μ M were tested, the compounds were added prior to initiation of perfusion of 210,000 platelets/ μ L and the effects measured for 30 minutes.

PHASE CONTRAST MICROSCOPY

The formation of platelet aggregates on the crystal surface was studied using a Zeiss microscope (Axiovert 200M, UK). First, PRP and PPP suspensions were perfused for 30 minutes through Q-Sense. The crystals were then taken for phase-contrast microscopy imaging using a 20x objective. Photomicrographs were captured using a digital camera and Zeiss software (Axiovision 4.7).

CONFOCAL MICROSCOPY

For the study of activated platelets PRP was perfused through Q-Sense for 30 minutes on fibrinogen-coated crystals. Afterwards, the crystals were placed in a 24 well plate and washed very gently three times with PBS. Each sample was then treated with fluorescein isothiocyanate (FITC) conjugated PAC-1 (BD

Biosciences, UK/Ireland) (150 μ L/well) for 30 minutes in the dark. The platelets were then fixed with 2% formaldehyde for 30 minutes at room temperature and permeabilized with 0.1% triton for 3 minutes. Finally, the samples were stained with Phalloidin Actin (Invitrogen, USA) (1:200 dilution) for 1 hour at room temperature, and mounted on a glass slide with mounting medium.

For the study of resting platelets, platelets were treated in suspension and mounted on a glass slide.

In both cases confocal images were taken using a 63x oil immersion objective, with a numerical aperture of 1.4, on a Zeiss LSM 510 Meta system (UK). The samples were excited using 488 nm and 561 nm and emission filters of band-pass 505-550 nm and long-pass 575 nm, respectively.

ATOMIC FORCE MICROSCOPY (AFM)

For the AFM imaging, PRP was perfused through Q-Sense for 30 minutes. Afterwards, samples were fixed using 2.5% glutaraldehyde for 30 minutes at 37°C. The platelets were then dehydrated through ascending grades of ethanol, (60% for 20 minutes, 80% for 20 minutes, 90% for 20 minutes and finally 100% for 30 minutes repeated once). Thereafter, crystals were mounted onto microscope slides with the cells facing upwards. The crystal-on-slide was mounted onto the microscope and clipped down to ensure no movement during acquisition. AFM images were then taken using an Ntegra Spectra (NT-MDT, Russia), AFM/Raman system. Imaging was carried out in dry-phase, semi-contact AFM with a silicon-nitride tip (NSG10, Golden silicon probes). The resonance frequency of the tip was found to be 280 KHz. Height AFM images, 70 μ m x 70 μ m scans, were taken five times for each sample, around the central

area of the crystal, at 0.55Hz. Image analysis was carried out on the height images using the Nova software (filter Fit Lines-X was used followed by subtract plane and finally grain analysis).

RHEOLOGY

The platelet aggregation rheology study was carried out based on the dimensions of the module chamber and assuming laminar flow along the crystal active measurement area. The Q-Sense modules are designed on the microfluidic basis of a parallel plate flow chamber with an internal total volume of 140 μL (flow channel $\sim 100 \mu\text{L}$, and above sensor crystal $\sim 40 \mu\text{L}$). The dimensions of the sensing area above the circular crystal are: diameter = 14 mm, height = 0.25 mm. This equates to $\sim 40 \mu\text{L}$ volume (**figure 24**).

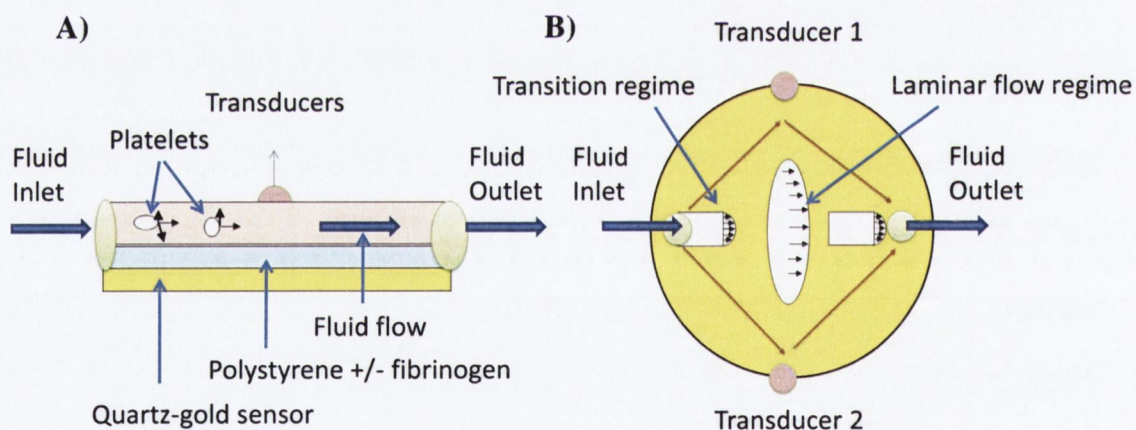


Figure 24: Q-Sense chamber

A schematic representation of the Q-Sense module chamber; transversal view (A) and from the top (B).

For all the experiments the volumetric flow rate Q injected through the peristaltic pumping system was incrementally fixed at 10, 20, 50 and 100 $\mu\text{L}/\text{minute}$. Shear rates and shear stresses on different platelet concentrations were calculated based on the PRP rheological changes.

SHEAR RATE

The mean velocity within the Q-Sense crystal sensor chamber during each experiment was calculated as $v_{mean} = Q/(wh)$, where Q is the flow rate, w is the width and h the height of the chamber inside the module. The *shear rate* γ in the middle of the crystal sensing area, was calculated by $\gamma = \delta v_{mean}/h$.

Density δ was calculated based on mass and the volume used (1 mL).

SHEAR STRESS

The *shear stress* was given by the formula $\tau = \delta \cdot v_{mean} \eta/h$, where δ is density and η is the dynamic viscosity.

The **dynamic viscosity** of PPP and PRP preparations was measured using a Vibro-Viscosimeter (SV-10 sine wave SV-10, A&D, USA). Before performing the measurements, prostacyclin, at a final concentration of 100 ng/mL, was added to each sample to inhibit platelet aggregation during the acquisition. The viscosity of PPP and PRP (at final concentrations of 100,000; 150,000 and 210,000 platelets/ μ L) was measured at four temperature ranges ($T_{mean} = 32, 34, 36, 38$ °C, $T_{bin} = 2$ °C).

STATISTICS

The results are expressed as f and D (from the 3rd overtone) or percentage of aggregation from at least three independent experiments. All means are reported with standard deviation. The data were analyzed using GraphPad Prism 5 software. The normality of the population was tested using D'Agostino-Pearson normality test. Paired Student's t-tests, One-way analyses of variance, repeated measures ANOVA and Dunnett's or Tukey-Kramer's multiple comparisons post test were performed, where appropriate. Statistical significance was considered when $P < 0.05$.

RESULTS

PERFUSION OF SENSOR CRYSTALS WITH PRP LED TO PLATELET AGGREGATION

As QCM-D is able to detect at nanogram level the deposition of mass on the crystal surface, **the core hypothesis** tested in my research was if measurable changes in f and D could be detected by the device during the perfusion of PRP through the system (**figure 25**).

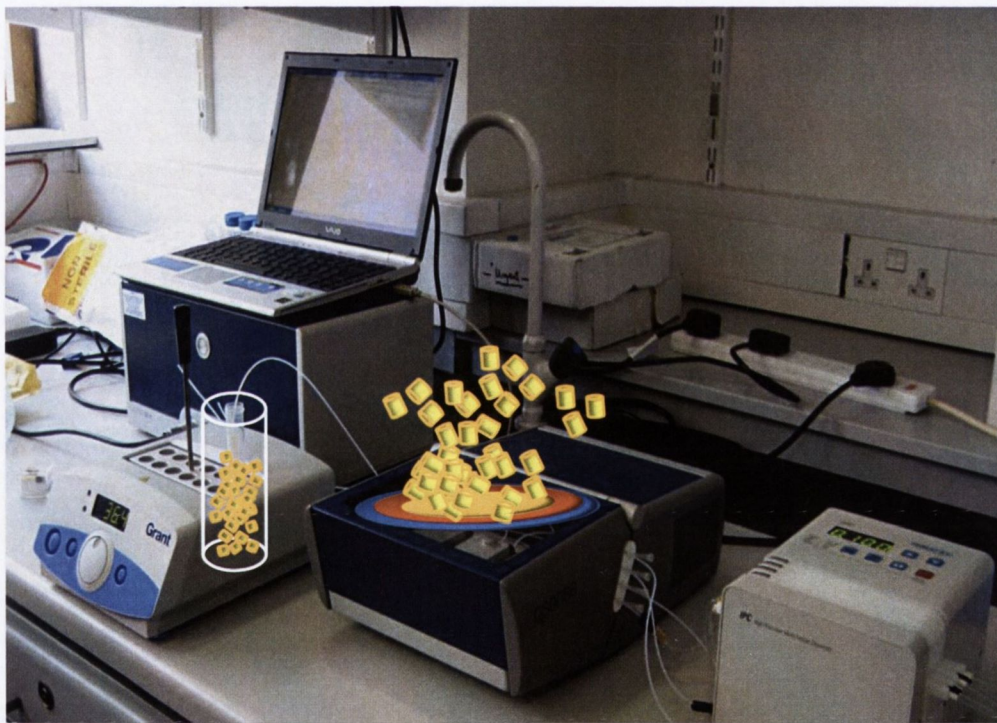


Figure 25: Sensor-induced platelet activation: a hypothesis underlying the experimental setup

I hypothesized that perfusion of platelets would lead to platelet aggregation and the deposition of mass (platelet aggregates) on the crystal surface resulting in a decrease in the f and an increase in the D as measured by the device.

As hypothesized, the perfusion of PRP on both, gold and polystyrene-coated crystals, induced a decrease in f and an increase in D indicating the deposition of platelets on the sensor surface (figure 26).

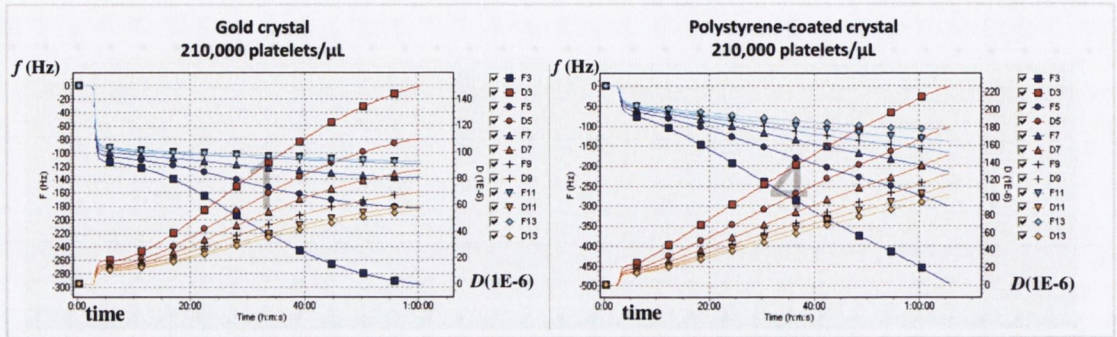


Figure 26: Effects of physiological concentration of platelets on frequency f and dissipation D

Perfusion of gold and polystyrene-coated crystals with PRP (210,000 platelets/ μL) led to a decrease in the f and increase in the D . The blue lines correspond to the changes in f and the red-orange lines correspond to the changes in D for the six different overtones (3rd, 5th, 7th, 9th, 11st and 13rd) measured during the experiment. The actual values for f (Hz) are shown in the left axis and for D (1E-6) in the right axis vs time.

Note: because the 3rd overtone (15MHz) was chosen for the statistical analysis, from now on only the 3rd overtone lines for f and D will be shown for the rest of the graphs along this thesis document (figure 27).

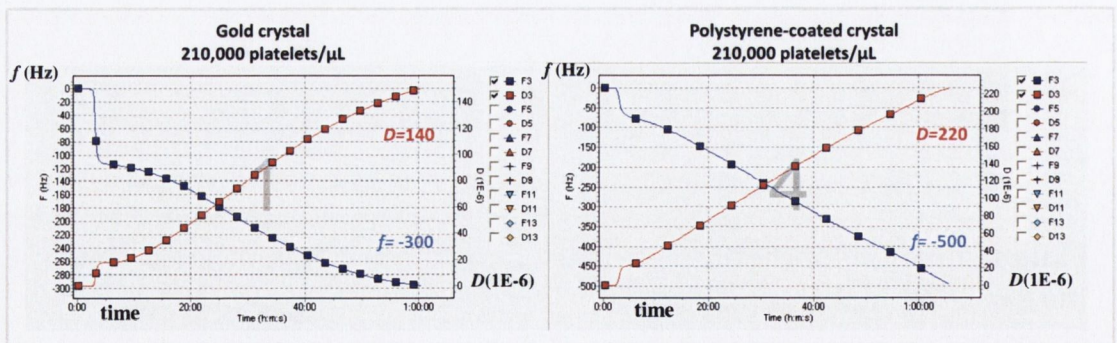


Figure 27: Effects of physiological concentration of platelets on frequency f and dissipation D for the 3rd overtone

The data from the experiment shown in figure 26.

EFFECTS OF FIBRINOGEN CONCENTRATIONS ON AGGREGATION

As fibrinogen is a plasma protein known to activate platelets, crystals were then coated with fibrinogen dissolved in PBS at two different concentrations, 100 $\mu\text{g}/\text{mL}$ and 500 $\mu\text{g}/\text{mL}$. Next, PRP (210,000 platelets/ μL) was perfused across the sensors for 60 minutes. No significant differences (Paired t test, two tailed, $n=3$) were found in f and D between both concentrations of fibrinogen at 30 minutes and at 60 minutes.

Note: Fibrinogen at 100 $\mu\text{g}/\text{mL}$ was used to coat crystals for all subsequent experiments.

EFFECTS OF FLOW RATE ON PLATELET AGGREGATION

Knowing that flow rate could affect platelet aggregation, the effects of the perfusion of PRP (210,000 platelets/ μL) across fibrinogen-coated crystals for 30 minutes at different flow rates were studied.

The perfusion of 210,000 platelets/ μL at 10, 20, 50 and 100 $\mu\text{L}/\text{minute}$ resulted in a significant decrease in f and increase in D with maximal effect at 50 and 100 $\mu\text{L}/\text{minute}$ (figure 28).

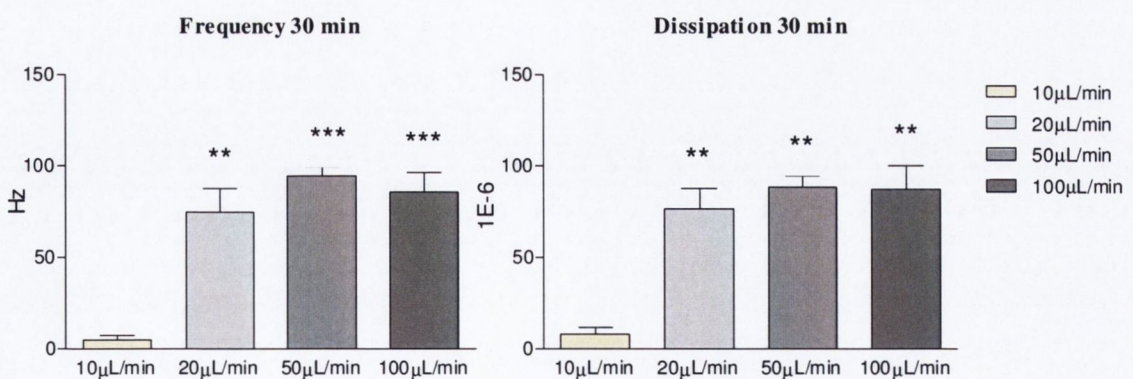


Figure 28: Effects of flow on frequency f and dissipation D

The perfusion of PRP resulted in a significant decrease in f and increase in D when flow rates of 10, 20, 50 and 100 $\mu\text{L}/\text{minute}$ were compared. One-way ANOVA; $n=3$; $P_f=0.0003$ and $P_D=0.0008$. Tukey's Multiple Comparison Test: ** $P<0.01$ vs 10 $\mu\text{L}/\text{minute}$; *** $P<0.001$ vs 10 $\mu\text{L}/\text{minute}$.

PLATELET AGGREGATION ON GOLD AND POLYSTYRENE-COATED CRYSTALS

The effects of different concentrations of platelets perfused on gold and polystyrene-coated crystals at a flow rate of 50 and 100 $\mu\text{L}/\text{min}$ were studied. In addition, differences between fibrinogen-uncoated and fibrinogen-coated crystals were also analysed. For this purpose PPP (control) and increased concentrations of platelets (100,000; 150,000 and 210,000 platelets/ μL) were perfused across fibrinogen-uncoated and fibrinogen-coated crystals for up to 60 minutes. Changes in f and D were recorded, calculated as percentage of aggregation (where the values for 210,000 platelets/ μL were considered as 100% of aggregation) and analysed at 15, 30, 45 and 60 minutes.

GOLD CRYSTALS

Perfusion of PRP at both 50 and 100 $\mu\text{L}/\text{min}$ across fibrinogen-uncoated and fibrinogen-coated gold crystals led to significant changes in f and D when compared to PPP at all different time-points. Although, no statistical differences were found in f when fibrinogen-coated crystals were compared to fibrinogen-uncoated crystals, significant changes were observed in D at 50 and 100 $\mu\text{L}/\text{min}$ (**figures 29-32, 37-40**).

POLYSTYRENE-COATED CRYSTALS

The perfusion of fibrinogen-coated polystyrene-coated crystals led to significant changes in f and D at both, 50 and 100 $\mu\text{L}/\text{minute}$ at all different time-points tested. The perfusion of fibrinogen-uncoated crystals with PPP and PRP under the same conditions also led to aggregation. However, these effects were lower when compared to fibrinogen-coated crystals at 100 $\mu\text{L}/\text{minute}$ but not at 50 $\mu\text{L}/\text{minute}$ (**figures 33-36, 41-44**).

Gold Crystals
Flow 50 μ L/minute
Perfusion time 15 minutes

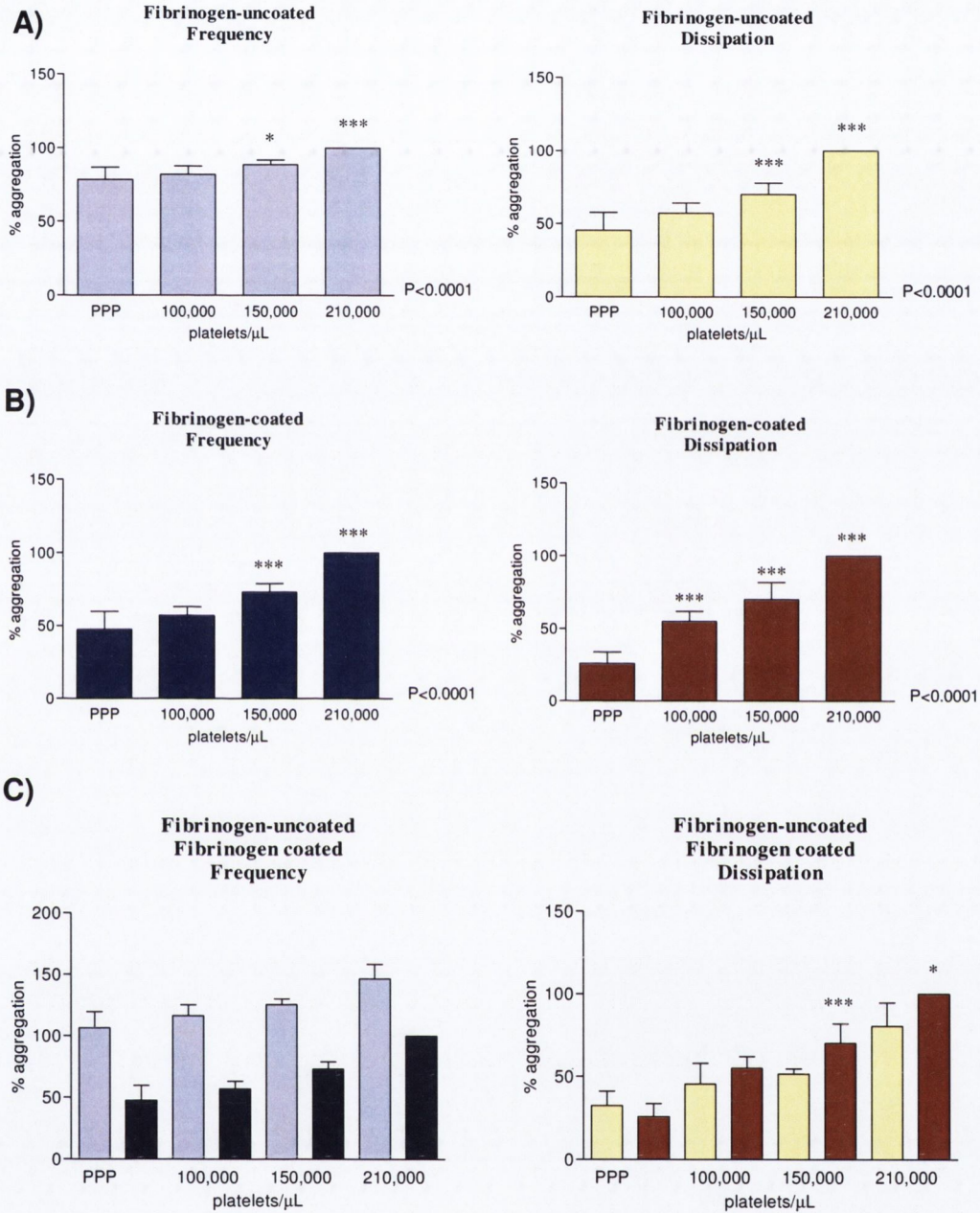


Figure 29: Frequency and dissipation in fibrinogen-uncoated and fibrinogen-coated gold crystals perfused with PPP and increasing concentrations of platelets (**A** and **B**) at 50 μ L/min (15 minutes). One-way ANOVA, Tukey's Multiple Comparison Test: * $P < 0.05$ vs PPP, *** $P < 0.001$ vs PPP. Figure **C** shows the comparison between uncoated and coated crystals. Repeated measures ANOVA, Tukey's Multiple Comparison Test: * $P < 0.05$ coated vs uncoated; *** $P < 0.001$ coated vs uncoated.

Gold Crystals
Flow 50 μ L/minute
Perfusion time 30 minutes

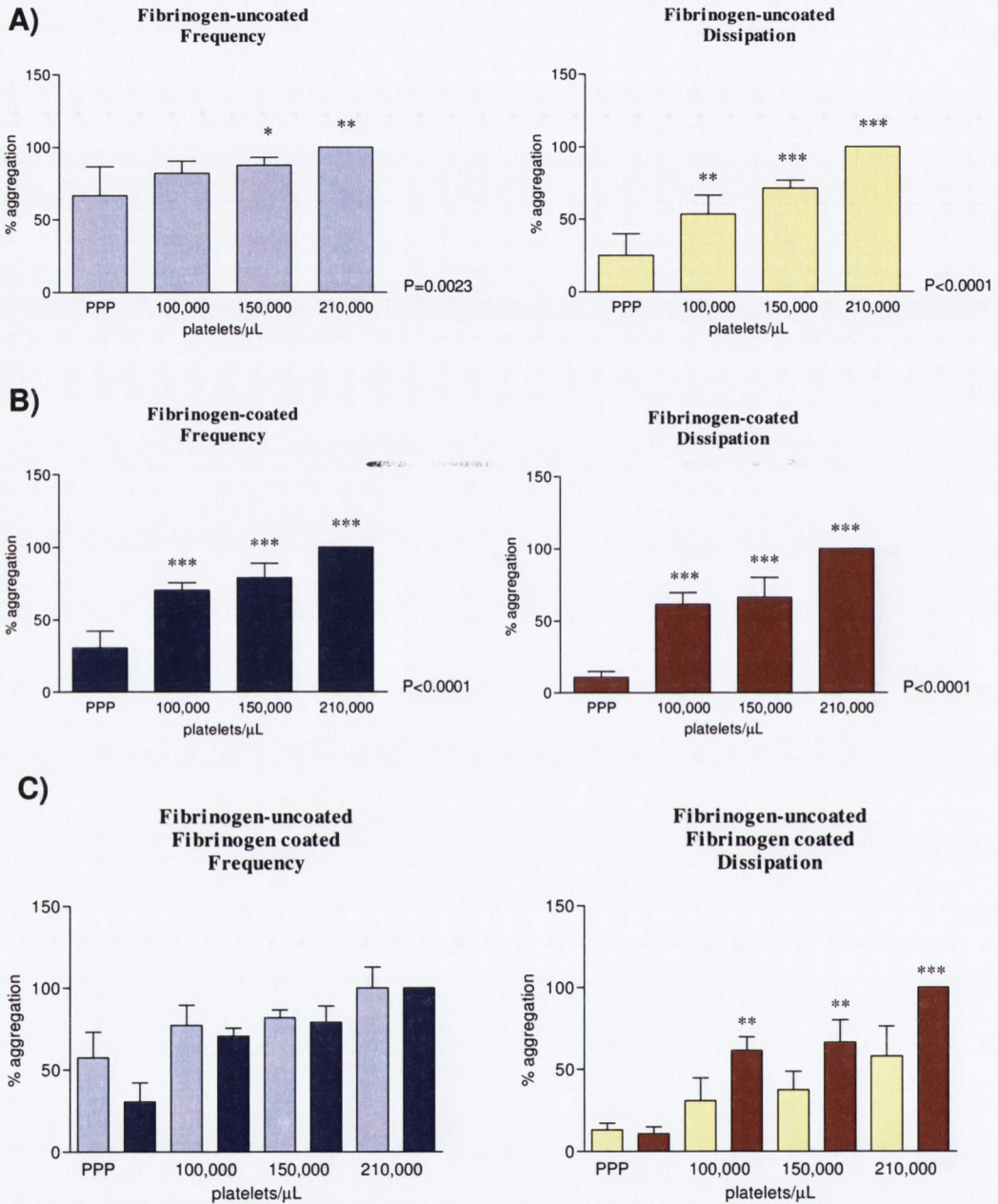


Figure 30: Frequency and dissipation in fibrinogen-uncoated and fibrinogen-coated gold crystals perfused with PPP and increasing concentrations of platelets (A and B) at 50 μ L/min (30 minutes). One-way ANOVA, Tukey's Multiple Comparison Test: * $P < 0.05$ vs PPP, ** $P < 0.01$ vs PPP, *** $P < 0.001$ vs PPP. Figure C shows the comparison between uncoated and coated crystals. Repeated measures ANOVA, Tukey's Multiple Comparison Test: ** $P < 0.01$ coated vs uncoated; *** $P < 0.001$ coated vs uncoated.

Gold Crystals
Flow 50 $\mu\text{L}/\text{minute}$
Perfusion time 45 minutes

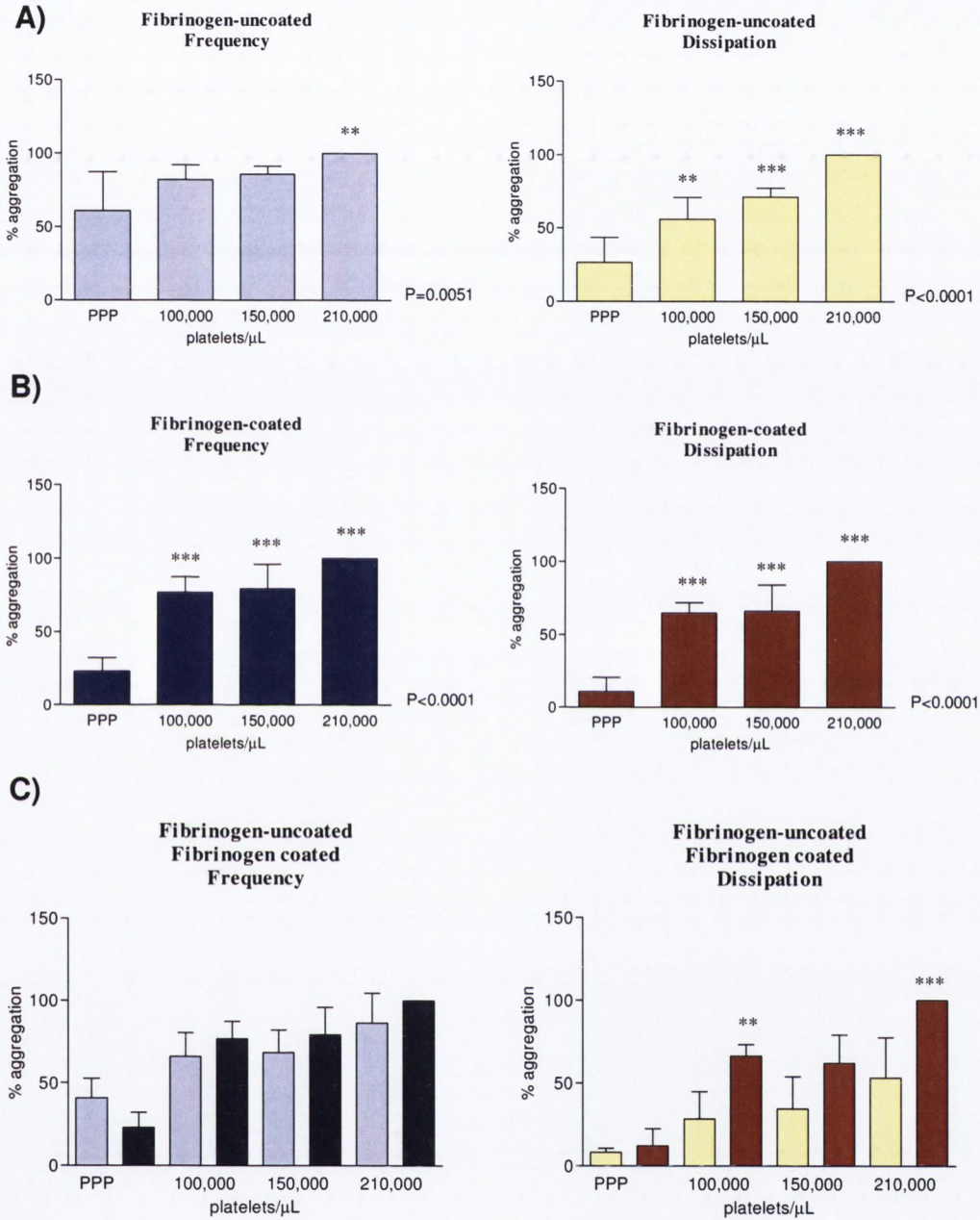


Figure 31: Frequency and dissipation in fibrinogen-uncoated and fibrinogen-coated gold crystals perfused with PPP and increasing concentrations of platelets (A and B) at 50 $\mu\text{L}/\text{min}$ (45 minutes). One-way ANOVA, Tukey's Multiple Comparison Test: ** $P<0.01$ vs PPP, *** $P<0.001$ vs PPP. Figure C shows the comparison between uncoated and coated crystals. Repeated measures ANOVA, Tukey's Multiple Comparison Test: ** $P<0.01$ coated vs uncoated; *** $P<0.001$ coated vs uncoated.

Gold Crystals
Flow 50 $\mu\text{L}/\text{minute}$
Perfusion time 60 minutes

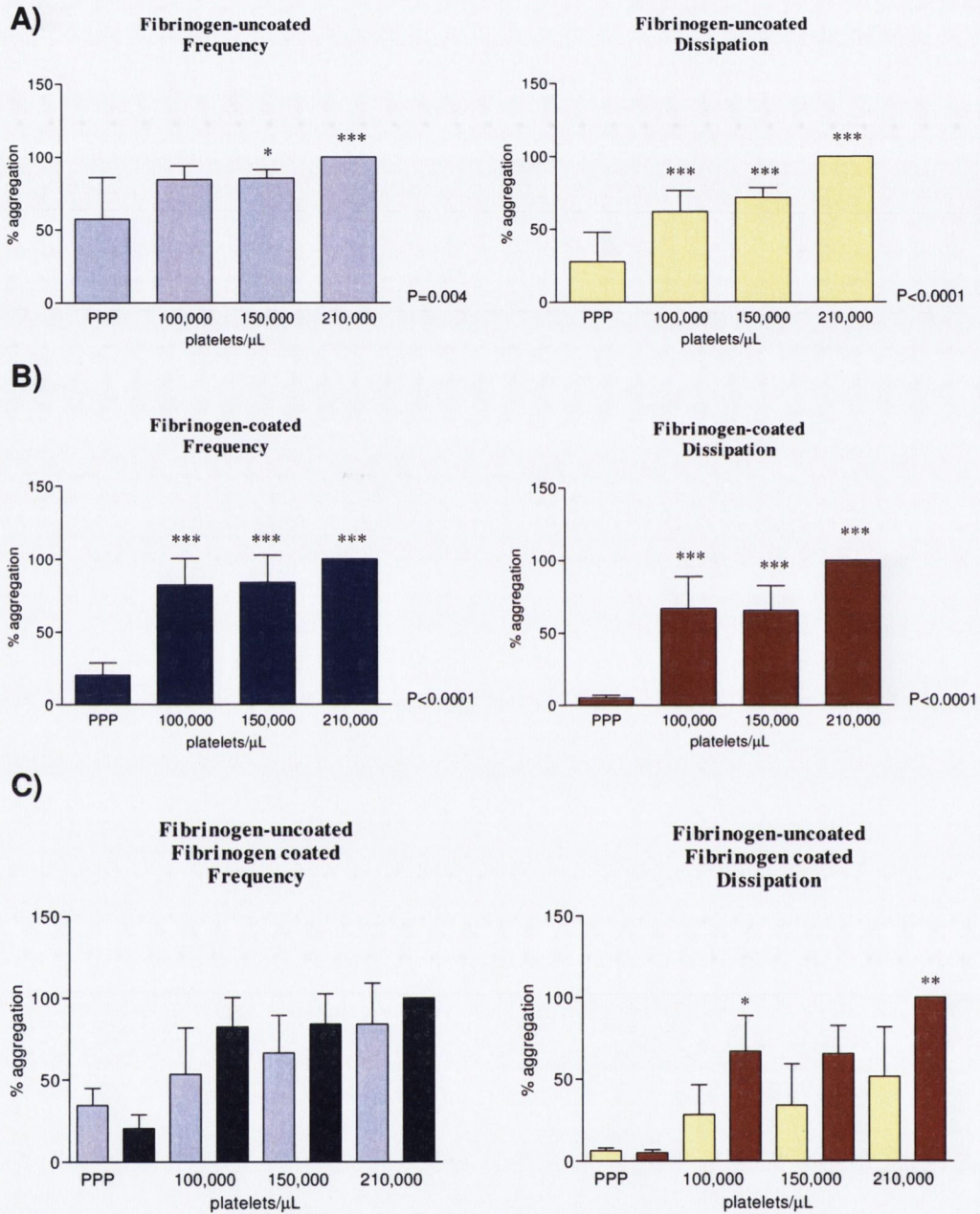


Figure 32: Frequency and dissipation in fibrinogen-uncoated and fibrinogen-coated gold crystals perfused with PPP and increasing concentrations of platelets (A and B) at 50 $\mu\text{L}/\text{min}$ (60 minutes). One-way ANOVA, Tukey's Multiple Comparison Test: * $P < 0.05$ vs PPP, *** $P < 0.001$ vs PPP. Figure C shows the comparison between uncoated and coated crystals. Repeated measures ANOVA, Tukey's Multiple Comparison Test: * $P < 0.05$ coated vs uncoated; ** $P < 0.01$ coated vs uncoated.

Polystyrene-coated Crystals
Flow 50 μ L/minute
Perfusion time 15 minutes

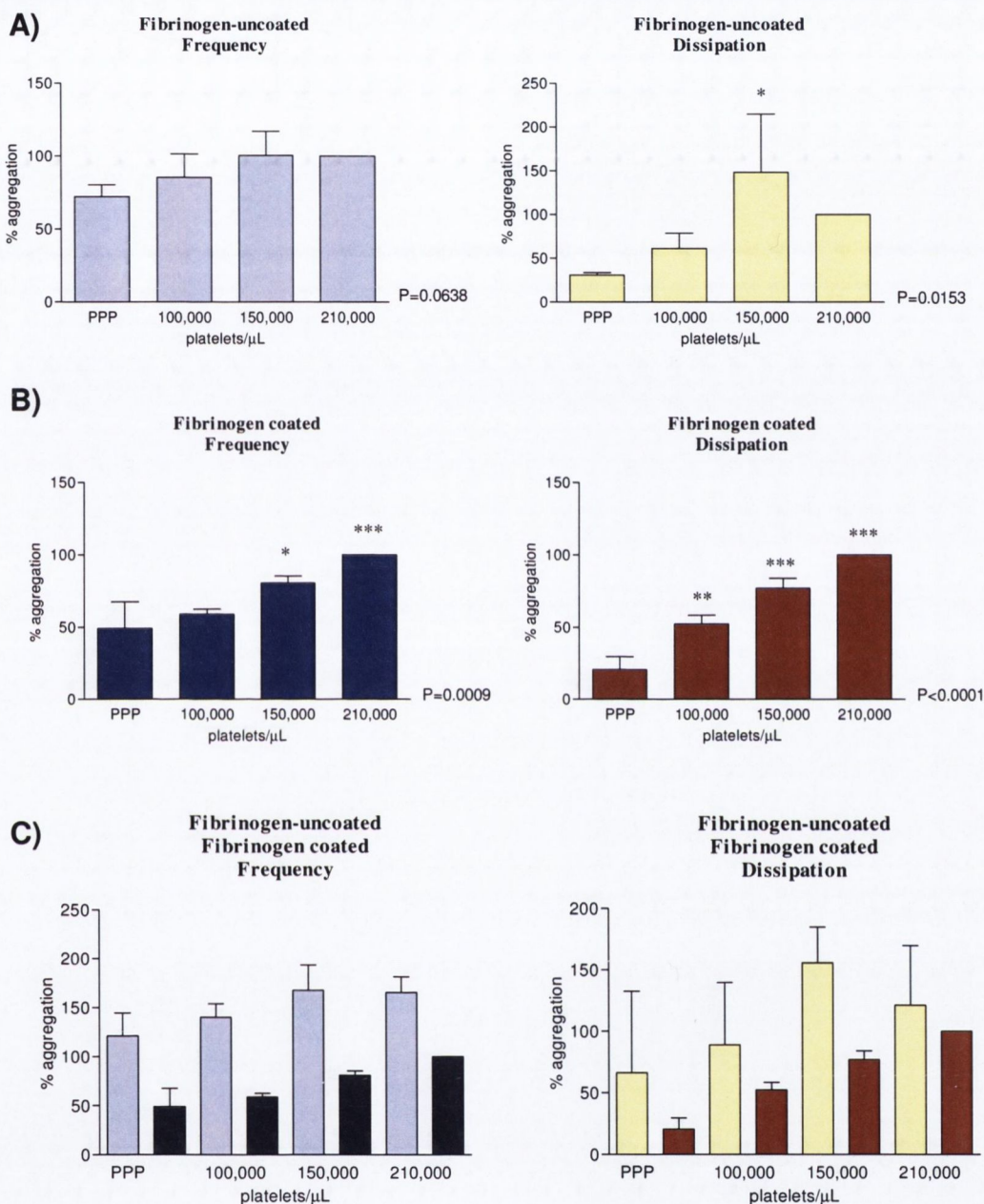


Figure 33: Frequency and dissipation in fibrinogen-uncoated and fibrinogen-coated polystyrene-coated crystals perfused with PPP and increasing concentrations of platelets (A and B) at 50 μ L/min (15 minutes). One-way ANOVA, Tukey's Multiple Comparison Test: * $P<0.05$ vs PPP, ** $P<0.01$ vs PPP, *** $P<0.001$ vs PPP. Figure C shows the comparison between uncoated and coated crystals.

Polystyrene-coated Crystals
Flow 50 $\mu\text{L}/\text{minute}$
Perfusion time 30 minutes

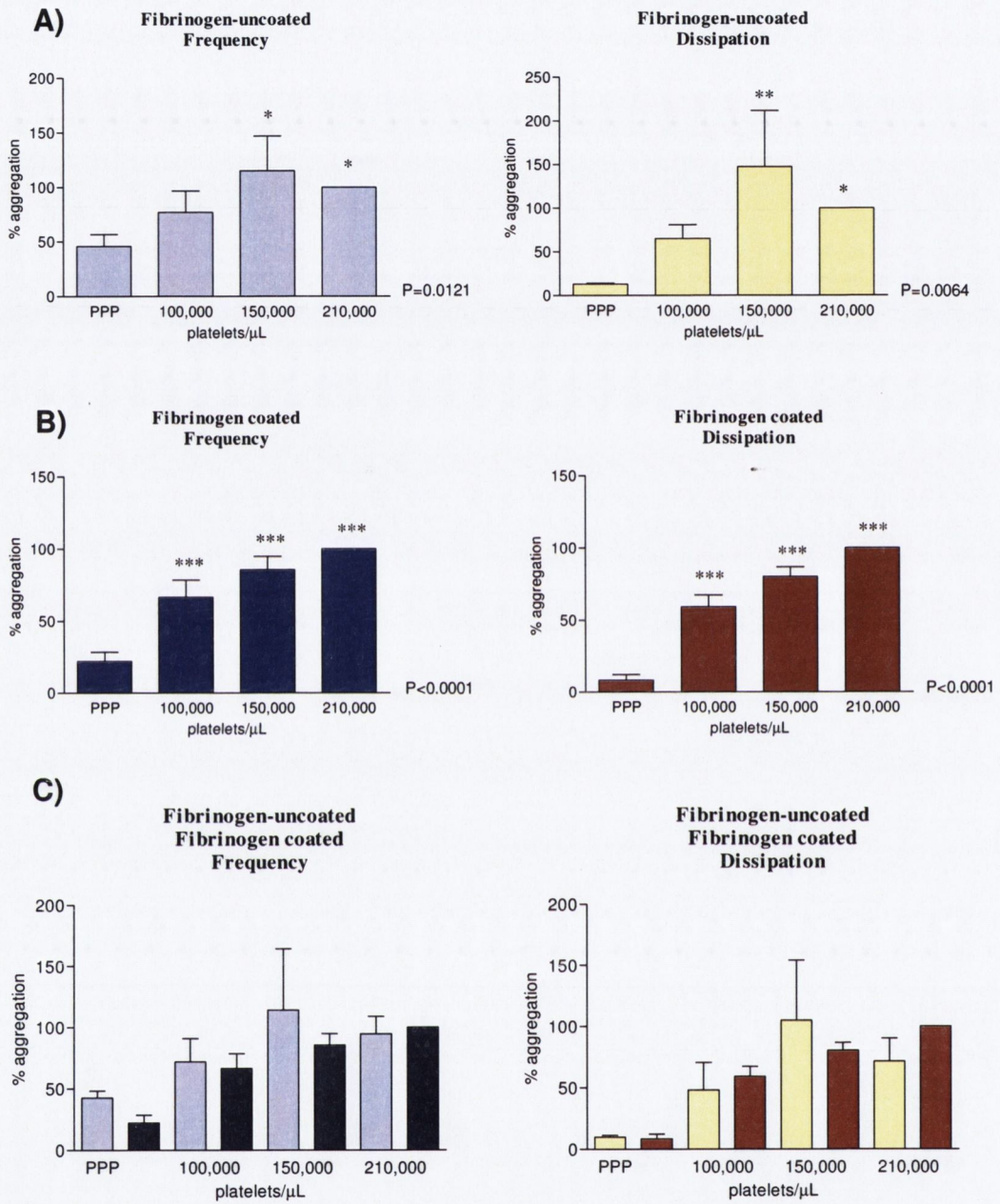


Figure 34: Frequency and dissipation in fibrinogen-uncoated and coated polystyrene-coated crystals perfused with PPP and increasing concentrations of platelets (A and B) at 50 $\mu\text{L}/\text{min}$ (30 minutes). One-way ANOVA, Tukey's Multiple Comparison Test: * $P<0.05$ vs PPP, ** $P<0.01$ vs PPP, *** $P<0.001$ vs PPP. Figure C shows the comparison between uncoated and coated crystals.

Polystyrene-coated Crystals
Flow 50 $\mu\text{L}/\text{minute}$
Perfusion time 45 minutes

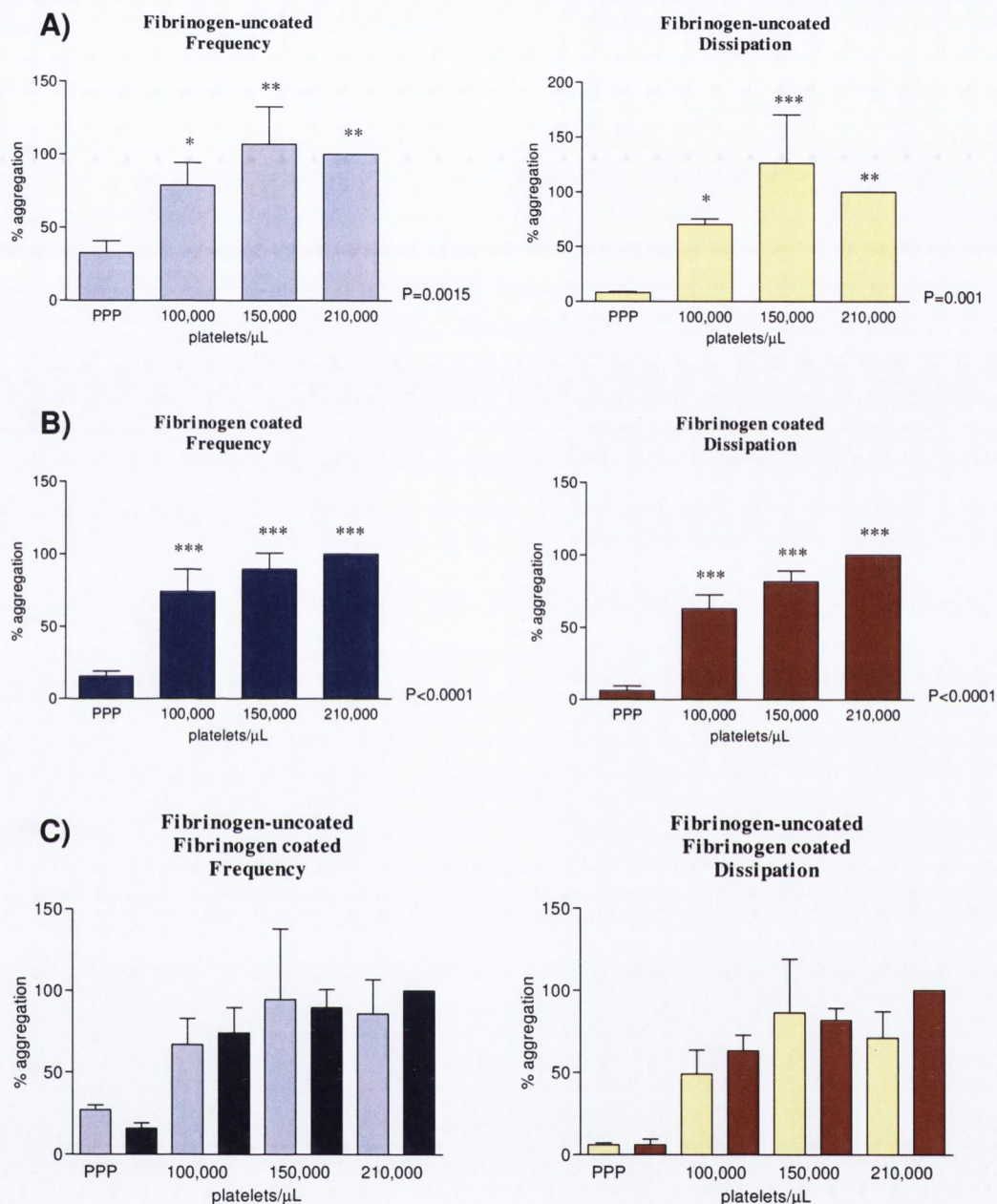


Figure 35: Frequency and dissipation in fibrinogen-uncoated and coated polystyrene-coated crystals perfused with PPP and increasing concentrations of platelets (A and B) at 50 $\mu\text{L}/\text{min}$ (45 minutes). One-way ANOVA, Tukey's Multiple Comparison Test: * $P < 0.05$ vs PPP, ** $P < 0.01$ vs PPP, *** $P < 0.001$ vs PPP. Figure C shows the comparison between uncoated and coated crystals.

Polystyrene-coated Crystals
Flow 50 μ L/minute
Perfusion time 60 minutes

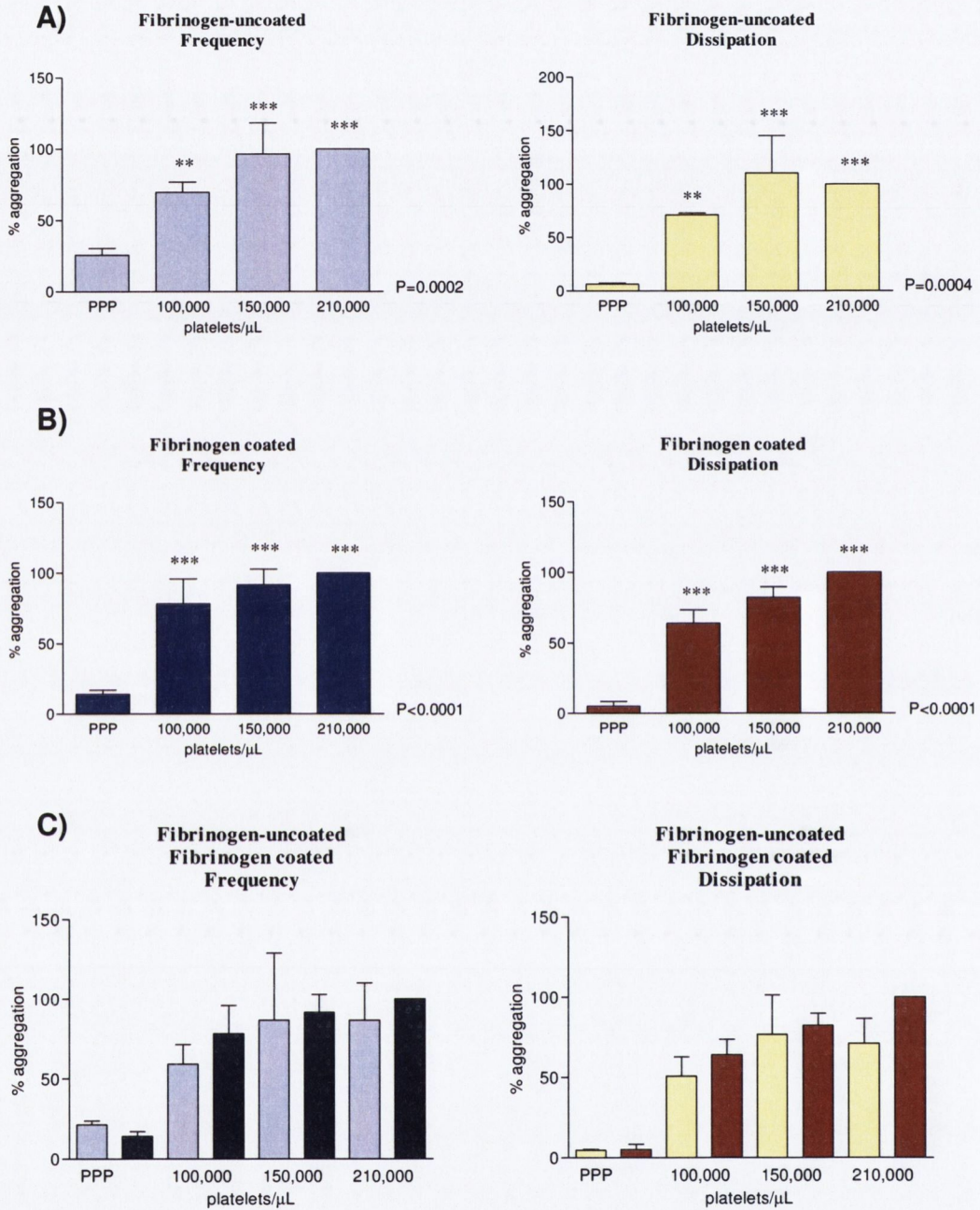


Figure 36: Frequency and dissipation in fibrinogen uncoated and coated polystyrene-coated crystals perfused with PPP and increasing concentrations of platelets (A and B) at 50 μ L/min (60 minutes). One-way ANOVA, Tukey's Multiple Comparison Test: **P<0.01 vs PPP, ***P<0.001 vs PPP. Figure C shows the comparison between uncoated and coated crystals.

Gold Crystals
Flow 100 $\mu\text{L}/\text{minute}$
Perfusion time 15 minutes

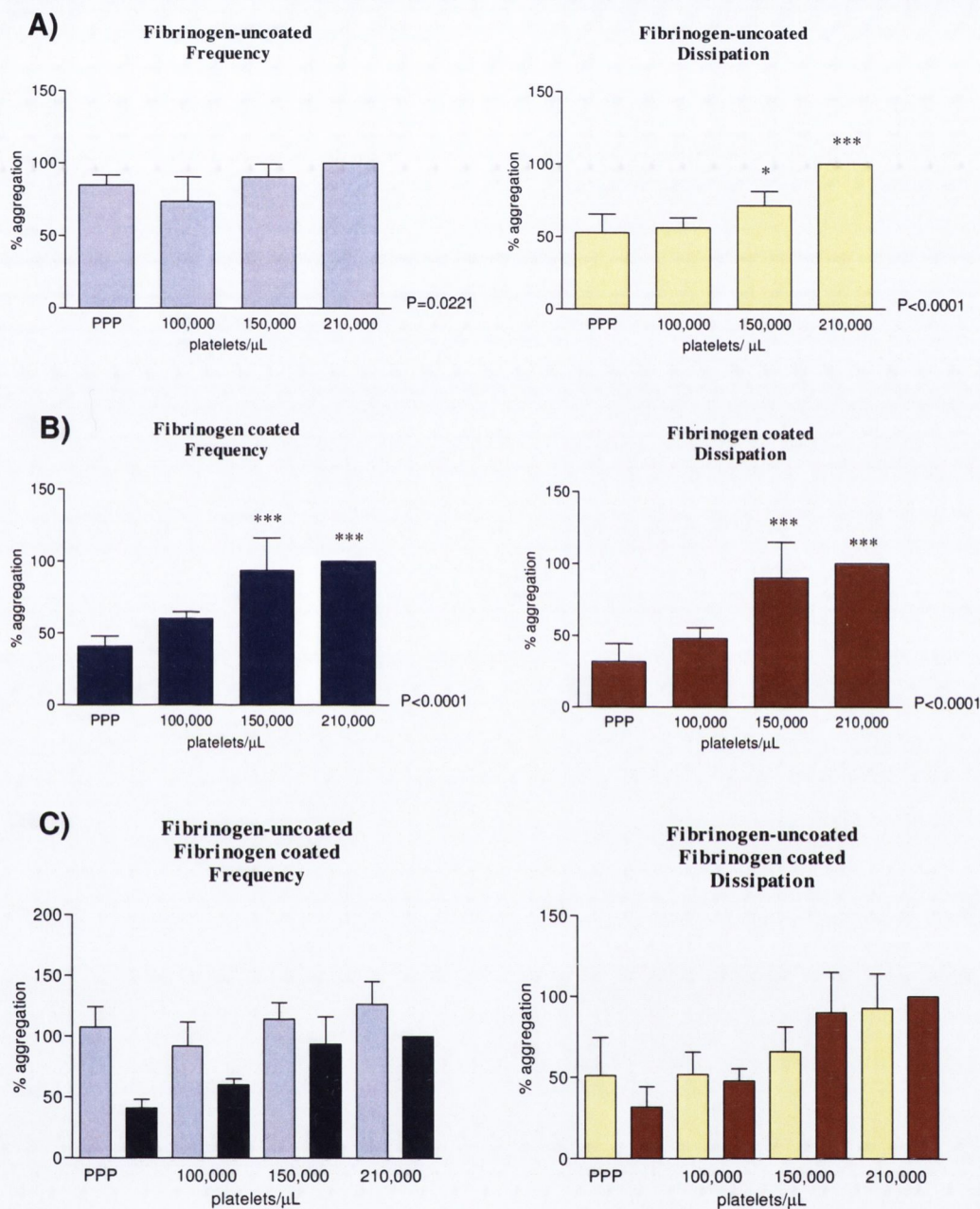


Figure 37: Frequency and dissipation in fibrinogen-uc coated and fibrinogen-coated gold crystals perfused with PPP and increasing concentrations of platelets (A and B) at 100 $\mu\text{L}/\text{min}$ (15 minutes). One-way ANOVA, Tukey's Multiple Comparison Test: * $P<0.05$ vs PPP, *** $P<0.001$ vs PPP. Figure C shows the comparison between uncoated and coated crystals.

Gold Crystals
Flow 100 μ L/minute
Perfusion time 30 minutes

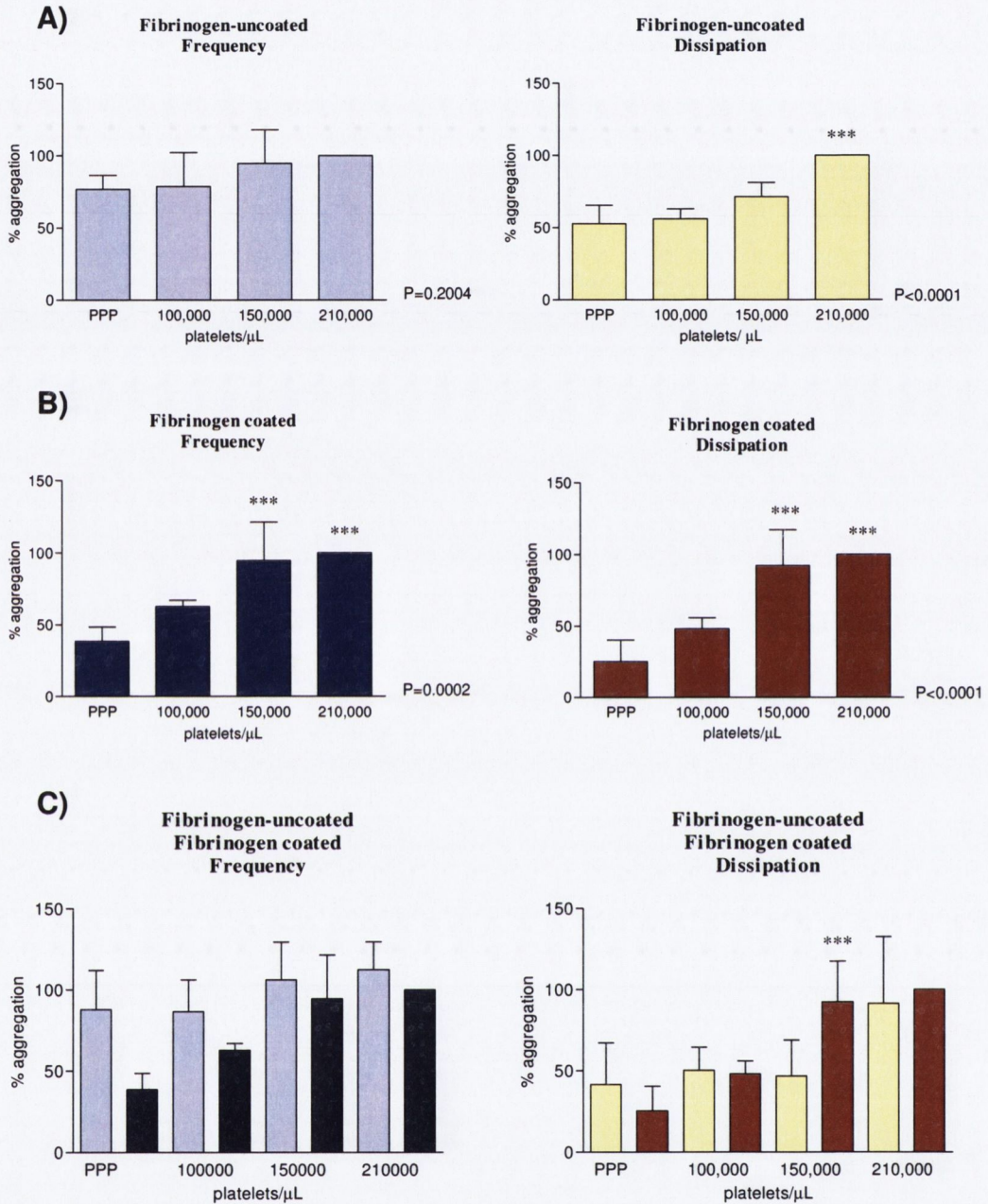


Figure 38: Frequency and dissipation in fibrinogen-uncoated and fibrinogen-coated gold crystals perfused with PPP and increasing concentrations of platelets (A and B) at 100 μ L/min (30 minutes). One-way ANOVA, Tukey's Multiple Comparison Test: ***P<0.001 vs PPP. Figure C shows the comparison between uncoated and coated crystals. Repeated measures ANOVA, Tukey's Multiple Comparison Test: ***P<0.001 coated vs uncoated.

Gold Crystals
Flow 100 $\mu\text{L}/\text{minute}$
Perfusion time 45 minutes

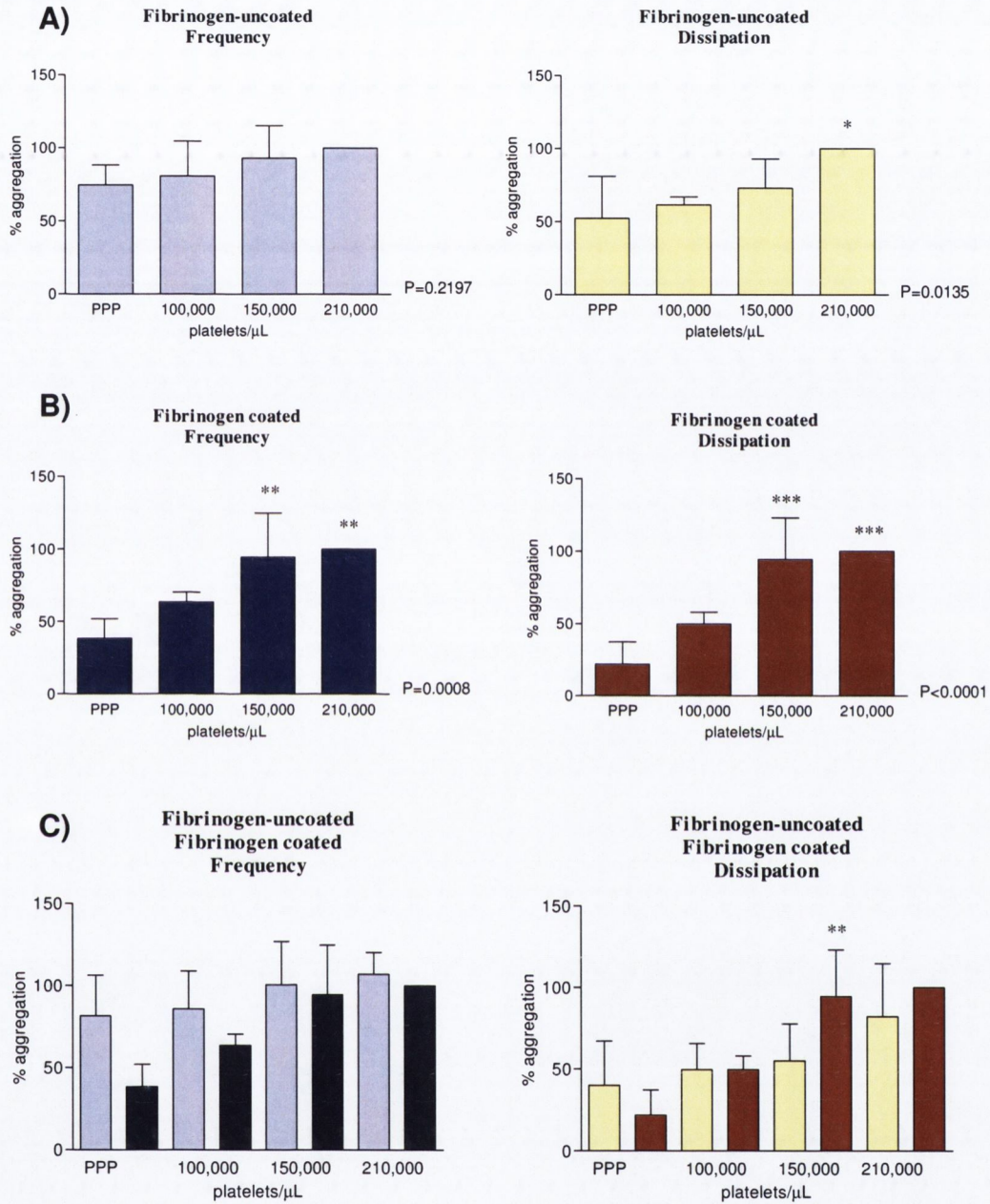


Figure 39: Frequency and dissipation in fibrinogen-uncoated and fibrinogen-coated gold crystals perfused with PPP and increasing concentrations of platelets (A and B) at 100 $\mu\text{L}/\text{min}$ (45 minutes). One-way ANOVA, Tukey's Multiple Comparison Test: * $P<0.05$ vs PPP, ** $P<0.01$ vs PPP, *** $P<0.001$ vs PPP. Figure C shows the comparison between uncoated and coated crystals. Repeated measures ANOVA, Tukey's Multiple Comparison Test: ** $P<0.01$ coated vs uncoated.

Gold Crystals
Flow 100 μ L/minute
Perfusion time 60 minutes

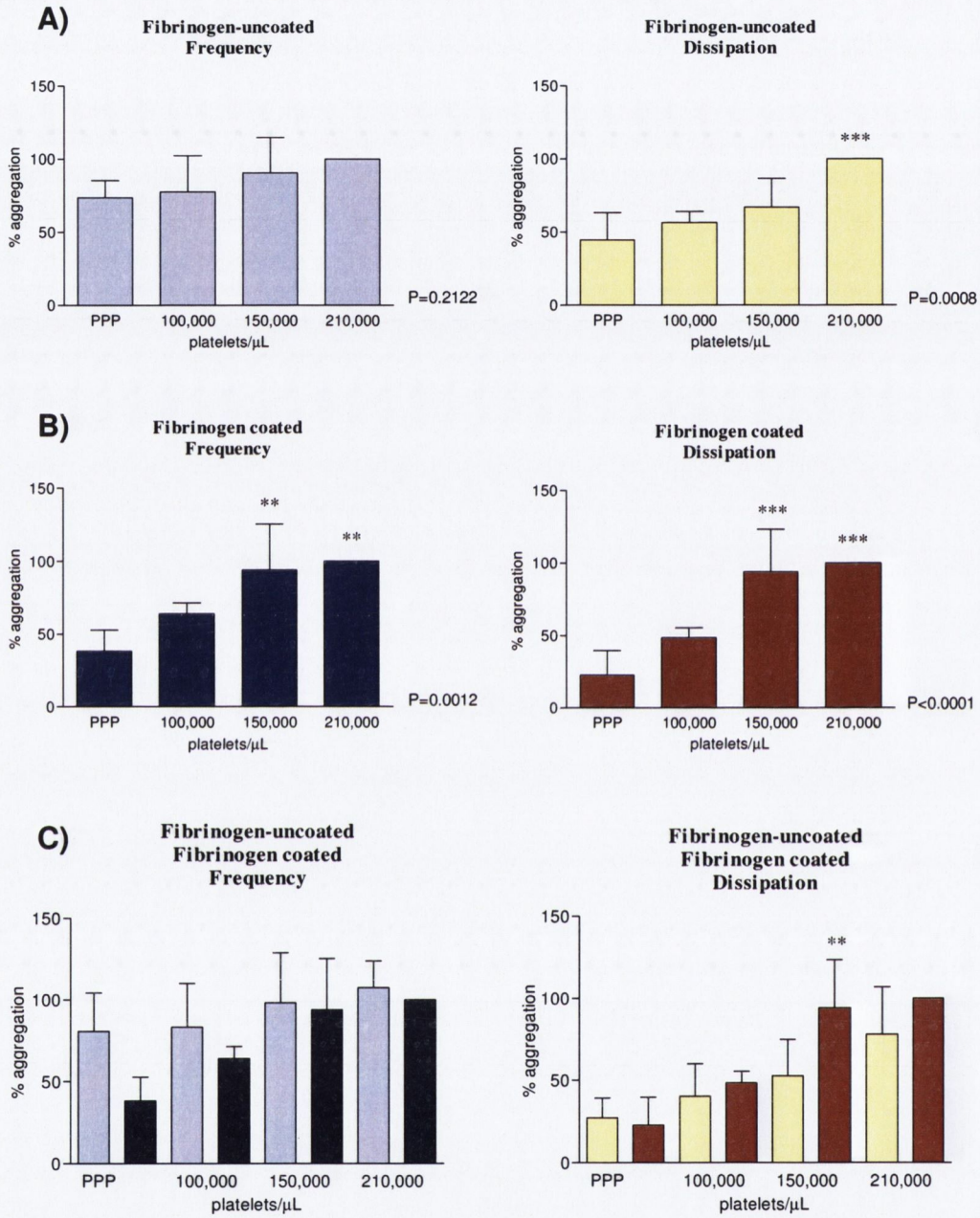


Figure 40: Frequency and dissipation in fibrinogen-uncoated and fibrinogen-coated gold crystals perfused with PPP and increasing concentrations of platelets (A and B) at 100 μ L/min (60 minutes). One-way ANOVA, Tukey's Multiple Comparison Test: ** $P<0.01$ vs PPP ***, $P<0.001$ vs PPP. Figure C shows the comparison between uncoated and coated crystals. Repeated measures ANOVA, Tukey's Multiple Comparison Test: ** $P<0.01$ coated vs uncoated.

Polystyrene-coated Crystals
Flow 100 $\mu\text{L}/\text{minute}$
Perfusion time 15 minutes

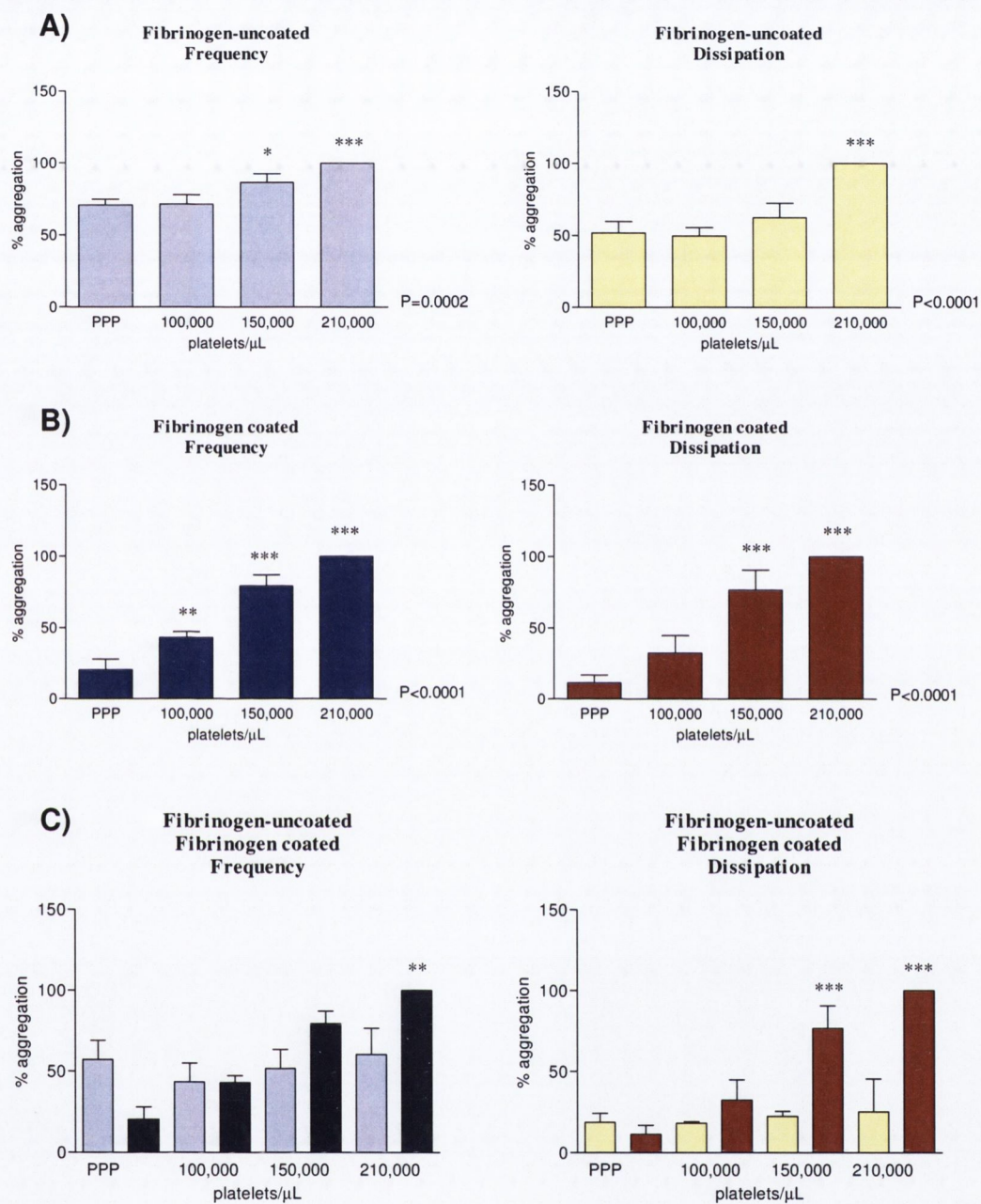


Figure 41: Frequency and dissipation in fibrinogen-uncoated and fibrinogen-coated polystyrene-coated crystals perfused with PPP and increasing concentrations of platelets (A and B) at 100 $\mu\text{L}/\text{min}$ (15 minutes). One-way ANOVA, Tukey's Multiple Comparison Test: * $P<0.05$ vs PPP, ** $P<0.01$ vs PPP, *** $P<0.001$ vs PPP. Figure C shows the comparison between uncoated and coated crystals. Repeated measures ANOVA, Tukey's Multiple Comparison Test: ** $P<0.01$ coated vs uncoated; *** $P<0.001$ coated vs uncoated.

Polystyrene-coated Crystals
Flow 100 $\mu\text{L}/\text{minute}$
Perfusion time 30 minutes

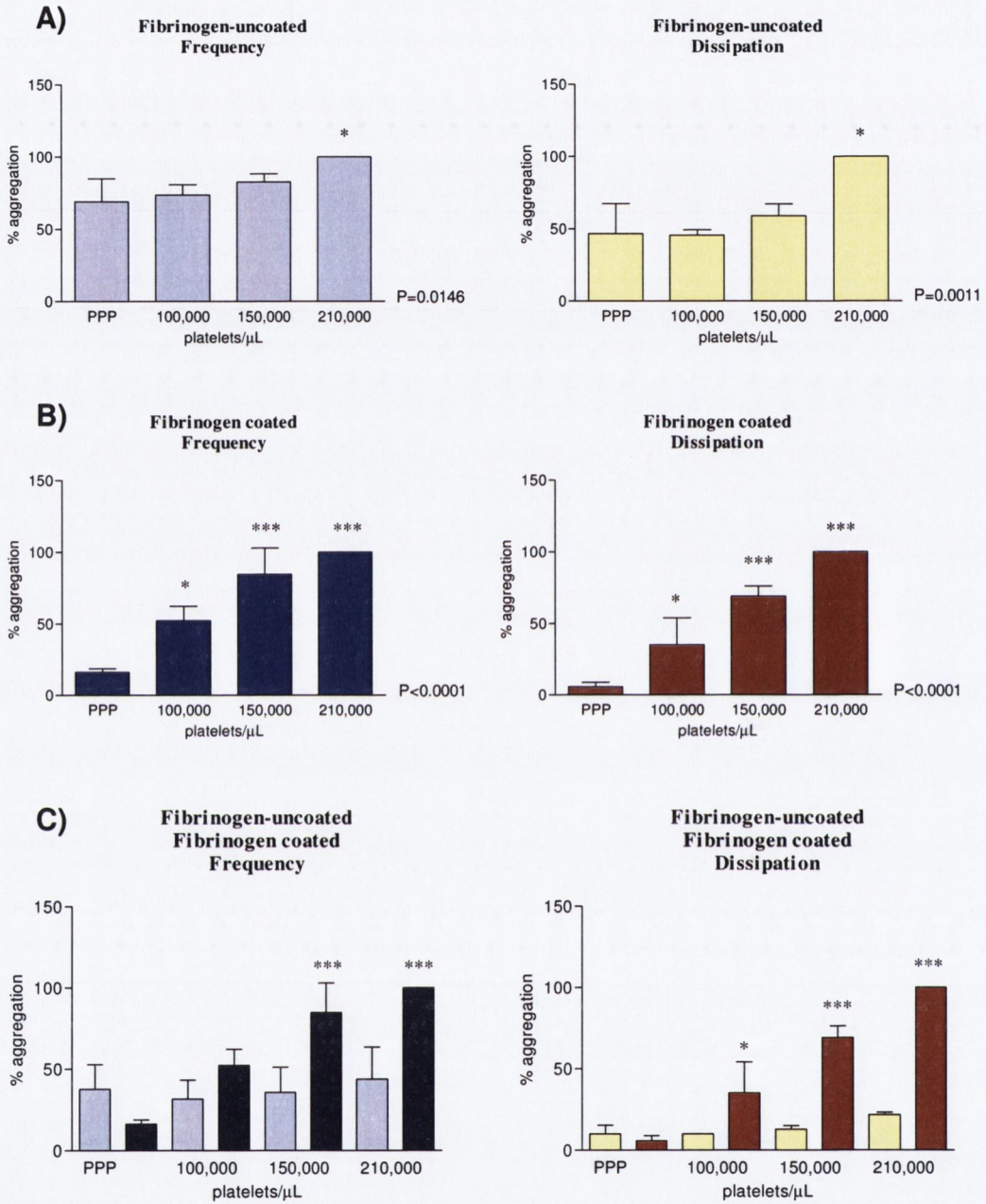


Figure 42: Frequency and dissipation in fibrinogen-uncoated and fibrinogen-coated polystyrene-coated crystals perfused with PPP and increasing concentrations of platelets (A and B) at 100 $\mu\text{L}/\text{min}$ (30 minutes). One-way ANOVA, Tukey's Multiple Comparison Test: * $P<0.05$ vs PPP, *** $P<0.001$ vs PPP. Figure C shows the comparison between uncoated and coated crystals. Repeated measures ANOVA, Tukey's Multiple Comparison Test: * $P<0.05$ coated vs uncoated; *** $P<0.001$ coated vs uncoated.

Polystyrene-coated Crystals
Flow 100 $\mu\text{L}/\text{minute}$
Perfusion time 45 minutes

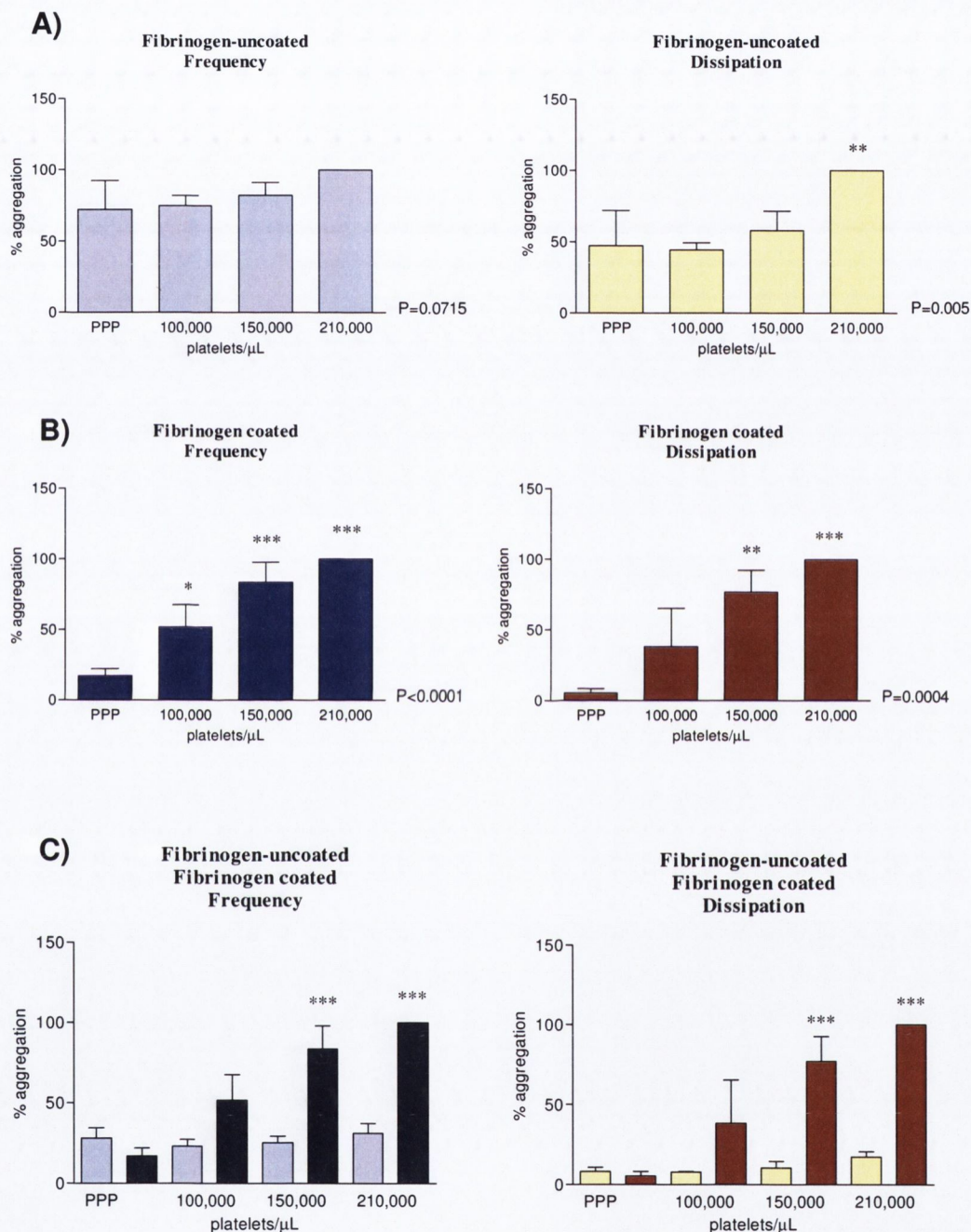


Figure 43: Frequency and dissipation in fibrinogen-uncoated and coated polystyrene-coated crystals perfused with PPP and increasing concentrations of platelets (**A** and **B**) at 100 $\mu\text{L}/\text{min}$ (45 minutes). One-way ANOVA, Tukey's Multiple Comparison Test: * $P<0.05$ vs PPP, ** $P<0.01$ vs PPP, *** $P<0.001$ vs PPP. Figure **C** shows the comparison between uncoated and coated crystals. Repeated measures ANOVA, Tukey's Multiple Comparison Test: *** $P<0.001$ coated vs uncoated.

Polystyrene-coated Crystals
Flow 100 μ L/minute
Perfusion time 60 minutes

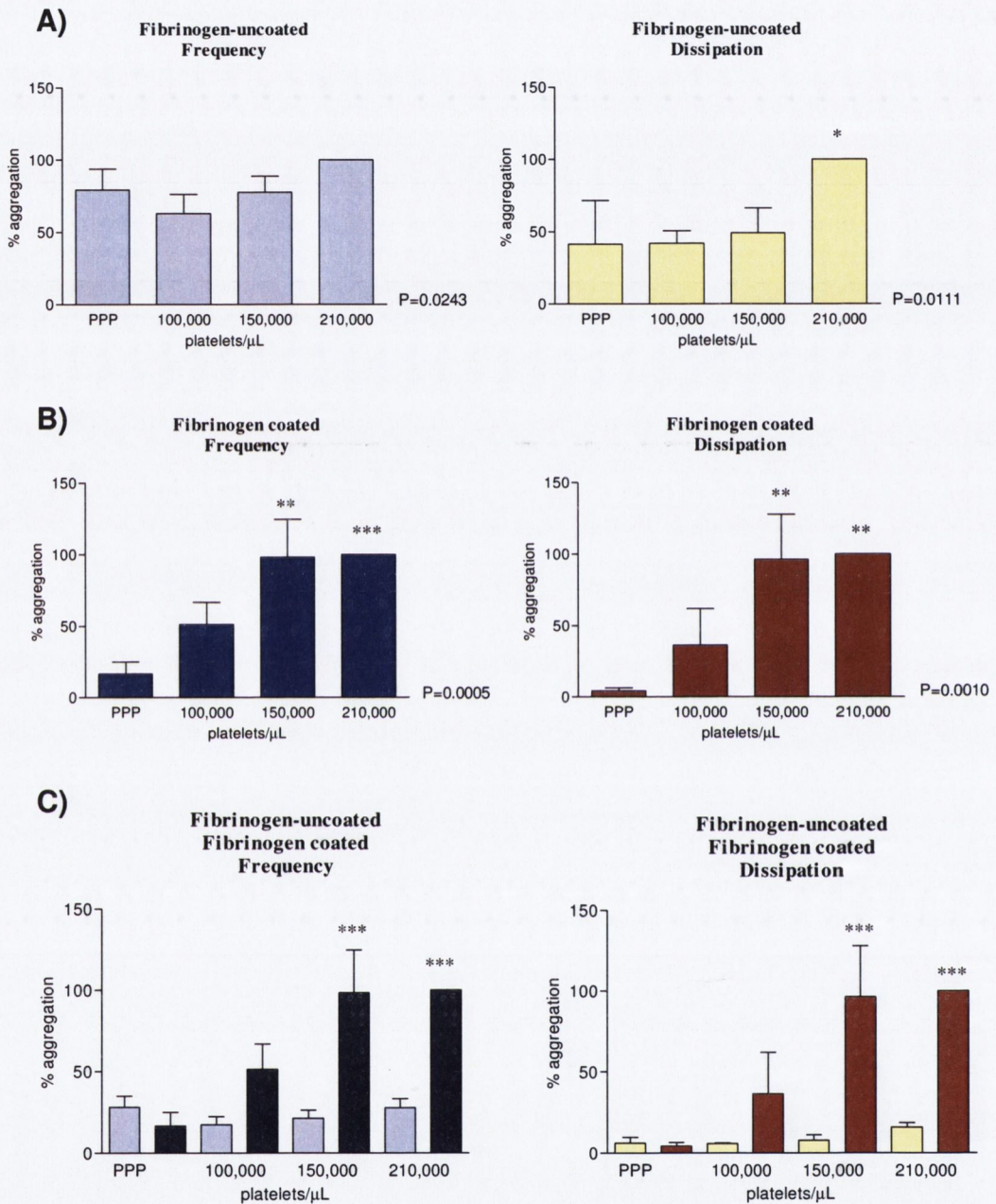


Figure 44: Frequency and dissipation in fibrinogen-uncoated and fibrinogen-coated polystyrene-coated crystals perfused with PPP and increasing concentrations of platelets (A and B) at 100 μ L/min (60 minutes). One-way ANOVA, Tukey's Multiple Comparison Test: * $P < 0.05$ vs PPP, ** $P < 0.01$ vs PPP, *** $P < 0.001$ vs PPP. Figure C shows the comparison between uncoated and coated crystals. Repeated measures ANOVA, Tukey's Multiple Comparison Test: *** $P < 0.001$ coated vs uncoated.

Polystyrene-coated Crystals
Flow 100 $\mu\text{L}/\text{minute}$
Perfusion time 60 minutes
Representative tracings

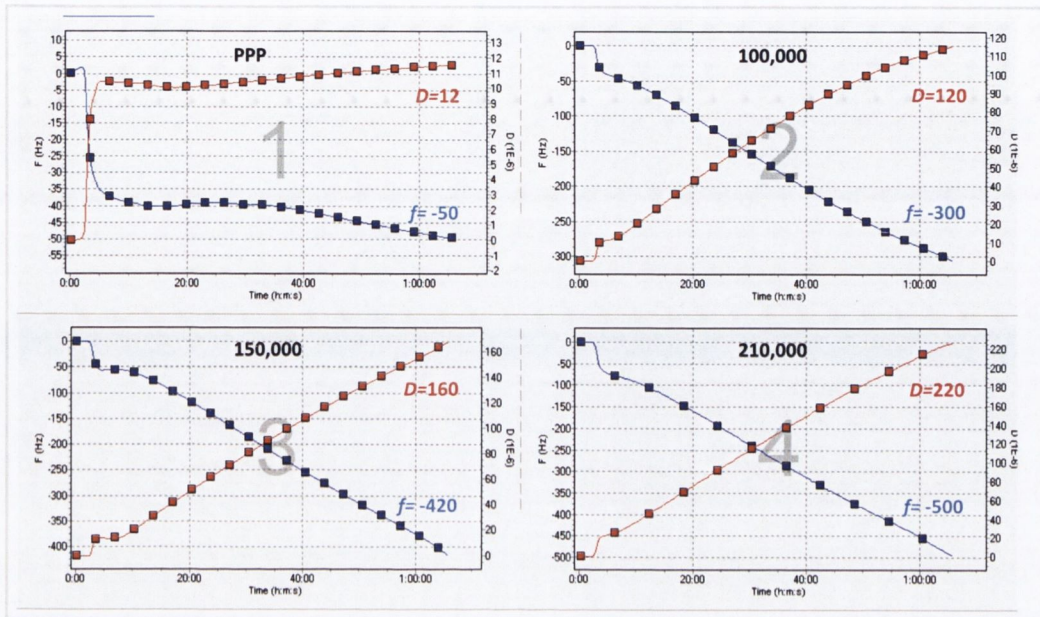


Figure 45: Effects of platelet concentrations on f and D . Representative tracings from experiments shown in Figure 44

The perfusion of fibrinogen-coated polystyrene-coated crystals at 100 $\mu\text{L}/\text{minute}$ led to a concentration-dependent decrease in f and increase in D . Representative tracings show the effects of PPP and increasing concentrations of platelets: 100,000; 150,000 and 210,000 platelets/ μL on f (blue line) and D (red line).

IMAGING OF SENSOR-INDUCED PLATELET AGGREGATION

PHASE CONTRAST MICROSCOPY

Sensor-induced platelet aggregation was first confirmed using phase-contrast microscopy. **Figure 46** shows platelet concentration-dependent formation of platelet aggregates on the surface of fibrinogen-coated polystyrene-coated crystals.

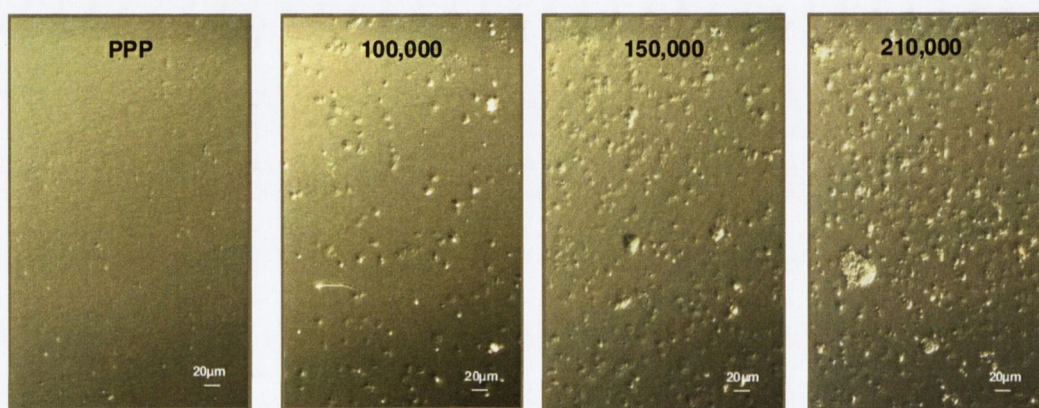


Figure 46: Effects of PPP and PRP perfused for 30 minutes on the microscopical appearance of fibrinogen-coated crystals as viewed in phase-contrast microscopy

Representative micrographs show accumulation of platelet aggregates on the surface of fibrinogen-coated crystals following perfusion of crystals with PRP (100,000; 150,000 and 210,000 platelets/ μ L), but not with PPP.

CONFOCAL MICROSCOPY

Following platelet activation, the major platelet receptor GPIIb/IIIa becomes activated and binds fibrinogen mediating platelet aggregation. At this stage platelets change their shape due to reorganisation of the platelet cytoskeleton. Therefore, immunofluorescence microscopy to study the interaction between the activated GPIIb/IIIa receptor (PAC-1) and the major cytoskeleton protein, actin was performed. As expected, the imaging revealed marked reorganization of the cytoskeleton (actin) with increased PAC-1 labelling on the surface of activated, but not resting platelets (**figure 47**).

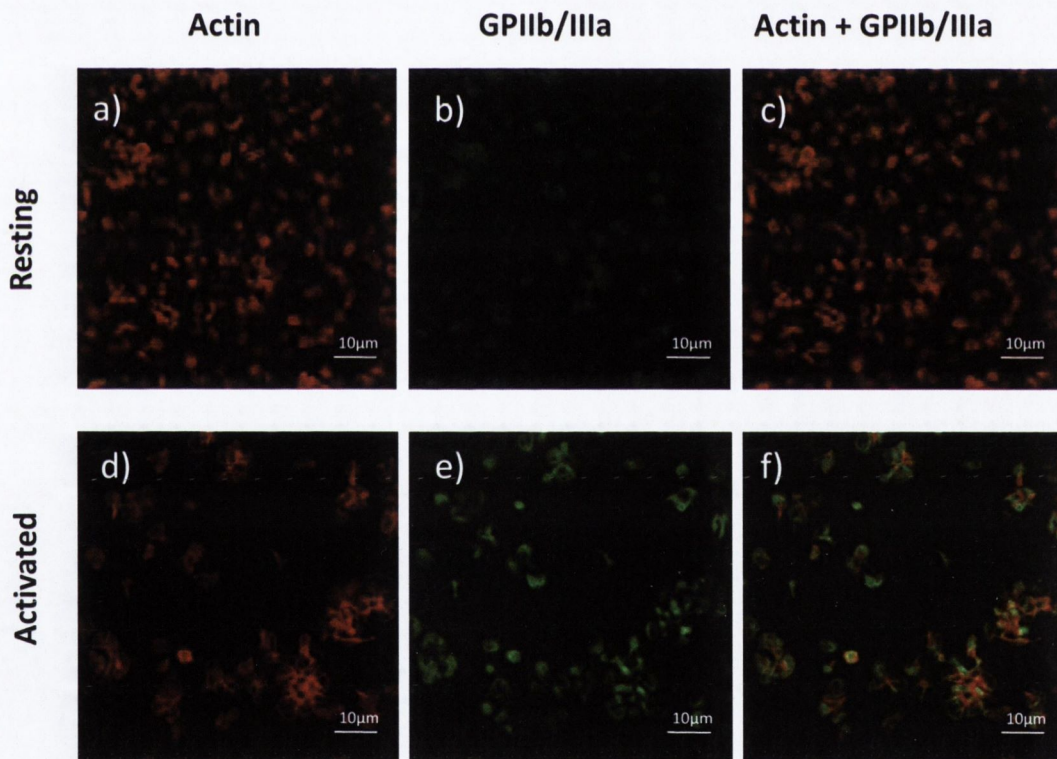


Figure 47: Co-localization of activated GPIIb/IIIa with actin in platelet cytoskeleton upon aggregation on sensor crystals.

Confocal microscopy of resting (a-c) and activated (d-f) platelets depict the interactions between GPIIb/IIIa, actin and cytoskeleton. Staining was performed with fluorescent-labeled antibodies against actin (a and d) or activated GPIIb/IIIa (PAC-1) (b and e). Digital merging of actin and PAC-1 images (c and f) shows co-localization of actin- and PAC-1-labeled structures. (*Imaging performed by Dr. Stephen Paul Samuels*)

ATOMIC FORCE MICROSCOPY

To study in detail morphological changes in activated platelets, atomic force microscopy was performed. In **figures 48** and **49** AFM height-based images with AFM-3D topography of platelets on fibrinogen-coated crystals show platelets aggregates and the morphological changes in single platelets with nanoscale resolution.

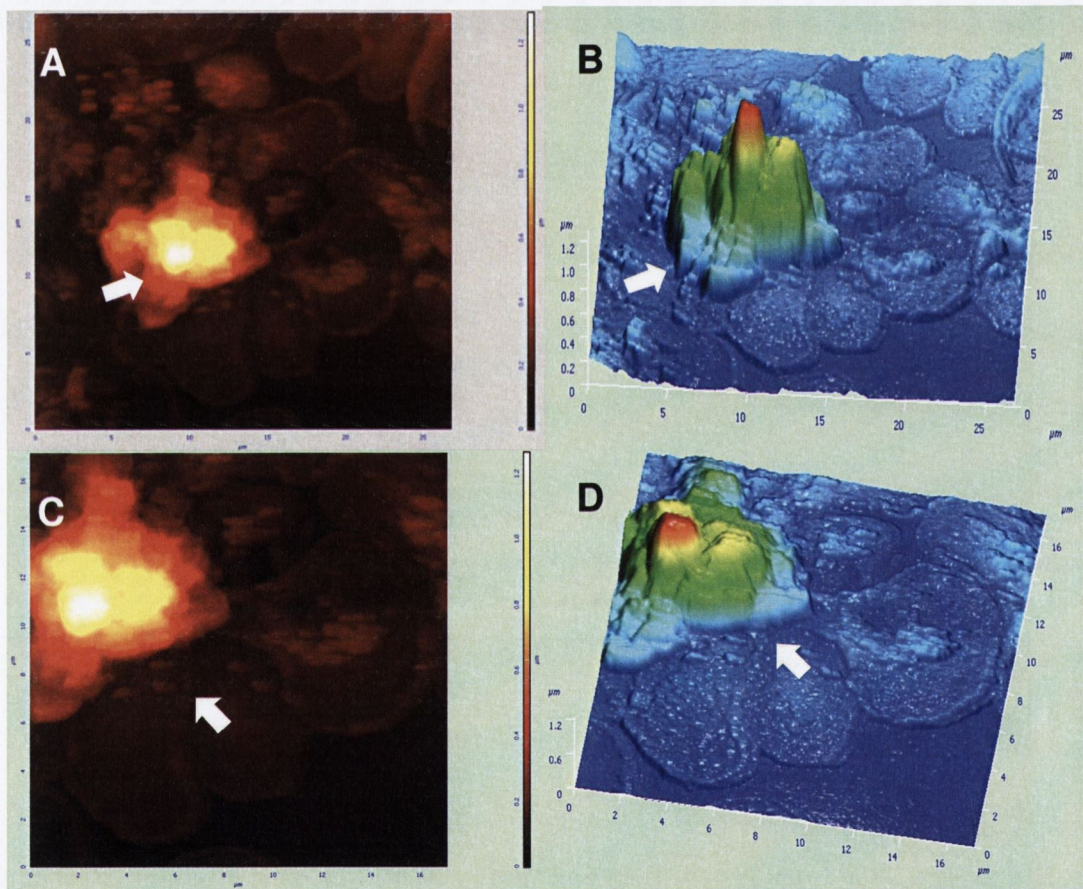


Figure 48: Platelet aggregation as imaged by AFM.

Platelets aggregates (white arrows) as imaged by AFM. Panels A and C show height images of platelet aggregates. Panels B and D show the same images in 3D. (Imaging performed by Dr. Stephen Paul Samuels)

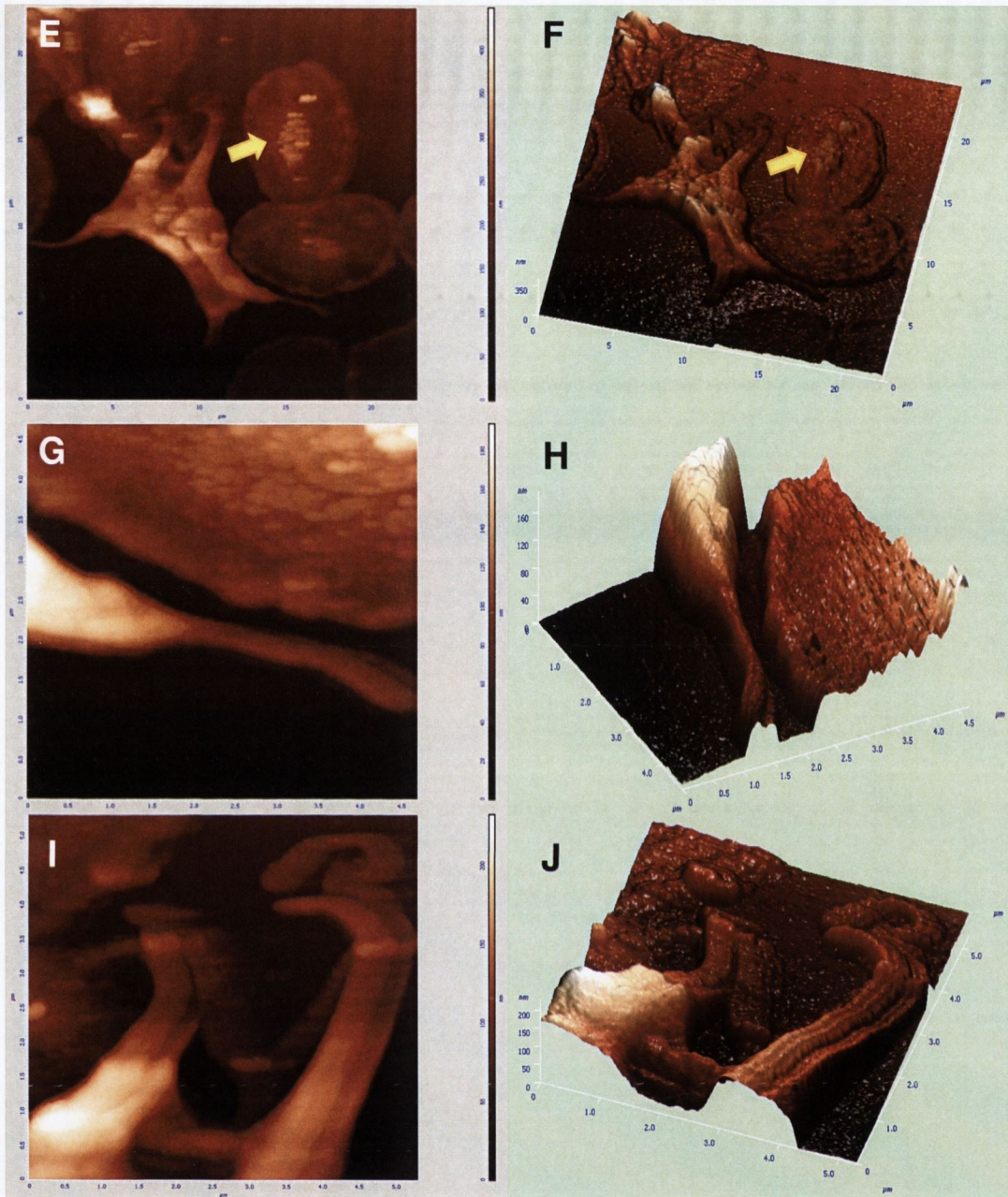


Figure 49: Activated single platelets as imaged by AFM.

Panels E, G and I show height images of platelets. Panels F, H and J show the same images in 3D. Panels E and F reveal the sequence of early and later stages of aggregate formation including spreading and shape change. Granular centralization and budding contributes to the formation of a pseudonucleus (fried egg-like) structure (yellow arrows) in single platelets. The appearance of finger-like projections (pseudopodia) heralds the later stages of platelet activation. Panels G, H, I and J show more in detail the pseudopodia. *(Imaging performed by Dr. Stephen Paul Samuels)*

EFFECTS OF PLATELET AGONISTS ON PLATELET AGGREGATION

Note: fibrinogen-coated polystyrene-coated crystals perfused with PRP at 100 $\mu\text{L}/\text{minute}$ for 30 minutes were chosen for these experiments.

For the investigation of the effects of platelets agonists under flow conditions using Q-Sense, fibrinogen-coated crystals were perfused with PRP in the presence or absence of ADP and TRAP. Both agonists enhanced D but not f as shown in **figures 50** and **51**. In addition, phase-contrast microscopy showed formation of larger aggregates in the presence of ADP and TRAP (**figure 52**).

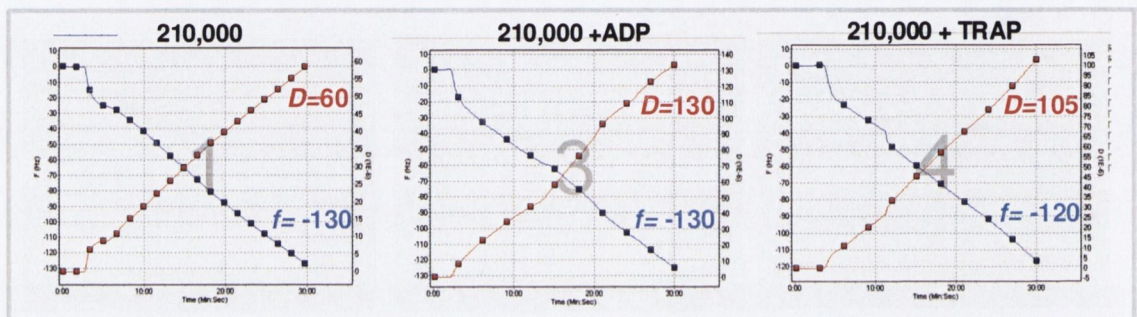


Figure 50: Effects of ADP and TRAP on f and D as measured by the device

Representative graphs show the effects of ADP and TRAP on f (blue line) and D (red line) for the 3rd overtone.

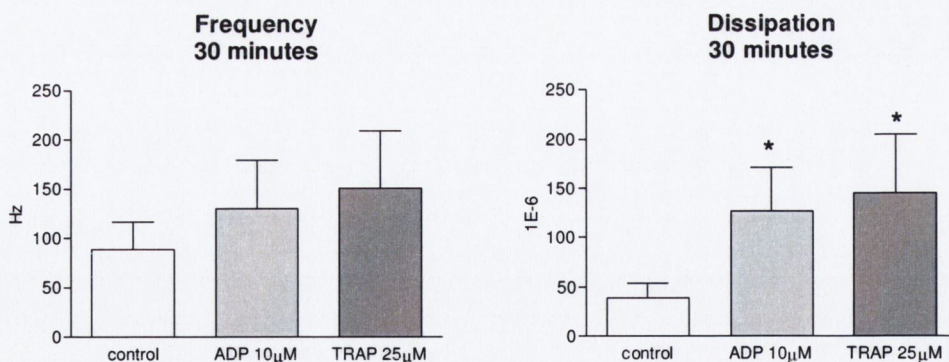


Figure 51: Effects on f and D of ADP and TRAP on fibrinogen-coated crystals

Both agonists did not significantly change f (repeated measures ANOVA, $n=4$; $P_f = 0.1371$) but increased D compared to control ($P_D = 0.0139$). Dunnett's Multiple Comparison Test: * $P < 0.05$ vs control.

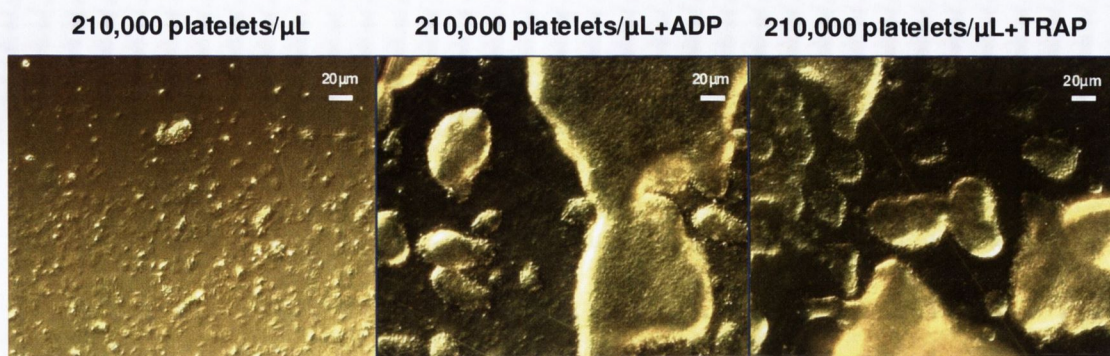


Figure 52: Potentiation by ADP and TRAP of platelet aggregation on fibrinogen-coated crystals as imaged by phase-contrast microscopy

Phase-contrast microscopy performed on the same samples showed the formation of larger platelet aggregates in the presence of ADP and TRAP when compared to control.

PHARMACOLOGY MODULATION OF PLATELET AGGREGATION

Note: fibrinogen-coated polystyrene-coated crystals perfused with PRP at 100 $\mu\text{L}/\text{minute}$ for 30 minutes were chosen for these experiments

The effects of a number of drugs that inhibit platelet aggregation acting at different stages of the platelet activation process were tested using the device. Changes in f and D measured by the instrument were calculated as percentage of aggregation, where control (210,000 platelets/ μL) was considered as 100% of aggregation.

EFFECTS OF COX INHIBITION ON PLATELET AGGREGATION

For the study of the effects of Aspirin on platelet aggregation, fibrinogen-coated crystals were perfused with PRP in the presence or absence of the compound. Aspirin was able to inhibit platelet aggregation, reducing the changes in both f and D compared to control (**figures 53 and 54**). In addition, phase-contrast microscopy showed the formation of smaller aggregates in the presence of ASA (**figure 55**).

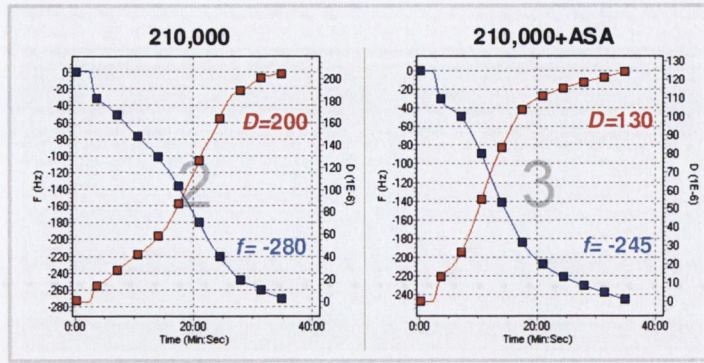


Figure 53: Effects of ASA on f and D on fibrinogen-coated crystals measured by the device

Representative graphs show inhibition by ASA of f (blue line) and D (red line) for the 3rd overtone compared to control.

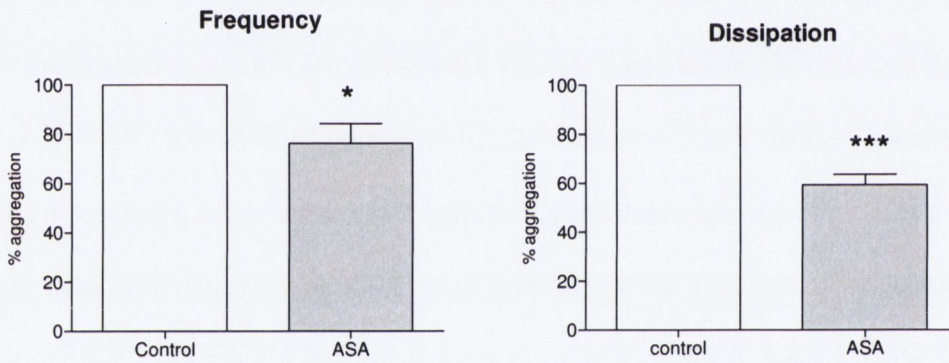


Figure 54: Statistical analysis of the inhibitory effects of ASA on sensor-induced aggregation

The inhibitory effect of ASA on platelet aggregation. Paired t-test, two tailed, $n=5$, *: $P_f=0.0409$, ***: $P_D=0.0007$.

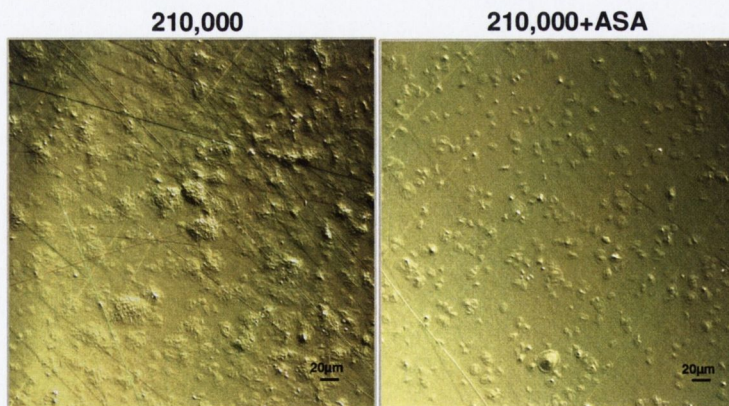


Figure 55: Reduction of aggregate size by ASA as imaged by phase-contrast microscopy

INHIBITION OF AGGREGATION BY MMP INHIBITOR, PHENANTHROLINE

The effects of a synthetic inhibitor of MMPs, phenanthroline, were investigated on fibrinogen-coated crystals perfused with PRP in the presence or absence of the compound. Phenanthroline inhibited platelet aggregation measured by the device (**figures 56 and 57**). When phase-contrast microscopy was performed, the presence of smaller aggregates in the presence of phenanthroline when compared to control was demonstrated (**figure 58**).

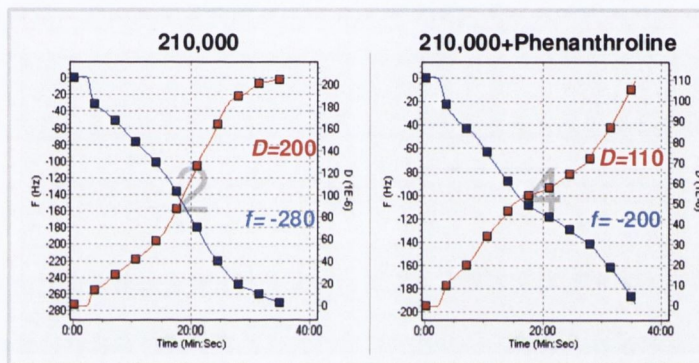


Figure 56: Inhibition by phenanthroline of f and D as measured by the device

Representative graphs show the effects of phenanthroline on f (blue line) and D (red line) for the 3rd overtone compared to control.

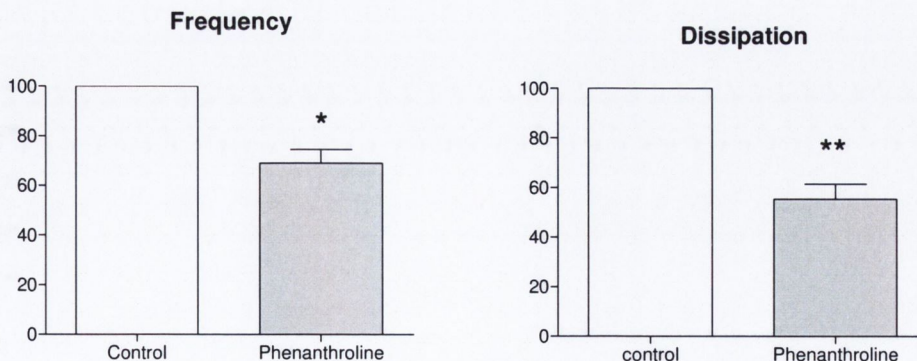


Figure 57: Inhibition by phenanthroline of f and D as measured by the device. The statistical analysis.

The perfusion of phenanthroline inhibited platelet aggregation. Paired t-test, two tailed, $n=4$, *: $P_f=0.0115$, **: $P_D=0.0055$.

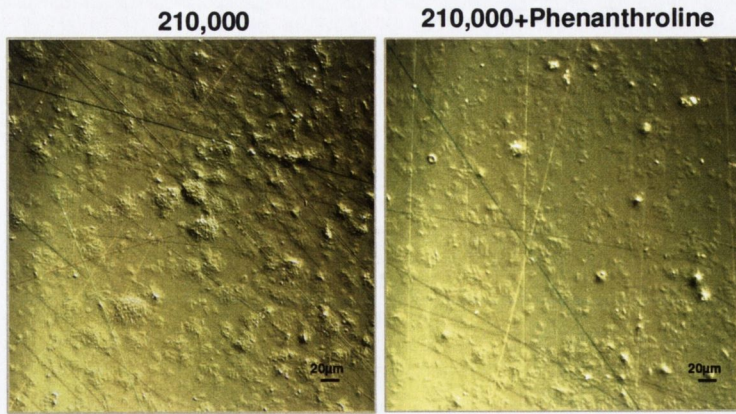


Figure 58: Inhibition by phenanthroline of aggregate size as imaged by phase-contrast microscopy

Phase-contrast, in the same donor, showed smaller platelet aggregates in the presence of phenanthroline when compared to control.

EFFECTS OF APYRASE AND MeSAMP ON PLATELET AGGREGATION

To test the contribution of the ADP-mediated pathway to platelet aggregation in the system, PRP in the presence or absence of apyrase and 2-MeSAMP was perfused on fibrinogen-coated crystals. Although 2-MeSAMP showed trend to decrease aggregation the effects of both compounds did not reach the statistical significance, none of the compounds significantly affected platelet aggregation (**figures 59 and 60**).

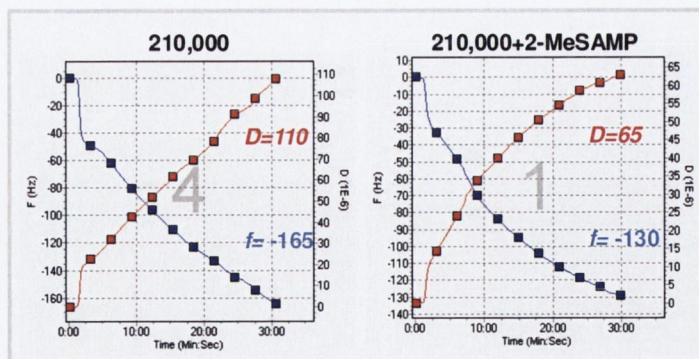


Figure 59: Effects of 2-MeSAMP on f and D as measured by the device

Representative graphs show the effects of 2-MeSAMP on f (blue line) and D (red line) for the 3rd overtone compared to control.

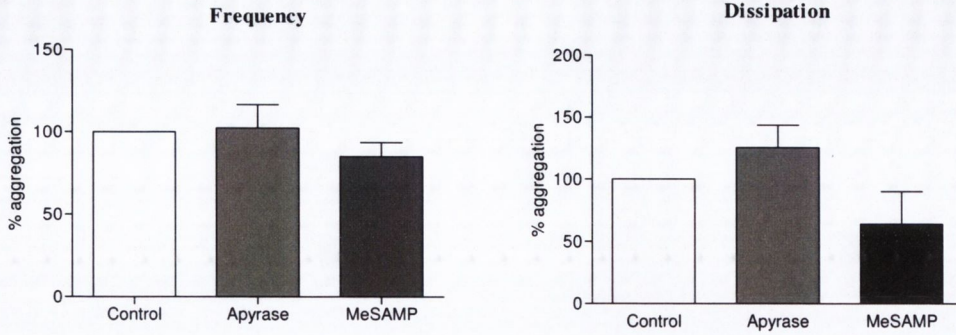


Figure 60: Effects of Apyrase and 2-MeSAMP on f and D . The statistical analysis

INHIBITION OF AGGREGATION BY GSNO AND SNAP

Since NO is a potent inhibitor of platelet activation and aggregation, we tested the effects of NO donors such as SNAP, a pharmacological agent, and GSNO, an endogenous inhibitor. Both compounds were able to inhibit platelet aggregation, reducing the changes in f and D compared to control (**figures 61 and 62**). Additionally, phase-contrast microscopy confirmed the formation of smaller number of aggregates in the presence of both NO donors (**figure 63**).

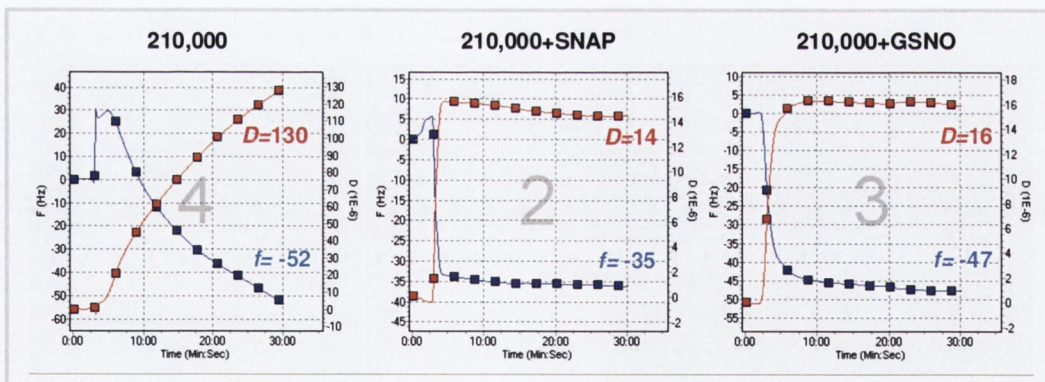


Figure 61: Inhibition by NO donors of f and D as measured by the device Representative graphs show the inhibitory effects of SNAP and GSNO on f (blue line) and D (red line) for the 3rd overtone compared to control.

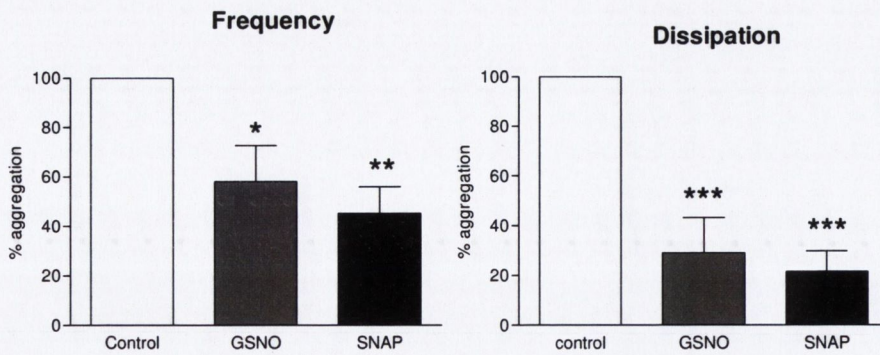


Figure 62: Inhibition by NO donors of *f* and *D*. The statistical analysis

The perfusion of GSNO and SNAP inhibited platelet aggregation. One-way ANOVA, $n=4$, $P_f=0.0125$, $P_D=0.0004$. Dunnet's Multiple Comparison Test: * $P<0.05$ vs control; ** $P<0.01$ vs control; *** $P<0.001$ vs control.

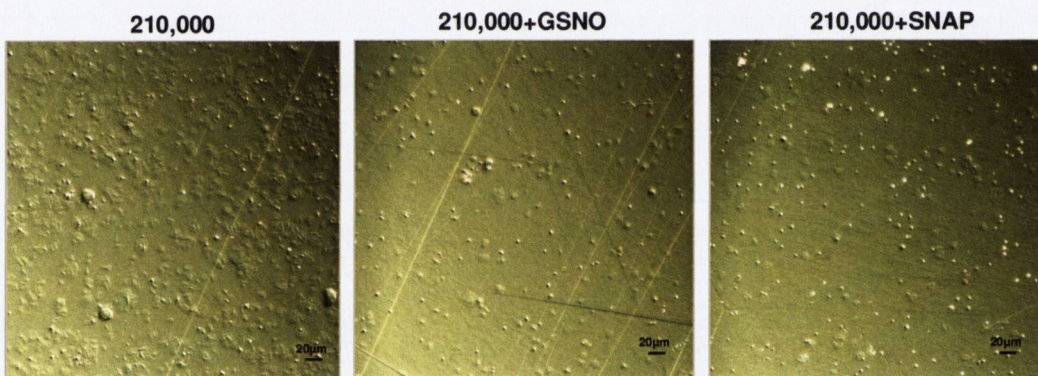
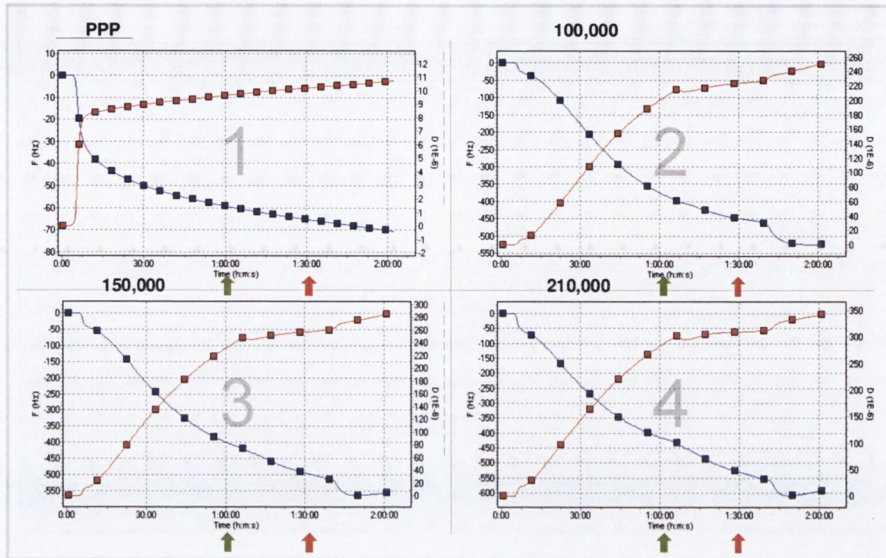


Figure 63: Reduction of platelet aggregate numbers by GSNO and SNAP as shown by phase-contrast microscopy

INHIBITION OF PLATELET ACTIVATION BY PROSTACYCLIN

Finally, as prostacyclin is the most potent endogenous inhibitor of platelet aggregation known so far, its effect on platelet aggregation in the system was tested. Prostacyclin was not only able to inhibit, but also reverse changes in *f* and *D* as shown in **figures 64 and 65**.

(A)



(B)

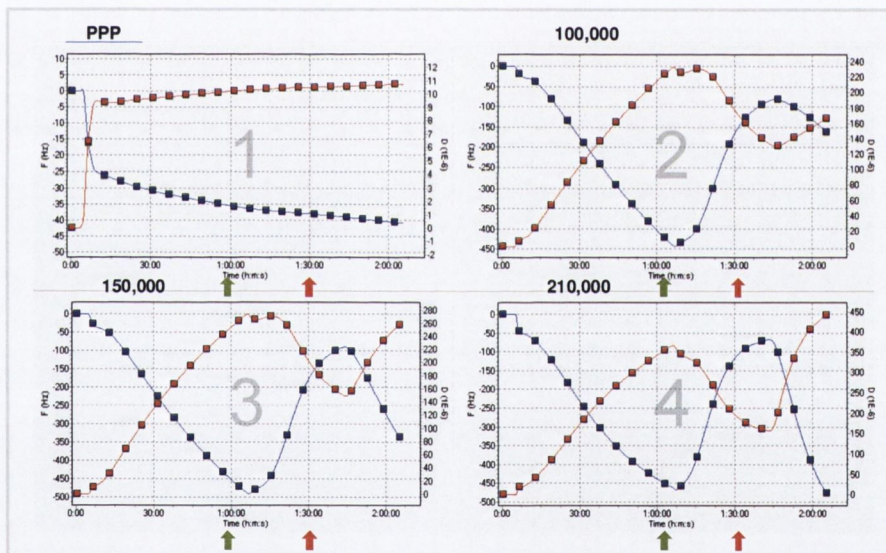


Figure 64: Prostacyclin-mediated inhibition of platelet activation.

Sensors were perfused with increasing concentrations of platelets (100,000; 150,000 and 210,000 platelets/ μL) or with platelet-free plasma (PPP) for 1 hour. Prostacyclin was then added for the remaining 30 min. Aggregation was measured for 30 min after the termination of prostacyclin infusion.

Prostacyclin inhibited (A) and reversed (B) the effects of platelet aggregation on f (blue line) and D (red line). As expected, prostacyclin exerted no significant effects on accumulation of PPP on the sensor surface. Green arrows: "prostacyclin on" and red arrows: "prostacyclin off". Tracings are representative of 3 similar experiments.

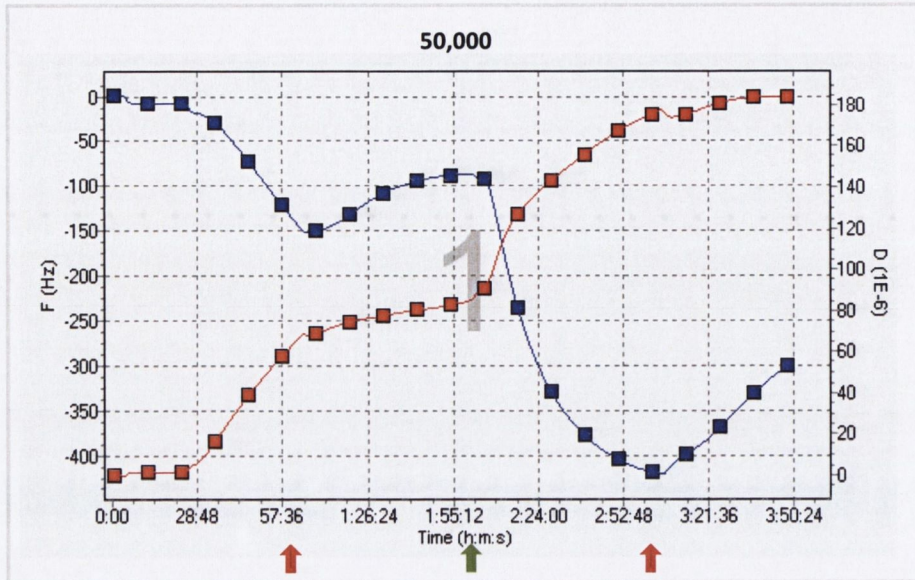


Figure 65: Prostacyclin-mediated inhibition of platelet activation in low-platelet-number samples

Sensors were perfused with 50,000 platelets/ μL for 1 hour. Prostacyclin was then added for the remaining 60 minutes. Aggregation was measured for 60 minutes after the termination of prostacyclin infusion and added again for another 40 minutes. Prostacyclin inhibited and reversed the effects of platelet aggregation on f (blue line) and D (red line). Green arrows: "prostacyclin on" and red arrow: "prostacyclin off". Tracings are representative of 3 similar experiments.

Q-TOOLS ANALYSIS USING VOIGT-BASED VISCOELASTIC MODEL

Using the Q-Tools software it is possible to estimate, with a Voigt-based viscoelastic model, the thickness and mass of the layer deposited on the surface crystal analyzing the f and D at three overtones. For this purpose, the changes in f and D induced by deposition of platelets and plasma proteins were measured simultaneously at 3rd, 5th and 7th overtones and modelled to calculate the thickness of the layer and the mass deposited on the crystal surface (figures 66-68).

In the next figures the Voigt-based viscoelastic modelling on experiments after the perfusion of different concentrations of PRP for the same donor are shown:

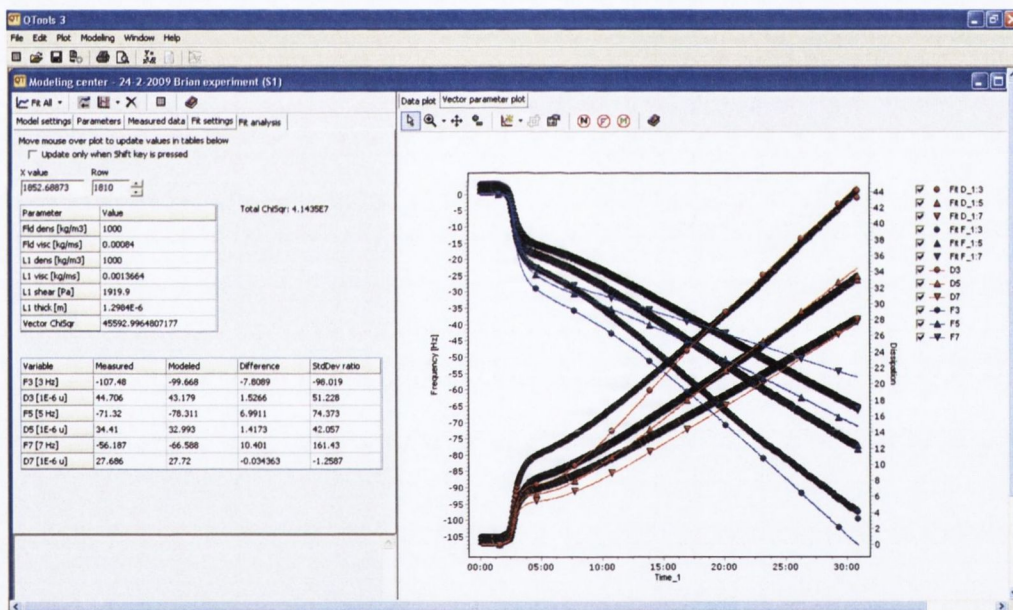


Figure 66: Q-Tools viscoelastic modelling screen for 100,000 platelets/ μ L

On the right, f and D responses for 3rd, 5th and 7th overtones vs time fitted using Q-Tools. On the left, parameters estimated using the Voigt-based viscoelastic model (including thickness). Perfusion of fibrinogen-coated polystyrene-coated crystals with PRP (100,000 platelets/ μ L) for 30 minutes led to a decrease in the f (blue lines) and increase in the D (red lines). The fitted lines are shown in blank colour. In this case the lines for the f and D measured by the Q-Soft and the fitted lines are not perfectly overlapped. The estimated thickness of the layer in this case is 1.298E-6 m (1.298 μ m).

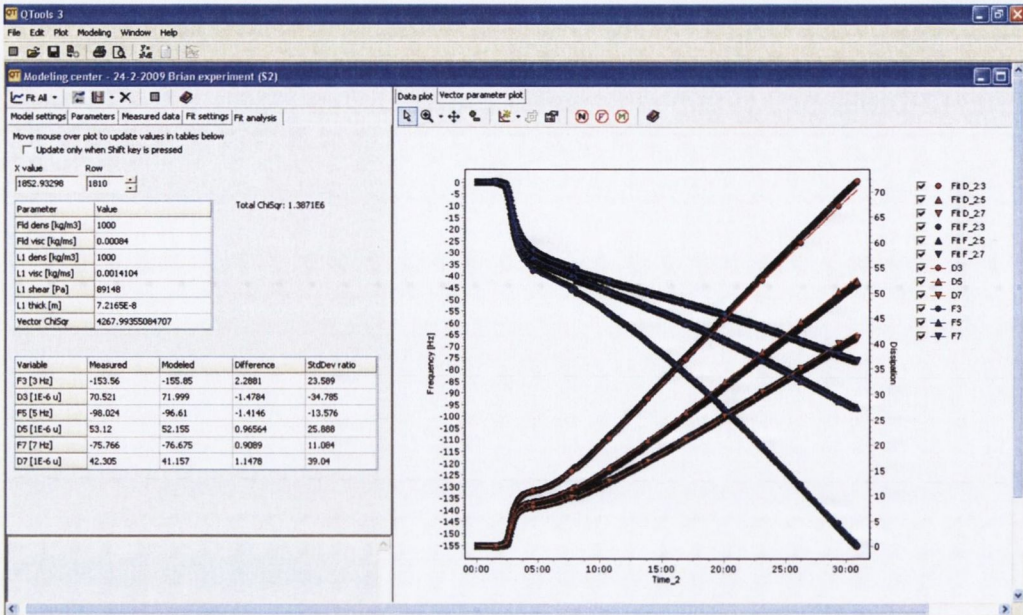


Figure 67: Q-Tools viscoelastic modelling screen for 150,000 platelets/ μL
Perfusion of fibrinogen-coated polystyrene-coated crystals with PRP (150,000 platelets/ μL) for 30 minutes led to a decrease in the f and increase in the D measured at three overtones (3^{rd} , 5^{th} and 7^{th}). In this case, the lines for the f and D measured by the Q-Soft and the fitted lines are perfectly overlapped. The estimated thickness of the layer is $7.2165\text{E-}8$ m (72.165 nm).

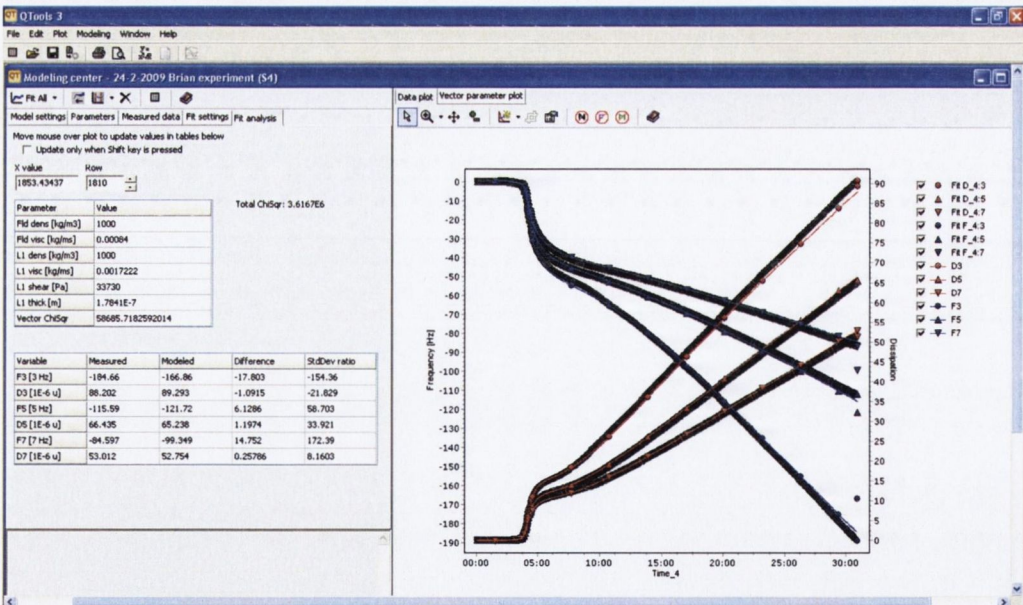


Figure 68: Q-Tools viscoelastic modelling screen for 210,000 platelets/ μL
Perfusion of fibrinogen-coated polystyrene-coated crystals with PRP (210,000 platelets/ μL) for 30 minutes led to a decrease in the f and increase in the D measured at three overtones (3^{rd} , 5^{th} and 7^{th}). In this case the lines for the f and D measured by the Q-Soft and the fitted lines are also perfectly overlapped. The estimated thickness of the layer is $1.784\text{E-}7$ m (178.4 nm)

Due to considerable differences in the fitting depending on the donor (data not shown) and the experimental conditions (**figures 66-68**), an alternative method was used to evaluate the accuracy of the Q-Tools modelling. For this purpose AFM imaging was performed on the same samples where the modelling was applied. Next, the image analysis on the height images was carried out using the Nova software (**figure 69**) and the average height for the fibrinogen layer and platelet aggregates was calculated (*by Ms. Jennifer Conroy*) and compared to the ones obtained using the Voigt-based model in the Q-Tools (**table 1**).

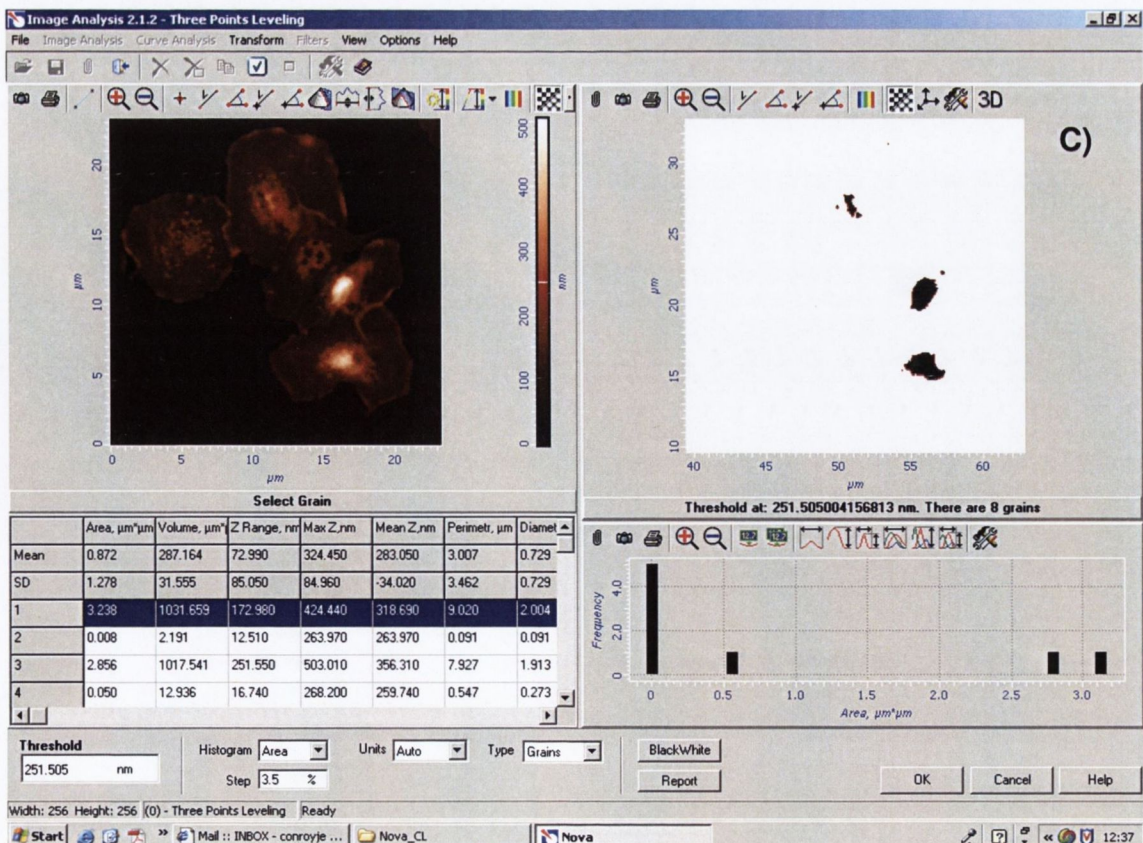
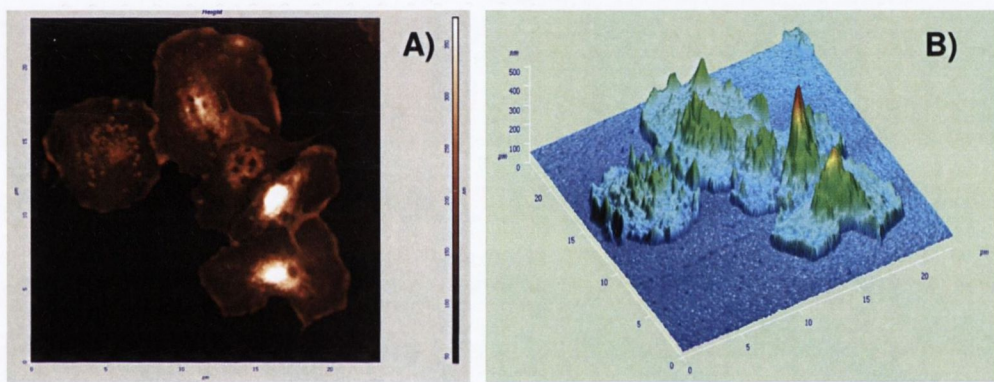


Figure 69: Atomic force microscopy analysis

Representative AFM height based images (A) with AFM-3D topography of platelets (B) on fibrinogen-coated crystals and analysis on the height images using the Nova software (C).

PRP concentrations	Q-Tools (Voigt-based model)	AFM (Nova software)
100,000 platelets/ μ L	1.298 μ m	570 nm+100nm*
150,000 platelets/ μ L	72.165 nm	503.2 nm+100nm*
210,000 platelets/ μ L	178.4 nm	1.314 μ m+100nm*

100nm* = fibrinogen layer thickness

Table 1: Thickness of the layer deposited on fibrinogen coated crystals

Estimated thickness by Q-Tools and AFM of the layer deposited on the crystal surface after perfusion of different concentrations of PRP for 30 minutes.

RHEOLOGY

The influence of flow rates and platelet concentrations on shear stress inside the perfusion chamber within the crystal active measurement area was also studied. The effect of bulk shear stress on platelet aggregation was quantified for 10, 20, 50, and 100 $\mu\text{L}/\text{min}$ at 37 $^{\circ}\text{C}$ (*calculations carried out by Dr. Adriele Prina-Mello*).

The volumetric flow rate Q injected through the peristaltic pumping system was incrementally fixed to 10, 20, 50 and 100 $\mu\text{L}/\text{minute}$ for all the experiments. The mean velocity was calculated using the formula $v_{mean} = Q/(wh)$ resulting in 0.17, 0.34, 0.84 and 1.7 mm/s respectively for the four flow rates and based on the geometry of the chamber. The shear rate γ in the crystal active measurement area was accounted for $\gamma = \delta v_{mean} / h$, where δ was calculated based on the mass and volume of the sample. The shear stress was given by $\tau = \gamma \cdot \eta$ where η was the dynamic viscosity measured for PPP and PRP at the three different concentrations of platelets (100,000; 150,000 and 210,000 platelet/ μL) and at four temperature ranges ($T_{mean} = 32, 34, 36$ and 38 $^{\circ}\text{C}$, $T_{bin} = 2$ $^{\circ}\text{C}$) (**figures 70-72**).

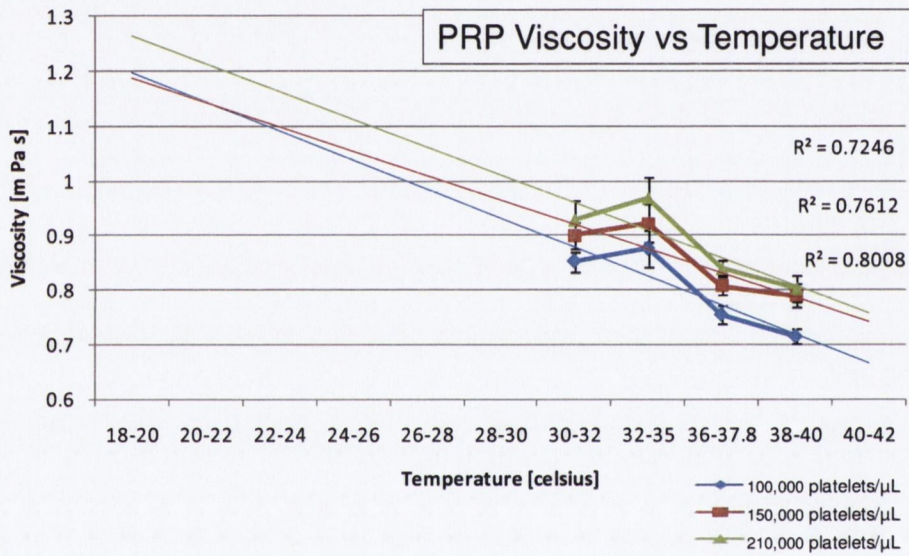
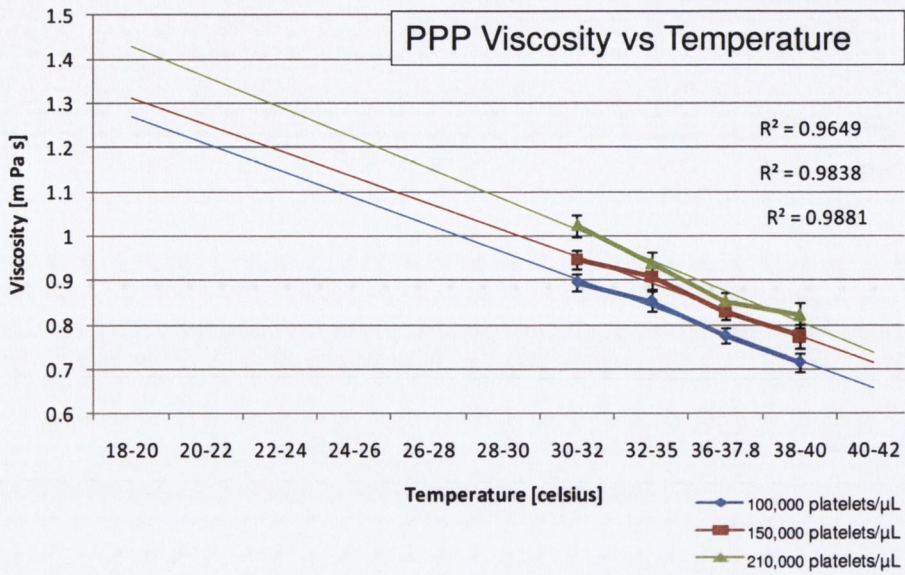


Figure 70: PPP and PRP viscosity measurements vs temperature

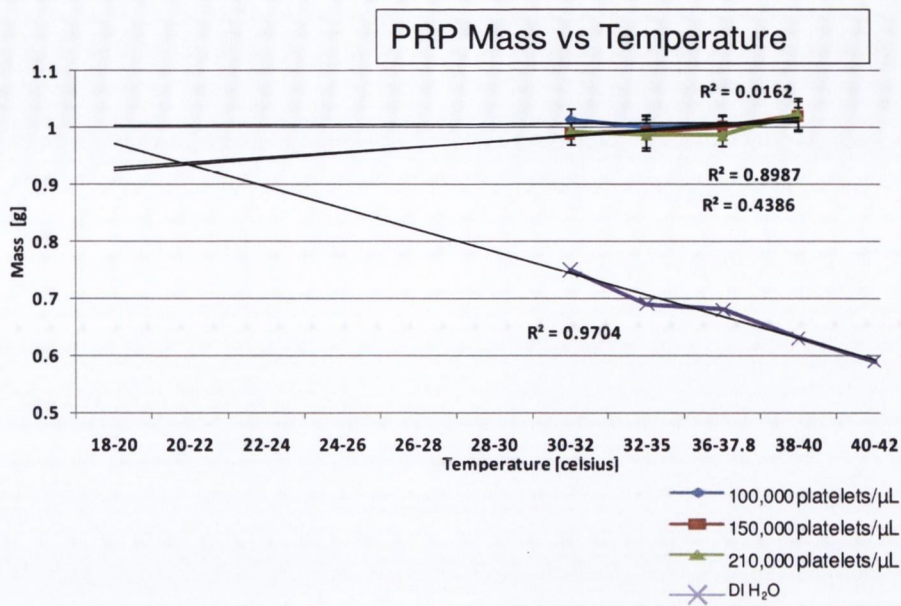


Figure 71: PRP mass measurements vs temperature

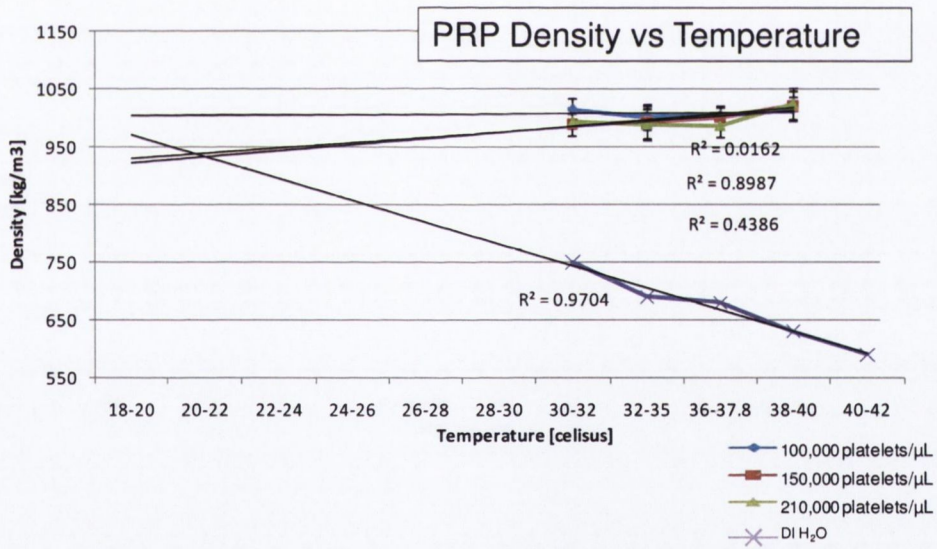


Figure 72: PRP density measurements vs temperature

Finally, to estimate the shear stresses at the same conditions where the experiments were performed, the averages of the measured density and dynamic viscosity at 37 °C were used for further calculations. As a result, the estimated shear stresses for the different concentrations of PRP (100,000; 150,000, and 210,000 platelets/ μL) and for the four different flow rates (10, 20, 50 and 100 $\mu\text{L}/\text{minute}$) ranged between 0.2 and 4.0 dyne/cm^2 (**figure 73**).

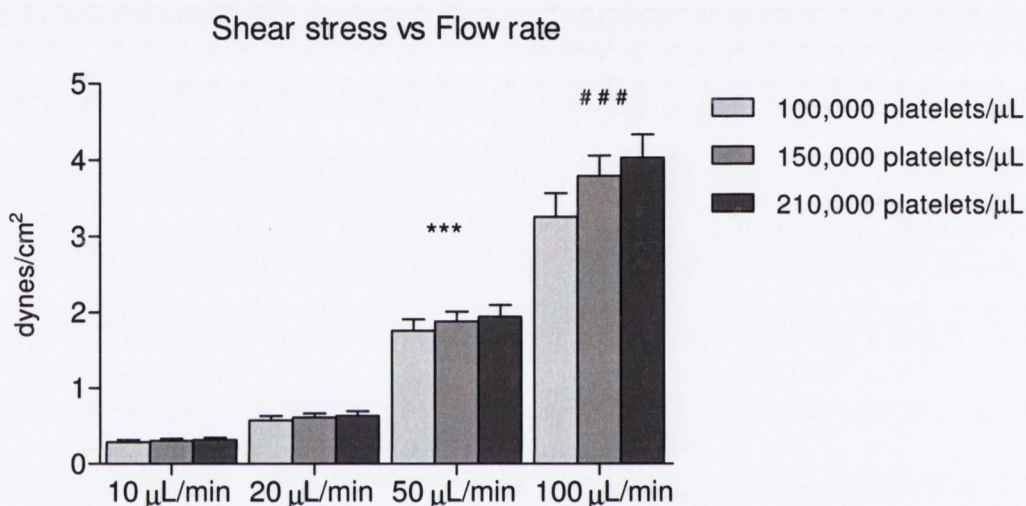


Figure 73: Shear stress vs flow rate

The increases in the flow rate were associated with an increase in the shear stress for all the different concentrations of platelets. One-way ANOVA, $n=8$, $P<0.001$. Tukey–Kramer’s multiple comparison tests: *** $P<0.001$, 10 $\mu\text{L}/\text{minute}$ vs 50 $\mu\text{L}/\text{minute}$; ### $P<0.001$, 50 $\mu\text{L}/\text{minute}$ vs 100 $\mu\text{L}/\text{minute}$.

DISCUSSION

The main physiological role of platelets is essential and fundamental contribution to haemostasis, the protective mechanism that prevents haemorrhage when the continuity of the vascular system is interrupted by traumatic injury. To exert their function, platelets survey the vascular system and adhere to the sites where alterations of the endothelial cell lining, accompanied or not by exposure of subendothelial matrix components, are detected (Ruggeri and Mendolicchio 2007). However, the frontier between physiological haemostasis and pathological thrombosis is very narrow, and it is recognized that platelets are at least partially responsible for the pathological development of atherothrombosis, the leading cause of death in the developed world (Davi and Patrono 2007). As a consequence, the participation of platelets in haemostasis and thrombosis has been extensively studied in the last decades. To date, different anti-platelet drugs have been used to inhibit platelet activation and thrombosis. The clinical effectiveness of such treatment with flagship drugs such as aspirin or clopidogrel is undeniable. However, monitoring the pharmacological effects of these drugs and individualizing treatments has been challenging as most of available assays test platelet function work under static conditions and/or in macroscale. There is widespread recognition of the need for a sensitive test of platelet function under flow conditions in nanoscale, which would allow the monitoring of the functional efficacy of drug in patients. Therefore, the main aim of my research was to investigate whether the QCM-D (Q-Sense E₄), a commercially available nanoscale resolution device, could be useful to measure flow-induced platelet aggregation.

METHOD CHARACTERISTICS

Three important questions needed to be addressed. Since nanoscale devices have great sensitivity and measure deposition of mass in nanograms, the first question to be addressed was if crystal sensors coated with fibrinogen could provide a platelet-activating surface and induce platelet aggregation. Secondly, whether using this system, the flow rate and shear stress could influence platelet aggregation. Finally, the effects of platelet agonists and inhibitors on platelet aggregation needed to be investigate using this device in order to compare them to other platelet aggregation-measuring devices.

FIBRINOGEN AS COATING SURFACE TO INDUCE PLATELET ACTIVATION AND AGGREGATION

Two different sensor crystals, polystyrene and gold quartz crystals, were used to study their interactions with platelets *in vitro* under flow conditions. Both crystals were previously coated with fibrinogen, a plasma protein, which is both necessary and sufficient for platelet interactions leading to platelet adhesion and aggregation. Indeed, an early feature of activation of platelets by different agonists is the exposure of specific glycoprotein receptors, particularly GPIIb/IIIa to which fibrinogen molecules bind with high affinity (Tailor, Cooper et al. 2005). In fact, patients suffering from fibrinogen disorders have been found to have long bleeding times (Vu and Neerman-Arbez 2007). In addition, fibrinogen is present in plasma and is adsorbed on biomaterial surfaces in much higher quantity than other adhesion proteins. Perfusion of fibrinogen-coated crystals with PRP led, as monitored in real-time by the device, to reduced f and increased D , and therefore accumulation of mass on the sensor

surface, in a platelet concentration-dependent manner. Moreover, the presence of platelet aggregates was confirmed by phase-contrast microscopy. In addition, perfusion of uncoated crystals with PRP led to reduced aggregation supporting the hypothesis that fibrinogen plays an important role facilitating platelet adhesion and aggregation on the surface of sensor crystals. Chin et al (Chinn, Horbett et al. 1991) have previously shown the similarity in the patterns of fibrinogen adsorption and platelet adhesion to surfaces exposed to a series of diluted plasma, suggesting a role for fibrinogen in mediating platelet adhesion to plasma preadsorbed surfaces. In addition, the same authors also showed that platelet adhesion to plasma-preadsorbed Biomer was almost completely inhibited when the plasma was deficient of human fibrinogen. Moreover, reconstitutions of afibrinogenemic plasma with exogenous fibrinogen lead to platelet adhesion in a dose-dependent manner. When confocal microscopy was performed on fibrinogen-coated crystals after perfusion of PRP using Q-Sense E₄, platelet cytoskeleton reorganization (visualized by anti-actin antibody) and the presence of activated GPIIb/IIIa receptors (stained with PAC-1 antibody) on the platelet membrane surface was shown. Furthermore, nanometer scale imaging analysis by AFM showed fried-egg-like platelets with budding granules and extended pseudopodia, that clearly indicated platelet activation (Karagkiozaki, Logothetidis et al. 2009). These results are consistent with previous studies which have shown that adhesion of platelets to materials coated with either fibrinogen or collagen can lead to platelet activation (Grunkemeier, Tsai et al. 1998).

However, it is not surprising that both crystals in the absence of fibrinogen also induced platelet aggregation. It is well known that exposure of different

materials to blood may lead to platelet activation, a key event in thromboembolic complications of different prosthetic devices in contact with the blood. In fact, platelet adhesion to biomaterials is often used as *in vitro* indicator of haemocompatibility (Salzman 1978; Study Group Of The Working Group On Valvular Heart Disease Of The European Society Of, Gohlke-Barwolf et al. 1995). When platelet aggregation induced by either fibrinogen-coated polystyrene or fibrinogen-coated gold crystals was compared, polystyrene crystals were found to be the best ones for the study of platelet aggregation in this *in vitro* model. Fibrinogen is a “sticky” protein with a strong tendency to adsorb well on most surfaces; in fact, it is well known that fibrinogen is an adhesive protein which is very well adsorbed on polystyrene (Chinn , Horbett et al. 1991; Tsai , Grunkemeier et al. 1999; Grunkemeier, Tsai et al. 2000). Indeed, Tsai et al (Tsai, Grunkemeier et al. 1999) studied the role of fibrinogen in mediating platelet adhesion to Immulon I, a polystyrene 96-well microtiter plate. They found that fibrinogen adsorption to polystyrene from afibrinogenemic plasma was much lower than that from normal plasma. Replenishment of fibrinogen into afibrinogenemic plasma caused an increase in platelet adhesion to Immulon I. Furthermore, when fibrinogen concentration in afibrinogenemic plasma reached that found in normal plasma, platelet adhesion level was comparable to that observed with normal plasma. Zhang et al (Zhang, Wu et al. 2008) studied the role of adsorbed fibrinogen in mediating platelet adhesion to polystyrene under flow conditions. Once again it was demonstrated that platelet adhesion to polystyrene pre-adsorbed with afibrinogenemic plasma was very low but restored in a dose-dependent manner with addition of fibrinogen. All these findings provide further support for

the conclusion that fibrinogen is the major plasma protein that mediates platelet adhesion to polymeric surfaces. Fibrinogen-coated gold crystals also induced platelet aggregation but to a lesser extent. It is possible that, in my experiments, fibrinogen adsorption onto the gold crystal surface was only partial, although some previous studies have shown that fibrinogen can be absorbed onto gold quartz crystals (Snopok, Kostyukevych et al. 1998; Hemmersam, Foss et al. 2005).

It should be also emphasized that other proteins, such as collagen and vWF are capable of inducing platelet activation via direct interaction with several platelet receptors. In fact, the initial binding of platelets at sites of vascular injury is mediated by GPIb/V/IX a structurally unique receptor complex expressed in megakaryocytes and platelets. Von Willebrand factor is the major ligand for one component of this complex, GPIb α , and the absence of the factor causes defects in primary haemostasis and coagulation (Mannucci 2004). Besides GPIb α , collagen receptors found on the platelet surface, particularly GPVI and GPIIb/IIIa also play an important role (Chen and Lopez 2005). For this reason, different experiments coating the crystals with collagen were also performed (data not shown), but the tubing was completely blocked after a few minutes of perfusion probably due to formation of large collagen fibrils. Therefore, I believe that this protein cannot be used in this experimental model. It remains to be demonstrated if vWF could be used for crystal coating to study platelet aggregation using Q-Sense E₄.

INFLUENCE OF FLOW RATE ON PLATELET AGGREGATION

Knowing that flow rates may influence platelet function, I studied the influence of different flow rates on platelet aggregation. The perfusion of PRP at physiological concentration of platelets (210,000 platelets/ μ L) resulted in a flow rate-dependent increase in platelet aggregation with maximal effect at 100 μ L/minute reemphasizing the concept that flow rate is essential to study platelet responses *in vitro* or *ex vivo*.

To date, the kinetics of aggregation has largely been studied under stirring in light transmission aggregometers with the following limitations. First, platelets normally adhere to damaged vessel walls in flowing conditions following three steps: 1) platelet activation and formation of pseudopodia; 2) formation of microaggregates; and 3) build-up of microaggregates to form large aggregates. Therefore, when platelet activation is weak and proceeds at low shear rates (such as generated by stirring) this results in large visible aggregates, which dissociate to microaggregates at near physiological shear rates. In contrast, strong platelet activation yields both microaggregates and large aggregates in stirred suspensions. For this reason, the study of platelet aggregation under stirring could underestimate the presence of microaggregates (Pedvis, Wong et al. 1988). Although Q-Sense E₄ is a low shear rate and shear stress flow system, it is extremely sensitive being capable of detecting ng quantities of mass deposited on the sensor surface. In fact, the presence of nano or microaggregates was detectable at real time by the device and demonstrated by different imaging techniques. Second, fluid shear rates in flowing blood may be minimal at the centre of the vessel, but become increasingly pronounced approaching the vessel wall (Kroll, Hellums et al. 1996). At the cellular level,

this has profound effects on initial contact, translocation, and firm adhesion of platelets under shear conditions. As platelet aggregation in our system is flow-dependent the method mimics well *in vivo* rheology. Third, antiplatelet agents presently available in clinical practice, which were originally tested in static or stirred conditions, have shown to be moderately successful in several thrombotic disorders. Therefore, pharmacological inhibitors of platelet aggregation should be ideally tested under conditions similar or identical to those of vascular blood flow.

PLATELET AGONISTS

The formation of a platelet aggregate requires the dramatic rearrangement of platelet cytoskeleton and may be induced by soluble activator agonists including thrombin and ADP. These factors trigger a biochemical cascade of events that is mediated via the release of major mediators from platelets including TXA₂ (Needleman, Moncada et al. 1976), ADP (Born 1962) and MMP-2 (Sawicki, Salas et al. 1997).

One of the most important proteins in haemostasis and vascular biology is thrombin, which is a multifunctional serine proteinase generated during the stimulation of coagulation. The main event in coagulation cascade is the conversion of soluble fibrinogen into insoluble fibrin, thus reinforcing the haemostatic plug. Thrombin also plays an important role in platelet activation and aggregation being the most potent platelet agonist *in vitro*. Thrombin actions are mostly mediated by proteinase-activated receptors (PARs) that convert an extracellular proteolytic cleavage event into an intracellular signal. It initiates a wide range of platelet responses: shape change, secretion of ADP,

serotonin and TXA₂, mobilization of the adhesion molecule P-selectin to the platelet surface, activation of GPIIb/IIIa complex, and the expression of procoagulant surface, which supports the generation of additional thrombin on platelet surface (Coughlin 2000). Four distinct PARs have been identified: the thrombin-sensitive receptors PAR1, PAR3 and PAR4, and the trypsin-activated receptor PAR2 (now known as F2R, F2RI1, F2RL2 and F2RL3, respectively). Mouse platelets express PAR3 and PAR4, whereas human platelets express PAR1 and PAR4. The activation of either PAR1 or PAR4 is sufficient to trigger platelet secretion and aggregation (Kahn, Nakanishi-Matsui et al. 1999).

ADP is a weak agonist that directly induces only shape change and reversible platelet aggregation, whereas the subsequent secretion and secondary aggregation are caused by the ADP-induced synthesis of TXA₂. However, ADP is essential in platelet function because, after being secreted from the platelet δ -granules, where it is stored, it amplifies the responses induced by other agonists. Pharmacological studies using selective antagonists have shown that ADP-induced platelet aggregation is largely mediated by P2Y₁ and P2Y₁₂ (Gachet 2001). P2Y₁₂ is the central receptor and target of thienopyridine antiplatelet drugs, which bind irreversibly to it. However, the coactivation of both P2Y₁ and P2Y₁₂ is necessary for normal ADP-induced aggregation to occur (Gachet 2008). The stimulation of P2Y₁ and P2Y₁₂ receptors by ADP assists in exposing the binding sites on the fibrinogen receptor, GPIIb/IIIa, culminating in platelet aggregation. If the contribution of P2Y₁ were eliminated, virtually no platelet activation by ADP would occur. In P2Y₁₂-deficient patients, the contribution of P2Y₁ would emerge on exposure to ADP, with the

associated shape change and then the transient aggregation response, but lacking the secondary wave for a full aggregation response (Gachet 2006).

In the present study, ADP and TRAP, which activates PAR1 and PAR4, were used as pharmacological agonists. It was found that both agents amplified platelet aggregation as monitored by increased D and large aggregate formation in phase-contrast microscopy when compared to control. Interestingly, the changes in f were not detected in these experiments. This is likely to be due to large aggregate formation and deposition of thick viscoelastic layer of platelets on the sensor surface. In fact, D appears to be more accurate than f to evaluate big viscoelastic layers. While both f and D reflect deposition of adhering platelets and small aggregates on crystals, the deposition of larger aggregates is more accurately reflected by changes in D .

PLATELET INHIBITORS

To evaluate the relative contribution of TXA₂, MMP-2 and ADP-dependent pathways to platelet aggregation using the device, respective inhibitors of these pathways such as aspirin (COX inhibitor), phenanthroline (MMP inhibitor), apyrase (ADP scavenger) and 2-MeSAMP, which is a selective P2Y₁₂ receptor antagonist, were tested. In the experiments described in this Thesis, both aspirin and phenanthroline were able to inhibit platelet aggregation showing the involvement of TXA₂ and MMP-2 in this process. However, apyrase and 2-MeSAMP did not exert significant effects on platelet aggregation indicating that the release of ADP from platelets was low under the experimental conditions used.

It's well known that TXA₂ is the major arachidonic acid product in platelets and that promotes thrombosis, aggregating platelets and inducing vasoconstriction in blood vessels. TXA₂ mediates platelet aggregation by stimulating platelet thromboxane receptors known as TP-receptors. This interaction leads to activation of PLC which results in the formation of IP₃ and DAG and therefore to an increase in intracellular Ca⁺⁺ and activation of PKC (Offermanns 2006). Aspirin reduces platelet aggregation inhibiting TXA₂ production by inhibiting platelet COX, an effect lasting for the entire life span of the platelet as platelets are anucleate elements and cannot synthesize *de novo* proteins such as COX (Burch, Stanford et al. 1978).

MMPs play an important role in platelet aggregation. The release of MMP-2 has been shown to mediate a novel pathway of platelet aggregation (Sawicki, Salas et al. 1997). During aggregation MMP-2 is translocated to the platelet surface membrane (Sawicki, Sanders et al. 1998). Recently it has been demonstrated that MMP-2 binds to the GPIIb/IIIa receptor on platelet surface upon platelet activation *in vitro* (Choi, Jeon et al. 2008) . Furthermore, MMP-9 has been shown to counteract the pro-aggregating effects of MMP-2 by inhibiting platelet aggregation (Fernandez-Patron, Martinez-Cuesta et al. 1999) . Phenantroline is a non-selective synthetic inhibitor of MMPs, therefore it can inhibit both MMP-2 and MMP-9. However, phenantroline was able to inhibit platelet aggregation using this flow system, suggesting that MMP-2 is the dominant MMP released during this process. These results are in agreement with previous studies in our laboratory which showed that phenantroline was able to inhibit platelet aggregation (Sawicki, Salas et al. 1997; Jurasz, Sawicki et al. 2001; Medina, Jurasz et al. 2006).

The vascular endothelium generates factors that modulate the interactions between platelets and the vascular wall. Endothelial cells synthesize and release a number of factors, including prostacyclin, NO, bradykinin, endothelium-derived hyperpolarising factor (EDHF), TXA₂ and endothelin, which regulate vascular tone and control platelet and leukocyte adhesion, aggregation and migration (Jurasz, Radomski et al. 2000). Prostacyclin and NO are the most important platelet inhibitors generated from endothelium. Impaired endothelial function leads to enhanced thrombogenicity due to increased adhesion of activated platelets and leukocytes. In fact, endothelial dysfunction plays a major role in the development of atherosclerosis and ischaemic heart disease, and both prostacyclin and NO deficiencies have been implicated in the pathogenesis of these vascular disorders (Egashira 2002). The inhibitory effects of prostacyclin on platelets are cAMP-dependent. It has been found that prostacyclin not only inhibits platelet aggregation, but also disaggregate platelets (Moncada 1981). Therefore, the effect of prostacyclin using Q-Sense E₄ was tested. Prostacyclin was not only able to inhibit platelet aggregation, but also caused disaggregation as monitored in real-time, an effect similar to that in vivo. These results are in agreement with a number of studies performed in our lab showing the antiplatelet effect of prostacyclin both in agonist and tumour cell-induced platelet aggregation (TCIPA) (Jurasz, Stewart et al. 2001; Radomski, Stewart et al. 2001).

Nitric oxide through a cGMP-dependent mechanism has the ability to maintain the vasodilator tone and inhibit platelet function. In fact, NO may inhibit both platelet adhesion to the endothelium (Radomski, Palmer et al. 1987c) , and subsequent platelet aggregation (Radomski, Palmer et al. 1987a). In the

experiments described in this Thesis, it was found that two NO-releasing agents, GSNO and SNAP, inhibited platelet aggregation as measured by the device and demonstrated by phase-contrast microscopy. Again, these results are in agreement with previous studies performed in our lab showing the inhibitory effect of these compounds both in agonist and TCIPA (Jurasz, Sawicki et al. 2001; Jurasz, Stewart et al. 2001; Radomski, Stewart et al. 2001). Indeed, it has been shown that both GSNO and SNAP may inhibit the release of MMP-2 during TCIPA, indicating a “cross-talk” between NO and MMP-2 (Jurasz, Sawicki et al. 2001).

METHOD EVALUATION

The use of the Q-Sense E₄ for the study of platelet function provides a new methodology to quantify the onset of aggregation and subsequent phenomena under conditions of low shear stress (<4 dyne/cm²). Under situations of low shear stress, bound fibrinogen promotes platelets to adhere firmly via platelet GPIIb/IIIa receptors (Savage, Saldívar et al. 1996). In fact, when fibrinogen-coated crystals were perfused with PRP platelet aggregation was demonstrated by imaging techniques such as phase-contrast microscopy and AFM, and increased expression of activated GPIIb/IIIa receptors was shown by immunofluorescence microscopy.

Previous studies adopted well-established and well-characterised models to carry out *ex vivo* measurements (Kroll, Hellums et al. 1996; Sakariassen, Hanson et al. 2001). These were based on large volume (mL/min), high shear rate (>1000 s⁻¹) and high shear stress (>100 dyne/cm²) models. With recent advances in nanotechnology it is now possible to custom-design a microfluidics system which can perform high-throughput screening of multiple antiplatelet agents with low shear stresses requiring only a few microlitre of blood (Gutierrez, Petrich et al. 2008). Nanotechnology, therefore, offers a unique scalability in the model validation of the shear-dependant platelet aggregation. The Q-Sense balance is a commercially available research device equipped with micrometre sized flow chambers, requiring 0.3-3.0 mL of PRP for each assay. This makes it less suitable for high-throughput screening (in the current Q-Sense configuration only four samples are simultaneously measured). This method does allow, however, real-time, *ex vivo*, high-sensitivity, precise measurements of platelet aggregation in physiological, clinical and

pharmacological studies. These measurements can be easily supplemented by direct imaging of platelet aggregates on the sensor crystals using standard phase-contrast microscopy, highly advanced confocal imaging, AFM or scanning electron microscopy. In a previous study the QCM-D has been used to quantify platelet morphological changes by electron microscopy focusing on the platelet primary adhesion process on a mix of fibronectin and albumin deposited on silica crystals (Fatisson; Merhi et al. 2008). Weber et al. (Weber, Wendel et al. 2005) have investigated the binding kinetics of GPIIb/IIIa to polymer-adsorbed fibrinogen using QCM-D correlating the results with platelet adhesion to the polymer surfaces by scanning electron microscopy. However, this is the first time that a QCM-D has been used for the study quantitatively and qualitatively platelet function with nano resolution. Furthermore, it has been demonstrated that sensor-induced platelet aggregation is amenable to regulation by standard physiological and pharmacological agents.

The sensitivity limits of the Q-Sense system allow for platelet measurement within the sensor area which is almost 1000 times larger than a platelet. Interestingly, Reynolds numbers were found to be all <1 which guarantees continuous laminar flows with negligible non-linear effects. Since the surface shear stress is proportional to the channel depth, the adhesion of platelets to the substrate is expected to increase the shear stress. However as an aggregate had an average height of $\sim 1.5 \mu\text{m}$ (measured by AFM technique), the reduction in channel depth by platelet aggregation on the surface of crystals accounted for only 0.5 % of channel depth, which in the other hand facilitate the Q-Sense precise measurements.

Real-time, dynamic measurements of the effects of prostacyclin on aggregation induced at very low concentrations of platelets (50,000/ μ L) point to the ability of this method to quantify platelet function in low-platelet concentrations samples such as from patients with thrombocytopenia or neonates.

Q-TOOLS ANALYSIS

An increase in the mass bound to the quartz crystal causes the crystal's oscillation frequency to decrease. The linear Sauerbray equation has been widely used to quantify the mass added to the surface at nanogram level. However, the Sauerbray equation does not apply in situations where the mass bound to the surface behaves as a complex viscoelastic layer. In these cases it is difficult, if not impossible, to extract corresponding mass binding quantities from decreases observed in the crystal frequency (Marx 2003). In cellular adsorption applications, the f and Sauerbray relationship would greatly underestimate the adsorbed mass of cells. When the adsorbed mass is viscous and sufficiently soft it does not follow the sensor oscillation perfectly (such as in the case of cells) leading to internal friction (due to the deformation) and thus to dissipation. Therefore, monitoring cell adsorption requires using the D parameter to fully characterize the adsorption of a viscoelastic cellular structure (Dixon 2008). Interestingly, the inapplicability of the Sauerbray equation to cell attachment has been demonstrated in a study with platelets (Muratsugu, Romanschin et al. 1997). In that study the f response produced by binding human platelets was compared to the calculated cell mass bound via measuring a ^{51}Cr radiolabel incorporated into the cells. Using the measured f decrease following cell attachment, converted to effective bound mass using

the Sauerbray equation, the value was found to be 200 times less than the actual bound cell mass based on their radiolabeled measurements. However, using a Voigt-based viscoelastic model included in the Q-Tools software, it is theoretically possible to estimate the adsorbed mass of the layer deposited on the surface-sensor taking into account not only f but also D recorded by the device at three different overtones. When the model was applied to estimate the thickness and mass of platelets deposited on the sensor surface in my experiments, some concerns arisen. First, when the Voigt-model was applied to a set of experiments, the fitting obtained differed depending on the donor. Secondly, even when the model was applied to different experiments from the same donor differences in the fitting were also observed. To overcome these problems, the real density and viscosity measured by viscosimeter for the different concentrations of PRP was introduced in the calculations without any improvement in the fitting as a result. Therefore, AFM was performed to find out the accuracy of the Q-Tools modelling. Atomic force microscopy was carried out to estimate the actual height of the aggregates deposited on the crystal surface and consequently the average thickness of the layer. These results were compared to those obtained with Q-Tools for the same donor. It was demonstrated that the use of Q-Tools software leads to underestimation of the thickness as shown by AFM, Therefore, the software does not allow for precise mass measurement when the deposition of non-homogenous layer of platelets takes place. In contrast, the Voight-based model has been successfully applied to the measurements of adsorbed proteins as well as to some polymer films (Voinova, Rodahl et al. 1999). However, when absorbed proteins do not conserve their shape during adsorption or they flow under shear deformation

the application of this mathematical model is not accurate enough (Voinova, Rodahl et al. 1999). In fact, the use of this model for some biological purposes brings out the problem of accounting for the complex rheology of the biological interface, which is dominated by viscous effects (Voinova, Jonson et al. 2002). As we found using phase-contrast and AFM the distribution of the platelet aggregates is not always uniform through the sensor surface and the complexity in the viscoelastic structure of the platelet-aggregate layer makes the software unsuitable for the measurement of platelet aggregate. Therefore, in all my experiments f and D values were used to quantify the changes in platelet aggregation.

ATOMIC FORCE MICROSCOPY

Atomic force microscopy is a novel method for high-resolution imaging of any surface including those of living and fixed cells (Kuznetsova, Starodubtseva et al. 2007). This powerful technique is also used for characterization of the mechanical, electrical and magnetic characteristics of samples to be studied both qualitatively and quantitatively. Atomic force microscopy operation is based on the detection of repulsive and/or attractive surface forces. The interaction between the sample surface and a tip (probe) located very close to it corresponds to the force between the atoms of the sample and those of the tip that scans its surface. Image contrast is generated by monitoring the forces of interaction between the tip and the surface. This technique can be operated in a number of different imaging modes depending on the nature of the interaction between the tip and sample surface. The micromechanical properties of cell surface and subsurface layers can be detected either by contact mode AFM

techniques (force modulation, lateral force microscopy and force-curve analysis) or by phase imaging in the tapping mode AFM (intermittent, semi contact) (Kuznetsova, Starodubtseva et al. 2007).

In vascular biology, AFM has been used so far for the study of the molecular level visualization of plasma proteins, protein aggregation and multimer assembly, and structural and morphological details of vascular cells under aqueous conditions (Fritz, Radmacher et al. 1994, Walch, Ziegler et al. 2000). To date only few authors have used AFM to study platelet activation (Fritz, Radmacher et al. 1993; Fritz, Radmacher et al. 1994; Radmacher, Fritz et al 1996; Karagkiozaki, Logothetidis et al. 2009). In the most recent publication the authors used stoichiometric and nonstoichiometric titanium nitride ($TiN(x)$) films to investigate platelet adhesion to these surfaces (Karagkiozaki, Logothetidis et al. 2009). The published images, however, were not clear enough and did not allow for determination of morphology of single platelets. In contrast, images acquired in our experiments revealed with great detail the subcellular components of activated platelets showing budding granules, pseudopodia and adhesion contact areas between the adjacent platelets fibrinogen and the crystal surface. Furthermore, AFM could be used for quantification of height of platelets aggregates deposited on the crystal surface.

I feel, therefore, that our AFM protocol is robust and suitable for studies on the interactions between biological and non-biological surfaces and platelets.

CONCLUSIONS

1. Q-Sense E₄ is a suitable device for the measurement of fibrinogen-induced platelet aggregation under flow conditions

Perfusion of PRP through fibrinogen-coated crystals induced platelet aggregation as measured by the device and confirmed by imaging techniques.

2. Microaggregates were detected in a platelet concentration-, flow-dependent manner

The best conditions for the study of platelet aggregation using this device was found at a flow rate of 100 $\mu\text{L}/\text{minute}$ on fibrinogen-coated polystyrene crystals.

3. Q-Sense is a low shear stress flow system

The estimated shear stresses at 100 $\mu\text{L}/\text{minute}$ for the different concentrations of PRP range from 3.26 dyne/cm^2 for 100,000 platelets/ μL to 4.03 dyne/cm^2 for 210,000 platelets/ μL .

4. Platelet aggregation can be pharmacologically modulated

Both platelet agonists and inhibitors tested, except Apyrase and 2-MeSAMP, were able to modify platelet response. In addition, prostacyclin was not only able to inhibit, but also reverse changes in platelet aggregation measured by the device.

5. Q-Sense is suitable for the study of platelet function with low platelet counting or limited amount of blood

Due to its sensitivity this device allows the study of platelet function in situations such as thrombocytopenia or limited amount of blood available such as in neonates.

6. Q-sense can be used for testing haemobiocompatibility of biomaterials

Crystal sensors provide a substrate not only for the coating with haemostatic proteins such as fibrinogen, but also for studies of platelet-compatibility of biomaterials used in medicine.

7. Q-Tools modelling underestimate the deposition of platelet aggregates

The Voigt-based viscoelastic modelling supplied with the Q-Sense is not suitable for estimating the thickness and therefore the mass deposited in sensor after the perfusion of platelets through the system. Platelet function should be studied by changes in f and D .

8. In summary, Q-sense is a valuable device for the study of platelet function in physiological and pathological circumstances and for pharmacological studies

FURTHER DIRECTIONS

Characterization of tumour cell-platelet interactions under flow conditions in nanoscale.

Tumour-induced platelet aggregation (TCIPA), blood coagulation and thrombosis play an important role in the pathophysiology of metastasis. Therefore, modulating tumour cell-platelet interactions and thrombosis may represent an effective therapeutic approach to prevent or reduce tumour metastasis. There is evidence that tumour cells have the ability to stimulate the release of platelet granules leading to the liberation of several pro-aggregatory agents, such as TXA₂ and ADP. Interestingly, there is strong evidence implicating platelet receptors in TCIPA, including GPIb α , GPIIb/IIIa and P-selectin. TCIPA confers a number of advantages to the survival of the tumour cell in the vasculature and in its successful metastasis. When covered with a coat of platelets, a tumour cell acquires the ability to evade the body's immune system. Indeed, it has been shown that platelets protect tumours from TNF- α -mediated cytotoxicity. In addition, platelets may shield cancerous cells from high shear forces seen in flowing blood that could potentially damage the tumour cell. Another survival advantage for the tumour cell is the tendency for the tumour cell-platelet aggregate to embolize the microvasculature at a new extravasation site. Furthermore, platelets facilitate the adhesion of tumour cells to the vascular endothelium, and release a number of growth factors that can be used by tumour cells for growth.

To date, only anticoagulant drugs have been used to inhibit tumour cell-platelet interactions (Cochrane Database of Systematic Reviews 2007, Issue 3. Art. No.: CD006468. DOI: 10.1002/14651858.CD006468.pub2}. Potential

pharmacological inhibitors of TCIPA need to be tested under conditions similar or identical to those of vascular blood flow and ideally they should selectively inhibit platelet-cancer, but not platelet-platelet interactions.

After establishing the use of Q-Sense as a unique method to study platelet aggregation at nanoscale resolution, I would like to use this method for the measurement of TCIPA.

I have just started the set up of the new TCIPA *in vitro* model using this device. To perform these experiments, first gold crystals were placed in 24 well plates. Afterwards, Caco-2 cells, adenocarcinoma colon cancer cells, were seeded in different concentrations on the top of the crystal surface and maintained for up to 48h or until confluency was reached in the incubator at 37 °C and 5% CO₂. Crystals were then placed in the chambers and washed with tyroide's buffer for 20 minutes (100 μL/min) to remove tumour cells and debris not bound to the surface. As shown in **figures 74-75**, changes in f and D were monitored at real time with the device and platelet aggregates were formed when PRP (210,000 platelets/μL) was perfused through the system and interact with cells grown on the top of the crystal surface.

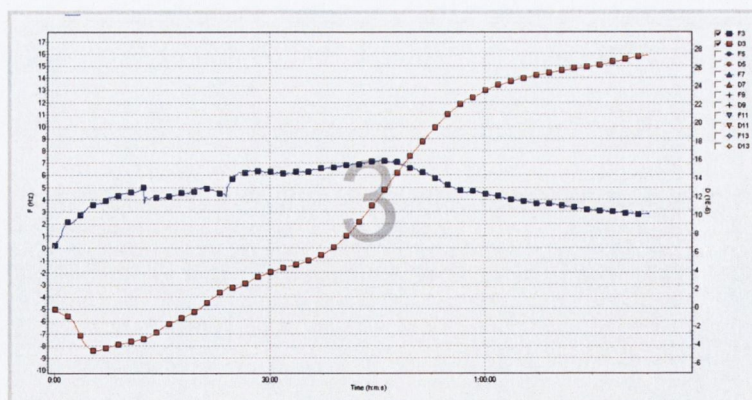


Figure 74: Aggregation of platelets on Caco2 cells grown on gold crystals

The perfusion of PRP (210,000 platelets/ μL) induced a decrease in the f and increase in D measured by Q-Sense.



Figure 75: Representative phase-contrast microscopy of TCIPA (20x). Platelet aggregates (red arrow) are formed on the top of Caco-2 cells.

Impact of the Proposed Research on Health and Cancer

Nowadays, there is no cure for cancer metastasis. In addition, the study of cancer metastasis is based on different imaging techniques which in some cases are only able to detect metastasis when they are big enough. Therefore, micro- or nano-metastasis often are not detectable until cancer becomes advanced. This device would be a fantastic tool to study cancer metastasis at early stage as is capable of detecting ng quantities of mass; therefore, the presence of nano- and micro-metastasis might be detectable. Moreover, I will use a flow system to further characterize tumour cell-platelet interactions mimicking the vascular blood flow. This research will provide novel information on the biology of cancer metastasis. Therefore, this information can be used in order to design new therapeutic strategies in cancer patients.

Pharmacological studies: Nanodelivery systems

I would like also to use this new method for the development of a highly selective therapeutic approach for the treatment of platelet activation and TCIPA using nanopharmacology (nanodelivery systems). For pharmacological studies I will use the following inhibitors of platelet function that act via various mechanisms: aspirin and other non-steroidal antiinflammatory drugs (inhibitors of COX and thromboxane generation), antagonists of purinergic receptor (2-MeSAMP), phenanthroline (inhibitor of MMPs), prostacyclin (cAMP stimulator), S-nitroso-glutathione (NO donor and cGMP stimulator). The drugs will be loaded into nanocarriers functionalized with antibodies such as PAC-1 or P-Selectin that will selectively deliver the drug to activated platelets targeting platelet-cancer aggregates but not to platelets which are not associated with cancer cells. In our group it has been recently optimized the use of nanocarriers chitosan and poly(lactide-co-glycolide) (PLGA) and selected chitosan and PLGA for further studies (Li, X, Radomski, A., Corrigan, O.I., Tajber L., De Sousa Menezes, F., Endter, S., Medina, C., and Radomski, M.W. The Platelet Compatibility of Poly(lactide-co-glycolide) (PLGA), Chitosan and PLGA- Chitosan Nanoparticles, Nanomedicine, in press)

REFERENCES

- Alonso-Escolano D., Medina C. et al. (2006). "PKC{delta} Mediates Platelet-Induced Breast Cancer Cell Invasion." Journal of Pharmacology and Experimental Therapeutics **318**:373-80.
- Alonso-Escolano D., Strongin A.Y. et al. (2004). "Membrane type-1 matrix metalloproteinase stimulates tumour cell-induced platelet aggregation: role of receptor glycoproteins." British Journal of Pharmacology **141**: 241-252.
- Armstrong R.A. (1996). "Platelet prostanoid receptors." Pharmacology and Therapeutics **72**(3): 171-91.
- Barret N.E., Jones L. et al. (2008). "Future innovations in anti-platelet therapies." British Journal of Pharmacology **154**: 918-939.
- Baumgartner H.R. and Haudenschild C. (1972). "Adhesion of platelets to subendothelium." Annals of the New York Academy of Sciences **27**(201): 22-36.
- Bergmeier W., Piffath C.L. et al. (2004). "Tumor Necrosis Factor- α -Converting Enzyme (ADAM17) Mediates GPIb α Shedding From Platelets In Vitro and In Vivo." Circulation Research **95**(7): 677-683.
- Best L.C., Martin T.J. et al. (1977). "Prostacyclin increases cyclic AMP levels and adenylate cyclase activity in platelets." Nature **267**(5614): 850-852.
- Bizzozero G. (1882). "Uber einen neuen Formbestandteil des Blutes und dessen Rolle bei der Thrombose und der Blutgerinnung." Virchows Arch. Pathol.Anat. Physiol **90**: 261.
- Blobel C.P. (2005). "ADAMS:key components in EGFR signalling and development." Nature Reviews Molecular Cell Biology **6**(1): 32-43.

- Born G.V. (1966). "Effects of adenosine diphosphate (ADP) and related substances on the adhesiveness of platelets in vitro and in vivo." British Journal of Haematology **12**(1): 37-8.
- Born G.V.R. (1962). "Aggregation of blood platelets by adenosine diphosphate and its reversal." Nature **194**: 972-9.
- Burch J.W., Stanford N. et al. (1978). "Inhibition of platelet prostaglandin synthetase by oral aspirin." The Journal of Clinical Investigation **61** (2): 314-319.
- Cardinal D.C. and Flower R.J. (1980). "The electronic aggregometer: a novel device for assessing platelet behavior in blood." Journal of Pharmacological Methods **3**(2): 135-158.
- Chen J. and Lopez J.A. (2005). "Interactions of Platelets with Subendothelium and Endothelium." Microcirculation **12**(3): 235-246.
- Cheng Y. (2006). "Cyclooxygenases, microsomal prostaglandin E synthase-1, and cardiovascular function." The Journal of Clinical Investigation **116**(5): 1391-1399.
- Chinn J.A., Horbett T.A. et al. (1991). "Baboon fibrinogen adsorption and platelet adhesion to polymeric materials." Thrombosis and Haemostasis **65**: 608-617.
- Choi W.S., Jeon O.H. et al. (2008). "MMP-2 regulates human platelet activation by interacting with integrin α IIb β 3." Journal of Thrombosis and Haemostasis **6**(3): 517-523.
- Chung A.W.Y., Jurasz P. et al. (2002). "Mechanisms of action of proteinase-activated receptor agonists on human platelets." British Journal of Pharmacology **135**(5): 1123-1132.

- Clemetson K.J. and Clemetson J.M. (2001). "Platelet collagen receptors. ." Thrombosis and Haemostasis **86**: 189-197.
- Colciaghi F., Borroni B. et al. (2002). "[alpha]-Secretase ADAM10 as well as [alpha]APPs is reduced in platelets and CSF of Alzheimer disease patients." Molecular Medicine **8**(2): 67-74.
- Coller B.S., Beer J.H. et al. (1989). "Collagen-platelet interactions: evidence for a direct interaction of collagen with platelet GPIa/IIa and an indirect interaction with platelet GPIIb/IIIa mediated by adhesive proteins." Blood **74**: 182-192.
- Coughlin S.R. (2000). "Thrombin signalling and protease-activated receptors." Nature **407**(6801): 258-264.
- Cramer E.M., Savidge G.F. et al. (1990). "Alpha-granule pool of glycoprotein IIb-IIIa in normal and pathologic platelets and megakaryocytes." Blood **75**(6): 1220-1227.
- Davi G. and Patrono C. (2007). "Platelet Activation and Atherothrombosis." The New England Journal of Medicine **357**(24): 2482-2494.
- Dixon M.C. (2008). "Quartz Crystal Microbalance with Dissipation Monitoring: Enabling Real-Time Characterization of Biological Materials and Their Interactions." Journal of Biomolecular Techniques **19**(3): 151-158.
- Djellas Y., Manganello J.M. et al. (1999). "Identification of Galpha 13 as one of the G-proteins That Couple to Human Platelet Thromboxane A₂ Receptors." Journal of Biological Chemistry **274**(20): 14325-14330.
- Donne A. (1842). "De L'origine des globules du sang, de leur mode de formation et de leur fin." Comptes Rendus de l'Académie des Sciences **14**: 366.

- Dopheide S.M., Yap C.L. et al. (2001). "Dynamic aspects of platelet adhesion under flow." Clinical and Experimental Pharmacology and Physiology **28**: 355-363.
- Dusting G.J., Moncada S. et al. (1982). "Prostacyclin: its biosynthesis, actions, and clinical potential." Advances in Prostaglandin Thromboxane and Leukotriene Research **10**: 59-106.
- Egashira K. (2002). "Clinical Importance of Endothelial Function in Arteriosclerosis and Ischemic Heart Disease." Circulation Journal **66**: 529-533.
- Fabre J.E., Nguyen M.T. et al. (1999). "Decreased platelet aggregation, increased bleeding time and resistance to thromboembolism in P2Y1-deficient mice." Nature Medicine **5**: 1199 - 1202.
- Falcinelli E., Giannini S. et al. (2007). "Platelets release active matrix metalloproteinase-2 "in vivo" in humans at a site of vascular injury: lack of inhibition by aspirin." British Journal of Haematology **138**(2): 221-230.
- Falcinelli E., Guglielmini G. et al. (2005). "Intraplatelet signaling mechanisms of the priming effect of matrix metalloproteinase-2 on platelet aggregation." Journal of Thrombosis and Haemostasis **3**(11): 2526-2535.
- Fatissou J., Merhi Y. et al. (2008). "Quantifying Blood Platelet Morphological Changes by Dissipation Factor Monitoring in Multilayer Shells." Langmuir **24**(7): 3294-3299.
- Fernandez-Patron C., Martinez-Cuesta M.A. et al. (1999). "Differential regulation of platelet aggregation by matrix metalloproteinases-9 and -2." Thrombosis and Haemostasis **82**(6): 1730-5.

- Fetalvero K.M., Martin K.A. et al. (2007). "Cardioprotective prostacyclin signaling in vascular smooth muscle." Prostaglandins and other Lipids Mediators **82**: 109-18.
- Fredriksson C., Kihlman S. et al. (1998). "The Piezoelectric Quartz Crystal Mass and Dissipation Sensor: A Means of Studying Cell Adhesion." Langmuir **14**(2): 248-251.
- Fritz M., Radmacher M. et al. (1993). "In Vitro Activation of Human Platelets Triggered and Probed by Atomic Force Microscopy." Experimental Cell Research **205**(1):187-190.
- Fritz M., Radmacher M. et al. (1994). "Granula motion and membrane spreading during activation of human platelets imaged by atomic force microscopy" Biophysical Journal **66**(5):1328-1334.
- Frojmovic M., Nash G. et al. (2002). "Definitions in biorheology: cell aggregation and cell adhesion in flow. ." Thrombosis and Haemostasis **87**(4): 771.
- Frojmovic M. (2008). "From in vitro blood rheology to useful bedside instrumentation for cardiovascular diseases: history and challenges." Annals of Biomedical Engineering **36**(4): 528-533.
- Fujikawa K., Suzuki H. et al. (2001). "Purification of human von Willebrand factor-cleaving protease and its identification as a new member of the metalloproteinase family." Blood **98**(6): 1662-1666.
- Fullard J.F. (2004). "The Role of the Platelet Glycoprotein IIb/IIIa in Thrombosis and Haemostasis." Current Pharmaceutical Design **10**: 1567-1576.

- Furchgott R.F. and Zawadzki J.V. (1980). "The obligatory role of endothelial cells in the relaxation of arterial smooth muscle by acetylcholine." Nature **288**(5789): 373-376.
- Furie B. and Furie B.C. (1988). "The molecular basis of blood coagulation." Cell **53**(4): 505-518.
- Furie B. and Furie B.C. (2008). "Mechanisms of Thrombus Formation." The New England Journal of Medicine **359**(9): 938-949.
- Gachet C. (2001). "Identification, characterization, and inhibition of the platelet ADP receptors." International Journal of Hematology **74**(4): 375-81.
- Gachet C. (2006). "Regulation of platelet function by P2 receptors." Annual Review of Pharmacology and Toxicology **46**(1): 277-300.
- Gachet C. (2008). "P2 receptors, platelet function and pharmacological implications." Thrombosis and Haemostasis **99**: 466-472.
- Galt S.W., Lindemann S. et al. (2002). "Outside-in signals delivered by matrix metalloproteinase-1 regulate platelet function." Circulation Research **90**(10): 1093-9.
- Gardiner E.E., Shen Y. et al. (2007). "Controlled shedding of platelet glycoprotein (GP)VI and GPIb-IX-V by ADAM family metalloproteinases." Journal of Thrombosis and Haemostasis **5**(7): 1530-1537.
- Garg U.C. and Hassid A. (1989). "Nitric oxide-generating vasodilators and 8-bromo-cyclic guanosine monophosphate inhibit mitogenesis and proliferation of cultured rat vascular smooth muscle cells." The Journal of Clinical Investigation **83**(5): 1774-1777.

- Gerzer R., Karrenbrock B. et al. (1988). "Direct comparison of the effects of nitroprusside, SIN 1, and various nitrates on platelet aggregation and soluble guanylate cyclase activity." Thrombosis Research **52**(1): 11-21.
- Gohlke-Barwolf et al. (1995). "Guidelines for prevention of thromboembolic events in valvular heart disease." European Heart Journal **16**(10): 1320-1330.
- Goto S., Tamura N. et al. (2002). "Involvement of glycoprotein VI in platelet thrombus formation on both collagen and von Willebrand factor surfaces under flow conditions." Circulation **106**: 266-272.
- Grunkemeier J.M., Tsai W.B. et al. (1998). "Hemocompatibility of treated polystyrene substrates: Contact activation, platelet adhesion, and procoagulant activity of adherent platelets." Journal of Biomedical Materials Research **41**(4): 657-670.
- Grunkemeier J.M., Tsai W.B. et al. (2000). "The effect of adsorbed fibrinogen, fibronectin, von Willebrand factor and vitronectin on the procoagulant state of adherent platelets." Biomaterials **21**(22): 2243-2252.
- Gutierrez E., Petrich B.G. et al. (2008). "Microfluidic devices for studies of shear-dependent platelet adhesion." Lab on a Chip. **8**(9): 1486-1495.
- Hamburger S.A. and McEver R.P. (1990). "GMP-140 mediates adhesion of stimulated platelets to neutrophils." Blood **75**(3): 550-4.
- Harrison P., Frelinger A. L. et al. (2007). "Measuring antiplatelet drug effects in the laboratory." Thrombosis Research **120**(3): 323-336.
- Hayward C.P.M., Harrison P. et al. (2006). "Platelet function analyzer (PFA)-100 closure time in the evaluation of platelet disorders and platelet function." Journal of Thrombosis and Haemostasis **4**(2): 312-319.

- Hechler B., Leon C. et al. (1998). "The P2Y1 Receptor Is Necessary for Adenosine 5'-Diphosphate-Induced Platelet Aggregation." Blood **92**(1): 152-159.
- Hemmersam A.G., Foss M. et al. (2005). "Adsorption of fibrinogen on tantalum oxide, titanium oxide and gold studied by the QCM-D technique." Colloids and Surfaces B: Biointerfaces **43**(3-4): 208-215.
- Hook F., Rodahl M. et al. (1998). "Energy Dissipation Kinetics for Protein and Antibody-Antigen Adsorption under Shear Oscillation on a Quartz Crystal Microbalance." Langmuir **14**(4): 729-734.
- Ignarro L.J., Buga G.M. et al. (1987). "Endothelium-derived relaxing factor produced and released from artery and vein is nitric oxide." Proceedings of the National Academy of Sciences of the United States of America **84**(24): 9265-9269.
- Ikeda Y., Handa M. et al. (1991). "The role of von Willebrand factor and fibrinogen in platelet aggregation under varying shear stress." The Journal of Clinical Investigation **87**(4): 1234-1240.
- Jantzen H.M., Gousset L. et al. (1999). "Evidence for Two Distinct G-protein-coupled ADP Receptors Mediating Platelet Activation" Thrombosis and Haemostasis **81**(1): 111-117.
- Jurasz P., Alonso-Escolano D. et al. (2004). "Platelet-cancer interactions: mechanisms and pharmacology of tumour cell-induced platelet aggregation." British Journal of Pharmacology **143**(7): 819-826.
- Jurasz P., North S. et al. (2003). "Matrix metalloproteinase-2 contributes to increased platelet reactivity in patients with metastatic prostate cancer: a preliminary study." Thrombosis Research **112**(1-2): 59-64.

- Jurasz P., Radomski A. et al. (2000). Nitric oxide and platelet function. Nitric oxide Biology and Pathobiology. I. L.J. San Diego San Francisco New York Boston Sydney Tokyo, Academic Press: 823-840.
- Jurasz P., Santos-Martinez M.J. et al. (2006). "Generation of platelet angiostatin mediated by urokinase plasminogen activator: effects on angiogenesis." Journal of Thrombosis and Haemostasis **4**(5): 1095-1106.
- Jurasz P., Sawicki G. et al. (2001). "Matrix Metalloproteinase 2 in Tumor Cell-induced Platelet Aggregation: Regulation by Nitric Oxide." Cancer Research **61**(1): 376-382.
- Jurasz P., Stewart M.W. et al. (2001). "Role of von Willebrand factor in tumour cell-induced platelet aggregation: differential regulation by NO and prostacyclin." British Journal of Pharmacology **134**(5): 1104-1112.
- Kahn M.L., Nakanishi-Matsui M. et al. (1999). "Protease-activated receptors 1 and 4 mediate activation of human platelets by thrombin." The Journal of Clinical Investigation **103**(6): 879-887.
- Karagkiozaki V., Logothetidis S. et al. (2009). "Atomic force microscopy probing platelet activation behavior on titanium nitride nanocoatings for biomedical applications." Nanomedicine **5**(1): 64-72.
- Kazes I., Elalamy I. et al. (2000). "Platelet release of trimolecular complex components MT1-MMP/TIMP2/MMP2: involvement in MMP2 activation and platelet aggregation." Blood **96**(9): 3064-3069.
- Knezevic I., Borg C. et al. (1993). "Identification of Gq as one of the G-proteins which copurify with human platelet thromboxane A₂/prostaglandin H₂ receptors." The Journal of Biological Chemistry **268**(34): 26011-26017.

- Konstantopoulos K., Kukreti S. et al. (1998). "Biomechanics of cell interactions in shear fields." Advanced Drug Delivery Reviews **33**(1-2): 141-164
- Kroll M.H., Hellums J.D. et al. (1996). "Platelets and shear stress." Blood **88**(5): 1525-1541.
- Kundu S.K., Heilmann E.J. et al. (1995). "Description of an in vitro platelet function analyzer-PFA-100." Seminars in Thrombosis and Hemostasis **21**(2): 106-112.
- Kuznetsova T.G., Starodubtseva M.N. et al. (2007). "Atomic force microscopy probing of cell elasticity." Micron **38**(8): 824-833.
- Larsen E., Celi A. et al. (1989). "PADGEM protein: a receptor that mediates the interaction of activated platelets with neutrophils and monocytes." Cell **59**(2): 305-12.
- Malinski T., Radomski M.W. et al. (1993). "Direct electrochemical measurement of nitric oxide released from human platelets." Biochemical and Biophysical Research Communications **194**(2): 960-5.
- Mannucci P.M. (2004). "Treatment of von Willebrand's Disease." The New England Journal of Medicine **351**(7): 683-694.
- Maree A.O. and Fitzgerald D.J. (2007). "Variable platelet response to aspirin and clopidogrel in atherothrombotic disease." Circulation **115**(16): 2196-2207.
- Martinez A., Salas E. et al. (2001). "Matrix metalloproteinase-2 in platelet adhesion to fibrinogen: interactions with nitric oxide." Medical Science Monitor **7**(4): 646-51.

- Marx K.A. (2003). "Quartz Crystal Microbalance: A Useful Tool for Studying Thin Polymer Films and Complex Biomolecular Systems at the Solution-Surface Interface." Biomacromolecules **4**(5): 1099-1120.
- Medina C., Jurasz P. et al. (2006). "Platelet Aggregation-Induced by Caco-2 Cells: Regulation by Matrix Metalloproteinase-2 and Adenosine Diphosphate." Journal of Pharmacology and Experimental Therapeutics **317**(2): 739-745.
- Michelson A.D. (2003). "How Platelets Work: Platelet Function and Dysfunction." Journal of Thrombosis and Thrombolysis **16**(1/2): 7-12.
- Moncada S. (1981). "Prostacyclin: Its Biosynthesis, Actions and Clinical Potential." Philosophical Transactions of the Royal Society B: Biological Sciences **294**: 305-329.
- Moncada S., Gryglewski R.J. et al. (1976). "An enzyme isolated from arteries transforms prostaglandin endoperoxides to an unstable substance that inhibits platelet aggregation." Nature **263**: 663–665.
- Moro M.A., Russel R.J. et al. (1996). "cGMP mediates the vascular and platelet actions of nitric oxide: confirmation using an inhibitor of the soluble guanylyl cyclase." Proceedings of the National Academy of Sciences of the United States of America **93**(4): 1480-1485.
- Mosesson M.W., Siebenlist K.R. et al. (2001). "The Structure and Biological Features of Fibrinogen and Fibrin." Annals of the New York Academy of Sciences **936**: 11-30.
- Murate T., Yamashita K. et al. (1997). "The production of tissue inhibitors of metalloproteinases (TIMPs) in megakaryopoiesis: possible role of platelet- and megakar." British Journal of Haematology **99**: 181-189.

- Muratsugu M., Romanschin A.D. et al. (1997). "Adhesion of human platelets to collagen detected by ^{51}Cr labelling and acoustic wave sensor." *Analytica Chimica Acta* **342**: 23-29.
- Nataraj C., Thomas D.W. et al. (2001). "Receptors for prostaglandin E₂ that regulate cellular immune responses in the mouse." *Journal of Clinical Investigation* **108**(8): 1229-1235.
- Needleman P., Moncada S. et al. (1976). "Identification of an enzyme in platelet microsomes which generates thromboxane A₂ from prostaglandin endoperoxides." *Nature* **261**(5561): 558-60.
- Offermanns S. (2006). "Activation of Platelet Function Through G Protein-Coupled Receptors." *Circulation Research* **99**: 1293-1304.
- Palmer R.M., Ferrige, A.G. et al. (1987). "Nitric oxide release accounts for the biological activity of endothelium-derived relaxing factor." *Nature* **17**(327): 524-526.
- Pedvis L.G., Wong T. et al. (1988). "Differential inhibition of the platelet activation sequence: shape change, micro- and macro-aggregation, by a stable prostacyclin analogue (Iloprost)." *Thrombosis Haemostasis* **59**: 323-8.
- Pirard B. (2007). "Insight into the structural determinants for selective inhibition of matrix metalloproteinases." *Drug Discovery Today* **12**(15-16): 640-646.
- Podda G.M., Bucciarelli P. et al. (2007). "Usefulness of PFA-100 testing in the diagnostic screening of patients with suspected abnormalities of hemostasis: comparison with the bleeding time." *Journal of Thrombosis and Haemostasis* **5**(12): 2393-2398.

- Rabie T., Strehl A. et al. (2005). "Evidence for a role of ADAM17 (TACE) in the regulation of platelet glycoprotein V." The Journal of Biological Chemistry **280**(15): 14462-14468.
- Radmacher M., Fritz M. (1996). "Measuring the viscoelastic properties of human platelets with the atomic force microscopy". Biophysical Journal **70**:556-567.
- Radomski A., Jurasz P. et al. (2002). "Identification, regulation and role of tissue inhibitor of metalloproteinases-4 (TIMP-4) in human platelets." British Journal of Pharmacology **137**(8): 1330-8.
- Radomski A., Stewart M.W. et al. (2001). "Pharmacological characteristics of solid-phase von Willebrand factor in human platelets." British Journal of Pharmacology **134**(5): 1013-1020.
- Radomski M. and Moncada S. (1983). "An improved method for washing of human platelets with prostacyclin." Thrombosis Research **30**(4): 383-9.
- Radomski M.W. and Moncada S. (1993). "Regulation of vascular homeostasis by nitric oxide." Thrombosis and Haemostasis **70**(1): 36-41.
- Radomski M.W., Palmer R.M. et al. (1987a). "The anti-aggregating properties of vascular endothelium: interactions between prostacyclin and nitric oxide." British Journal of Pharmacology **92**(3): 639-646.
- Radomski M.W., Palmer R.M. et al. (1987b). "The role of nitric oxide and cGMP in platelet adhesion to vascular endothelium." Biochemical and Biophysical Research Communications **148**(3): 1482-1489.
- Radomski M.W., Palmer R.M. et al. (1987c). "Endogenous nitric oxide inhibits human platelet adhesion to vascular endothelium." Lancet **2**(8567): 1057-1058.

- Radomski M.W., Palmer R.M. et al. (1990a). "Characterization of the L-arginine:nitric oxide pathway in human platelets." British Journal of Pharmacology **101**(2): 325-328.
- Radomski M.W., Palmer R.M. et al. (1990b). "An L-arginine/nitric oxide pathway present in human platelets regulates aggregation." Proceedings of the National Academy of Sciences of the United States of America **87**(13): 5193-5197.
- Radomski M.W., Rees D.D. et al. (1992). "S-nitroso-glutathione inhibits platelet activation in vitro and in vivo." British Journal of Pharmacology **107**(3): 745-749.
- Rivera J., Lozano M.L. et al. (2009). "Platelet receptors and signaling in the dynamics of thrombus formation" Haematologica **94**(5): 700-711.
- Ruggeri Z. M. (2002). "Platelets in atherothrombosis." Nature Medicine **8**(11): 1227.
- Ruggeri Z.M. and Mendolicchio G.L. (2007). "Adhesion mechanisms in platelet function." Circulation Research **100**(12): 1673-1685.
- Russell J., Cooper D. et al. (2003). "Low venular shear rates promote leukocytedependent recruitment of adherent platelets." American Journal of Physiology **284**: G123-G129.
- Sakariassen K.S., Hanson S.R. et al. (2001). "Methods and Models to Evaluate Shear-Dependent and Surface Reactivity-Dependent Antithrombotic Efficacy." Thrombosis Research **104**(3): 149-174.
- Sakariassen K.S., Muggli R. et al. (1989). "Measurements of platelet interaction with components of the vessel wall in flowing blood." Methods in enzymology **169**: 37-70.

- Salas E., Moro M. A. et al. (1994). "Comparative pharmacology of analogues of S-nitroso-N-acetyl-DL-penicillamine on human platelets." British Journal of Pharmacology **112**(4): 1071-6.
- Salzman E.W. (1978). "Influence of antiplatelet drugs on platelet-surface interactions." Advances in Experimental Medicine and Biology **102**: 265-283.
- Santos-Martinez M.J., Medina C. et al. (2008). "Role of metalloproteinases in platelet function." Thrombosis Research **121**(4): 535-542.
- Sauerbrey G. (1959). "Verwendung von Schwingquarzen zur wägung dünner schichten und zur mikrowägung." Z Phys **155**: 206-222.
- Savage B., Saldívar E. et al. (1996). "Initiation of Platelet Adhesion by Arrest onto Fibrinogen or Translocation on von Willebrand Factor." Cell **84**(2): 289-297.
- Sawicki G., Salas E. et al. (1997). "Release of gelatinase A during platelet activation mediates aggregation." Nature **386**(6625): 616-619.
- Sawicki G., Sanders E.J. et al. (1998). "Localization and translocation of MMP-2 during aggregation of human platelets." Thrombosis and Haemostasis **80**(5): 836-9.
- Schlondorff J. and Blobel C.P. (1999). "Metalloprotease-disintegrins: modular proteins capable of promoting cell-cell interactions and triggering signals by protein-ectodomain shedding." Journal of Cell Science **112**(21): 3603-3617.
- Schullek J., Jordan J. et al. (1984). "Interaction of von Willebrand factor with human platelets in the plasma milieu." Journal of Clinical Investigation **73**(2): 421-428.

- Schultze M. (1865). "Ein heizbarer objektisch and seine Verwendung bei Untersuchungen des Blutes." Arch. Mikv. Anat. **1**: 1.
- Seals D.F. and Courtneidge S.A. (2003). "The ADAMs family of metalloproteases: multidomain proteins with multiple functions." Genes and Development **17**(1): 7-30.
- Sheu J.R., Fong T.H. et al. (2004). "Expression of matrix metalloproteinase-9 in human platelets: regulation of platelet activation in in vitro and in vivo studies." British Journal of Pharmacology **143**(1):193-201.
- Smith J.W., Steinhubl S.R. et al. (1999). "Rapid platelet-function assay: an automated and quantitative cartridge-based method." Circulation **99**: 620-625.
- Snopok B.A., Kostyukevych K.V. et al. (1998). "A biosensor approach to probe the structure and function of the adsorbed proteins: fibrinogen at the gold surface." Semiconductor Physics, Quantum Electronics & Optoelectronics **1**: 121-134.
- Stenberg P.E., McEver R.P. et al. (1985). "A platelet alpha-granule membrane protein (GMP-140) is expressed on the plasma membrane after activation." The Journal of Cell Biology **101**(3): 880-886.
- Sternlicht M.D. and Werb Z. (2001). "How matrix metalloproteinases regulate cell behavior." Annual Review of Cell and Developmental Biology **17**(1): 463-516.
- Taylor A., Cooper D. et al. (2005). "Platelet-Vessel Wall Interactions in the Microcirculation." Microcirculation **12**(3): 275 - 285.

- Takasaki J., Kamohara M. et al. (2001). "Molecular cloning of the platelet P2TAC ADP receptor: pharmacological comparison with another ADP receptor, the P2Y1 receptor." Molecular Pharmacology **60**: 432-439.
- Thomas D.W., Mannon R.B. et al. (1998). "Coagulation defects and altered hemodynamic responses in mice lacking receptors for thromboxane A₂." Journal of Clinical Investigation **102**(11): 1994-2001.
- Tsai W.B., Grunkemeier J.M. et al. (1999). "Human plasma fibrinogen adsorption and platelet adhesion to polystyrene." Journal of Biomedical Materials Research **44**(2): 130-139.
- Turitto V.T. (1982). "Blood viscosity, mass transport, and thrombogenesis." Progress in Hemostasis Thrombosis **6**: 139-177.
- Turitto V.T. and Hall C.L. (1998). "Mechanical factors affecting hemostasis and thrombosis." Thrombosis Research **92**(6, Supplement 2): S25-S31.
- Visse R. and Nagase H. (2003). "Matrix Metalloproteinases and Tissue Inhibitors of Metalloproteinases: Structure, Function, and Biochemistry." Circulation Research **92**(8): 827-839.
- Voinova M.V., Jonson M. et al. (2002). "Missing mass, effect in biosensor's QCM applications." Biosensors and Bioelectronics **17**(10): 835-841.
- Voinova M.V., Rodahl M. et al. (1999). "Viscoelastic acoustic response of layered polymer films at fluid-solid interfaces: continuum mechanics approach." Physica Scripta **59**: 391-396.
- Vu D. and Neerman-Arbez M. (2007). "Molecular mechanisms accounting for fibrinogen deficiency: from large deletions to intracellular retention of misfolded proteins." Journal of Thrombosis and Haemostasis **5**(1): 125-131.

- Walch M., Ziegler U. (2000) "Effect of streptolysin O on the microelasticity of human platelets analyzed by atomic force microscopy." Ultramicroscopy **82**(1-4):259-67
- Watson S.P. (2009). "Platelet Activation by Extracellular Matrix Proteins in Haemostasis and Thrombosis." Current Pharmaceutical Design **15**(12): 1358-1372.
- Weber N., Wendel H.P. et al. (2005). "Formation of viscoelastic protein layers on polymeric surfaces relevant to platelet adhesion." Journal of Biomedical Materials Research Part A **72A**(4): 420-427.
- Wencel-Drake J.D., Painter R.G. et al. (1985). " Ultrastructural localization of human platelet thrombospondin, fibrinogen, fibronectin, and von Willebrand factor in frozen thin section." Blood **65**: 929-938.
- Wyler B., Bienz D. et al. (1986). "Glycoprotein Ib is the only phosphorylated major membrane glycoprotein in human platelets." The Biochemical Journal **234**: 373–379.
- Xia Z. and Frojmovic M.M. (1994). "Aggregation efficiency of activated normal or fixed platelets in a simple shear field: effect of shear and fibrinogen occupancy." Biophysical Journal **66**(6): 2190-2201.
- Zhang M., Wu Y. et al. (2008). "Fibrinogen and von Willebrand factor mediated platelet adhesion to polystyrene under flow conditions." Journal of Biomaterials Science-Polymer Edition **19**(10): 1383-1410.
- Zwaginga J.J., Sakariassen K.S. et al. (2006). "Flow-based assays for global assessment of hemostasis. Part 2: current methods and considerations for the future." Journal of Thrombosis and Haemostasis **4**(12): 2716-2717.